AD_____

Award Number: DAMD17-02-1-0581

TITLE: Analysis of Breast Cell-Lineage Response Differences to Taxol Using a Novel Co-Culture

PRINCIPAL INVESTIGATOR: Lauren S. Gollahon, Ph.D.

CONTRACTING ORGANIZATION: Texas Tech University
Lubbock, Texas 79409-1035

REPORT DATE: April 2003

TYPE OF REPORT: Annual

PREPARED FOR: U.S. Army Medical Research and Materiel Command
Fort Detrick, Maryland 21702-5012

DISTRIBUTION STATEMENT: Approved for Public Release;
Distribution Unlimited

The views, opinions and/or findings contained in this report are those of the author(s) and should not be construed as an official Department of the Army position, policy or decision unless so designated by other documentation.

20031104 095

# REPORT DOCUMENTATION PAGE

*Form Approved*
*OMB No. 074-0188*

Public reporting burden for this collection of information is estimated to average 1 hour per response, including the time for reviewing instructions, searching existing data sources, gathering and maintaining the data needed, and completing and reviewing this collection of information. Send comments regarding this burden estimate or any other aspect of this collection of information, including suggestions for reducing this burden to Washington Headquarters Services, Directorate for Information Operations and Reports, 1215 Jefferson Davis Highway, Suite 1204, Arlington, VA 22202-4302, and to the Office of Management and Budget, Paperwork Reduction Project (0704-0188), Washington, DC 20503

| 1. AGENCY USE ONLY (Leave blank) | 2. REPORT DATE | 3. REPORT TYPE AND DATES COVERED |
|---|---|---|
| | April 2003 | Annual (1 Apr 2002 - 31 Mar 2003) |

**4. TITLE AND SUBTITLE**

Analysis of Breast Cell-Lineage Response Differences to Taxol Using a Novel Co-Culture

**5. FUNDING NUMBERS**

DAMD17-02-1-0581

**6. AUTHOR(S)**

Lauren S. Gollahon, Ph.D.

**7. PERFORMING ORGANIZATION NAME(S) AND ADDRESS(ES)**

Texas Tech University
Lubbock, Texas 79409-1035

E-Mail: lgollaho@ttacs.ttu.edu

**8. PERFORMING ORGANIZATION REPORT NUMBER**

**9. SPONSORING / MONITORING AGENCY NAME(S) AND ADDRESS(ES)**

U.S. Army Medical Research and Materiel Command
Fort Detrick, Maryland 21702-5012

**10. SPONSORING / MONITORING AGENCY REPORT NUMBER**

**11. SUPPLEMENTARY NOTES**

Original contains color plates: All DTIC reproductions will be in black and white.

**12a. DISTRIBUTION / AVAILABILITY STATEMENT**

Approved for Public Release; Distribution Unlimited

**12b. DISTRIBUTION CODE**

**13. ABSTRACT (Maximum 200 Words)**

The purpose of this study is to investigate interactions occurring between normal breast cells and tumor cells grown together in a novel co-culture system. This is accomplished through the use of GFP technology. The scope of the work to date includes establishing optimal growth densities; generating hTERT cell lines to insure the availability of "normal" cells for continued analysis; and optimizing the conditions for valid efflux and transport experiments. Major findings: Preliminary results suggest that c-myc may be implicated in the ability for the tumor cells to resist Taxol insult through upregulation of the GLUT-1 transport mechanism. In addition, ER negative cells do not appear to be as influenced by the normal cells in co-culture growth experiments. Task associated progress report: We have determined growth curves and patterns for concurrent cell cultures of control epithelial, stromal and tumor cells (Task 1-3) and determined ratios of mammary epithelial, stromal and tumor cell types in co-culture (Tasks 1-3). Concurrently, my Co-PI has established the parameters for valid uptake and efflux transport experiments for normal mammary cells and tumor cells. In order to obtain valid efflux and transport mechanism results for our system, previous methods described in the literature had to be modified.

**14. SUBJECT TERMS**

Co-culture, GFP, Taxol, differential gene expression, cell lineage responses, uptake and efflux transport mechanisms

**15. NUMBER OF PAGES**

60

**16. PRICE CODE**

| 17. SECURITY CLASSIFICATION OF REPORT | 18. SECURITY CLASSIFICATION OF THIS PAGE | 19. SECURITY CLASSIFICATION OF ABSTRACT | 20. LIMITATION OF ABSTRACT |
|---|---|---|---|
| Unclassified | Unclassified | Unclassified | Unlimited |

## Table of Contents

**DOD 2003 Annual Report– Gollahon and Collie lab experiments**

## Introduction

Most studies on breast cancer development and progression focus on one cell type examined in isolation. This is due in part to the difficulty of culturing cell types with different growth requirements and in part to the inability to identify accurately the different cell types in a mixed culture. Of the breast lesions formed, 90% are derived from epithelial cells, with less than 10% from fibroblasts. This suggests an inherent difference in cell lineage responses to cancer initiation and progression. Our research goal is to show that different mammary cell types grown together in a novel co-culture system express discrete genes and respond differently to chemotherapy than do monolayers of homogeneous cell populations. The results from this co-culture system will be a critical step toward developing a three-dimensional culture model that more closely simulates the natural breast environment. The co-culture of normal human mammary cell types (epithelial and stromal) or of normal and tumor-derived cells will result in altered gene expression and differential sensitivity to Taxol. Taxol sensitivity of breast cells grown in co-culture is entirely unknown, as are the mechanisms that might contribute to Taxol responsiveness. Our model system will enable us to accurately monitor these expected differences in gene expression and Taxol responsiveness.

## Body

*Task 1. Co-culture human mammary epithelial (HME) cells and corresponding human mammary stromal (HMS) cells under normal growth conditions and in the presence of Taxol: Year 1*

*Task 1a. Determine growth patterns for concurrent cultures of control and treated HME-HMS cells using fluorescent microscopy.*

The goal of this set of experiments was to determine if growth patterns occurred for cells in control and treated co-cultures. We are currently completing this set of experiments. We had some initial setbacks. These included a delay of one month in transferring the graduate student (Sheree Case) to this project. Once the project experiments were underway, there was a problem with contamination. That took approximately 3 weeks to 1 month to isolate, clear and assess the damage to the cell lines.

However, in the process, several normal HMS and HME cells lines became infected. The depletion of the mortal cell stocks prompted our decision to introduce the catalytic reverse transcriptase enzyme component of telomerase (hTERT) through defective retroviral transfection. This construct was previously described in (Counter *et al.*, 1998; Takakura *et al.*, 1999). This was mentioned in the initial proposal as an alternative step to maintaining normal cell lines if the mortal, primary cell cultures became a limiting factor. It has been shown in the literature that introduction of hTERT does not induce transformation nor a tumorigenic phenotype in the cells (Jiang *et al.*, 1999; Morales *et al.*, 1999). To that end exogenous hTERT has been introduced into HME and HMS 73 and 87 respectively and selected with puromycin.

This procedure was previously described in (Jiang *et al.*, 1999; Morales *et al.*, 1999; McChesney *et al.*, 2000). We have prior experience with such techniques, (Shay *et al.*, 1995; Gollahon and Shay, 1996a; Gollahon *et al.*, 1998). The appended article Shay et al, 1995 describes the technique in detail. The only modification was the substitution of hTERT as the introduced species and selection under puromycin at concentrations between 25ng/ml to 50 ng/ml for 1 week). Upon selection of viable clones, the cells have been subcultured and frozen stocks replenished. This procedure took approximately 2 months to complete.

To directly address the objectives of Task 1, we determined the following as the best course of action. Cell cultures of HME, HMS and corresponding tumor cells were cultured as homogenous control populations. These cells included HME cells transfected with enhanced cyan fluorescent protein (CFP; Abs 433 nm, Em 475 nm); HMS cells transfected with enhanced green fluorescent protein (GFP; Abs 488 nm, Em 507 nm) and tumor cells transfected with red fluorescent protein (RFP; Abs 558 nm, Em 583) constructs. These constructs had been previously introduced into the cell lines of interest. Prior work in the lab already characterized cell growth curves for the cells with and without the constructs. Statistical analysis showed no significant differences in growth between the standard media and the co-culture medium (Fibroblast Basal Medium –FBM plus mammary growth supplements) (data shown in the original proposal manuscript and Master's Theses by Jim Zhang and Brian Herring). For exact medium conditions please see Shay et al, 1995 in the appendix.

Recently, the TTU - Howard Hughes Medical Institute purchased an Olympus IX-70 Deconvolution microscope and IX-80 microscope with confocal capabilities. This greatly facilitated our work due to the fact that it is located in the Department of Biological Sciences. In addition, Dr. Gollahon was recently named the University Imaging Center Director who insured access to the microscopes on a regular basis. The microscope has two excitation lasers. One is an Argon (488nm) and the second is a Green HeNe (543 nm). In addition the microscope is set for UV fluorescence and is equipped with a triple ban pass filter and a GFP filter (488 nm – 507 nm). The software is Fluoview. The cells were analyzed for growth patterns using confocal microscopy. However, in first starting this series of experiments, we realized that there was no true excitation source available for the cyan (Abs 433 nm and Em 475 nm). Thus we decided to freeze this set of HME cells for use when the correct laser could be added onto the scope. We are currently looking into the needs of the current users to decide whether a 442 HeCd laser or a 458 Multi Argon laser would be better suited. To continue progressing the proposal project, we transfected enhanced yellow fluorescent protein (YFP) into the HME cells. YFP has an Abs and Em spectrum shifted more toward the green (Abs 513 nm, Em 527 nm) than the GFP. We felt with the discrimination mirrors on the lasers, the scattered light would be reduced enough to possibly observe the green and the yellow concurrently. If this was not possible, the second alternative was to co-culture the HME and tumor cells and the HMS and tumor cells, but not the HME and HMS cells together. Transfection of the yellow into the HME cells was completed in approximately one month. We expect to have a third laser available on the confocal microscope by September of 2003.

The following are detailed descriptions of co-culture experiments corresponding to the figures included in the report. These descriptions also include observations made concerning cell

growth, morphology and overall empirical assessment of the cultures under analysis. Appended in Table 1, are the individual counts per experiment

**Figures 1-3.** These figures illustrate homogenous cultures of HME, Tumor and HMS plated in their corresponding media of SF170 or DMEM-supplemented with 10% Cosmic Calf Serum (Hyclone) and gentamycin sulfate (Sigma) respectively, as described in Shay et al, 1995. The cells were plated in Lab-Tek II 4-chamber slides (Nalg-Nunc), grown for 5 days and then visualized using confocal microscopy. Four different fields of vision were photographed digitally per chamber per slide. Cell types from 10 different fields of vision were counted per well per slide for ratio analysis unless specified otherwise. Population doublings were calculated for the parent cell lines that were concurrently maintained in T75 flasks.
**Observations:** The tumor cells grew much more rapidly than the HME and HMS and quickly dominated the chambers. This made it difficult to get a good view of the HME and HMS cells.

**Figures 4A-B.** Cells were co-cultured at concentrations of 30K HME, 10K Tumor, 30K HMS, 10K Tumor in a 4 well plate with FBM medium and were viewed after 5 days in culture. **A** - HME yellow with tumor red, B - HMS green with tumor red. The co-culture was viewed under 8 random fields of vision per chamber. Cells were counted for each field. Population doublings were calculated for the parent cell lines that were concurrently maintained in T75 flasks
A control was also done with the same concentration individually for each cell line in FBM medium. Each control cell type in FBM was photographed under 4 random fields of vision. Cell counts were done for each Field per chamber per slide.
**Observations**: Only tumor cells were observed in most of the field of visions. The picture taken for this figure was the only 1 that had a representation of both cell types out of 8 random fields of vision.

**Figures 5A-D.** Cells were co-cultured at concentrations of 50K HME, 3K Tumor, 50K HMS, 3K Tumor cells respectively in a 4-chamber slide with FBM medium and analyzed after 5 days in culture. **A** HMS green with tumor red, **B** - Overlay in A with increased magnification, **C** - HME yellow with tumor red, **D** - Overlay in C with increased magnification. The co-culture analyzed from 8 random fields of view. Cell counts were performed for each field per chamber per slide for each experiment.
Population doublings were calculated for the parent cell lines that were concurrently maintained in T75 flasks.
**Observations:** The tumor cells continued to dominate the mixed cultures. **Note:** No control was done at this time because the main focus of this series of experiments was to optimize the plating density for each cell type.

Although there was a more even distribution of cells when plated at 50-50-3, as stated earlier, the cell morphology for the HME and HMS cells did not reflect that of normal healthy cells. The are a number of possibilities why this occurred. One reason may simply be that the normal cells do not recover and go into cell cycle as quickly as the tumor cells. As they start to recover, the tumor cells with some factor that inhibits normal cell growth or causes a stress response may condition the medium. We are planning on investigating this possibility as a project tangential to the Tasks through a collaboration with Brian Reilly, Ph.D. in the department. He has expertise in protein isolation and identification. Another reason my simply be that the tumor cells depleted

the metabolites essential to the normal cells. Whatever, the reason, we decided to try a different strategy. Since the cells were not doing well together when harvested directly from the parent cell cultures and placed in the chamber slides, we decided to allow them to grow for several population doubling levels (PDLs) as a mixed population n a T75. At this time 50k-50k-3k HME-HMS-tumor cells were plated in a T75 flask and allowed that to grow for 5 days in FBM medium. Several different plating densities for HME-HMS-Tumor were performed including 50k-50k-50k, 30k-30k-10k and finally 50k-50k-3k. Interestingly, the 50-50-3 also appeared optimal in the T75 for yielding a more even cell distribution.

**Figures 6A-D.** These figures reflect the cells previously cultured together. For analysis using confocal microscopy 30K of the combined cell population was plated onto a 4-chamber slide. **A** - HME yellow with tumor red, **B** - Overlay in A under higher magnification, **C** - HMS green with tumor red, **D** - Overlay in C under higher magnification. Eight random fields of view were counted per chamber per slide. Population doublings were calculated for the parent cell lines that continued to grow in T75 flasks as well as the combined stock culture from which these cells were harvested.

**Observations**: The previous method of co-culture showed poor growth morphology for the normal cells. In addition, given a sufficient time, the tumor cells would eventually out number the normal cells and dominate the chamber surface area. When co-cultured on a larger surface area first, the tumor cells did not show an increased growth rate over the HME and HMS cells. They appeared to grow quickly as observed in the previous platings. However, once the population sizes for the HME and HMS cells reached a certain size, they appeared to better regulate tumor cell growth and although the tumor cells did not appear to stop growing, their growth was slowed down markedly to the point that there was a much more even distribution of cells in the combined populations. This cell population has been continually cultured for 2-3 months and the tumor cells have yet to grow over the normal cells. The possibility also exists that the tumor cells are secreting a growth-enhancing compound. However, due to the fact that this phenomenon was not observed in the separate cell populations that were plated together, this hypothesis seems unlikely. When viewed under confocal microscopy, it was interesting to note that the normal cells no longer demonstrated a stressed growth phenotype. The vacuolation, blebbing and other apoptotic traits were no longer present. The HME and HMS cells looked healthier. We are no confirming these data using the plate reader and finalizing the conditions for separation via FACsort as discussed in the proposal.

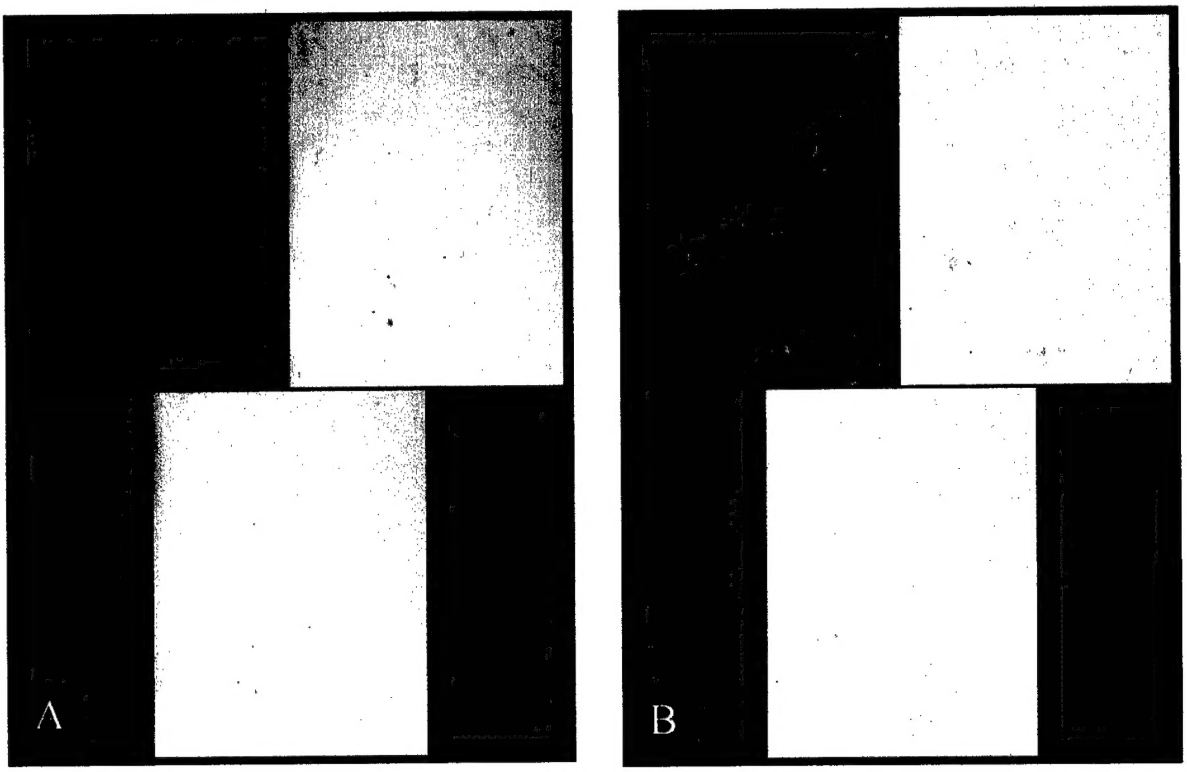


**Figure 1A-B. Homogenous cultures of HMS-GFP cells.** 50K cells were plated on a 4-chamber slide (Lab-Tek II) and cultured for 5 days in DMEM-XSG medium. Cells were viewed with an Olympus IX-80 inverted confocal microscope under 40X. Cells were excited with a 488 nm argon laser. GFP maximum excitation is 488 nm and maximum emission is 507 nm.
GFP= Green Fluorescent Protein

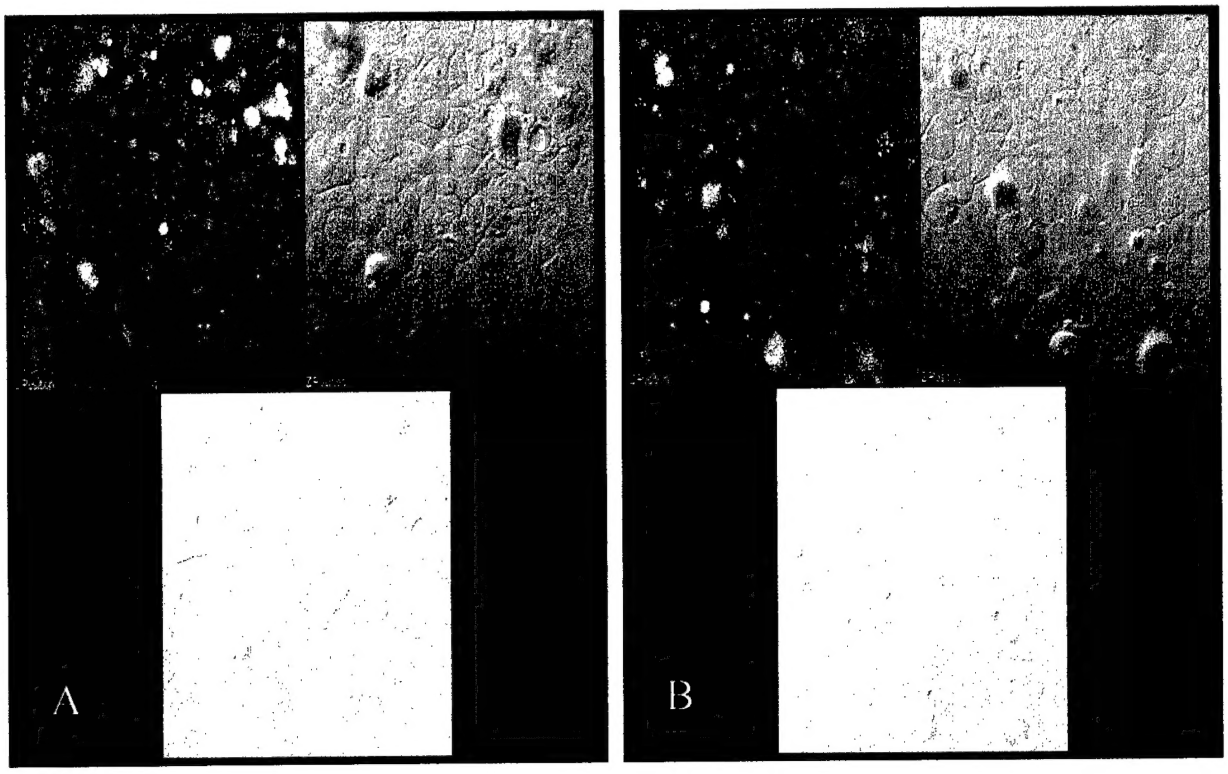


**Figure 2A-B. Homogenous culture of HME-EYFP cells.** 50K cells were plated on a 4-chamber slide (Lab-Tek II) and cultured for 5 days in SF170 medium. Cells were viewed with an Olympus IX-80 inverted confocal microscope under 60X. Cells were excited with a 488 nm argon laser or 543 green HeNe laser. EYFP maximum excitation is 513 nm and maximum emission is 527 nm.
EYFP= Enhanced Yellow Fluorescent Protein

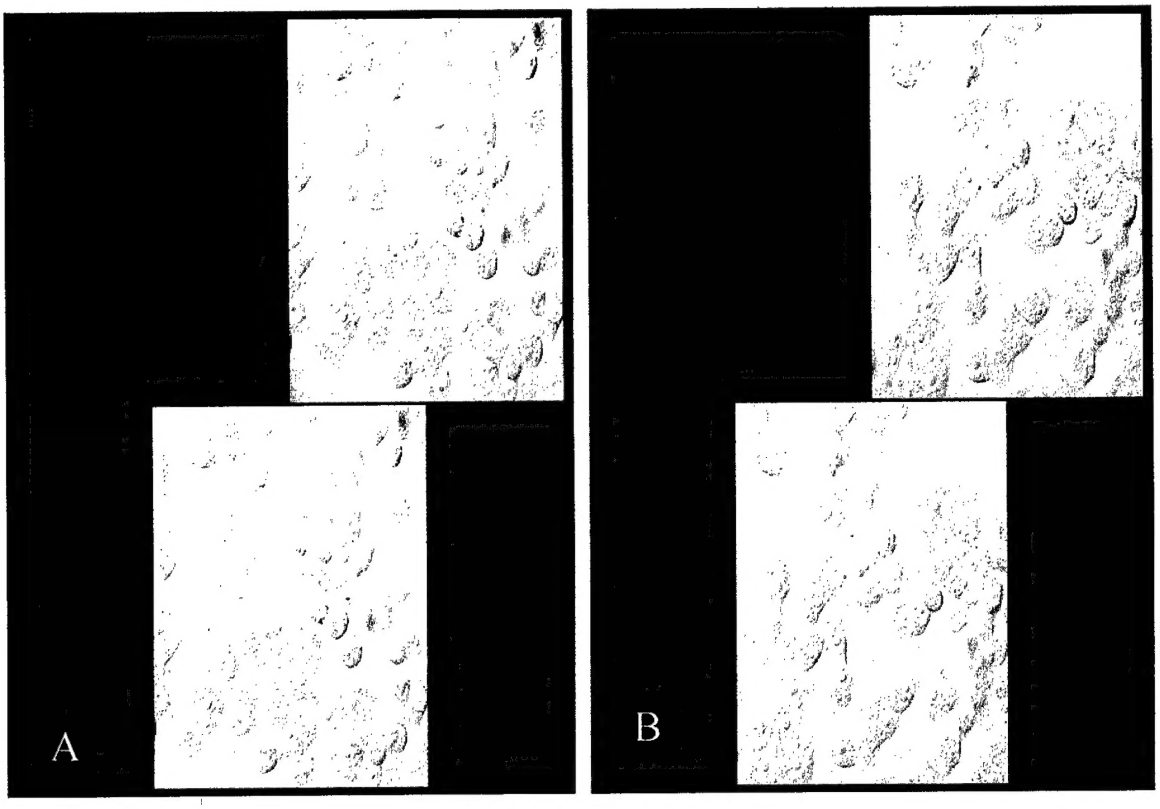


**Figure 3A-B. Homogenous culture of Tumor-DsRedFP cells.** 10K cells were plated on a 4-chamber slide (Lab-Tek II) and cultured for 5 days in DMEM-XSG medium. Cells were viewed with an Olympus IX-80 inverted confocal microscope under 60X. Cells were excited with a 543 nm green HeNe laser. DsRedFP maximum excitation is 558 nm and maximum emission is 583 nm.
DsRedFP=*Discisoma* sp Red Fluorescent Protein

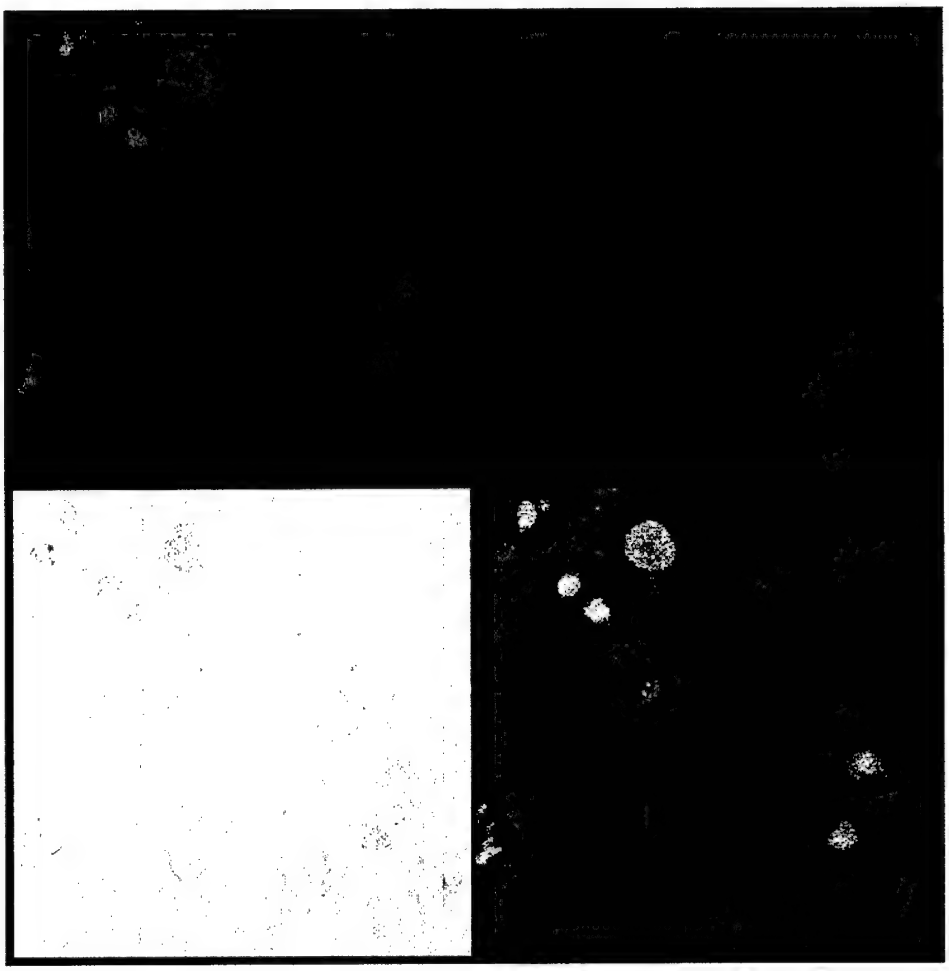

**Figure 4. Co-culture of HME-EYFP, HMS-GFP,and Tumor-DsRedFP cells.** 30K HMS-GFP and 10K Tumor-DsRedFP cells were plated on a 4-chamber slide (Lab-Tek II) and cultured for 5 days in FBM medium. Cells were viewed with an Olympus IX-80 inverted confocal microscope under 60X. (Upper Left) Cells were excited with a 488 nm argon laser. GFP maximum excitation is 488 nm and maximum emission is 507 nm. GFP= Green Fluorescent Protein. (Upper Right) Cells were excited with a 543 nm green HeNe laser. DsRedFP maximum excitation is 558 nm and maximum emission is 583 nm. DsRedFP=*Discisoma* sp Red Fluorescent Protein (Lower Left) Cell outlines visible through transmitted light in gray scale view. (Lower Right) Overlay view of upper left view and upper right view. Yellow indicates overlap of cells. Since the emission spectra are very different, the most likely explanation is that the cells are layered.

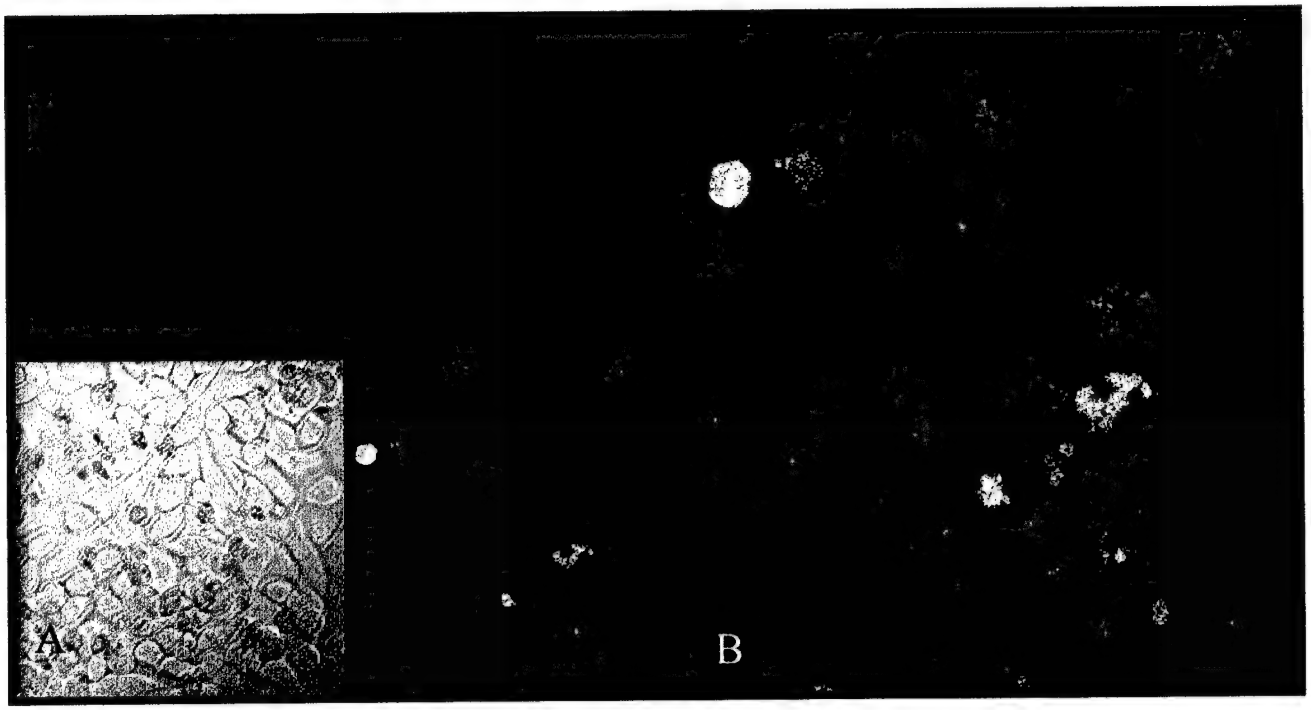


**Figure 5. Co-culture of HMS-GFPand TTU1-DsRedFP cells**. 50K HMS-GFP,and 3K TTU1-DsRedFP cells were plated on a 4-well chamber slide (Lab-Tek) and cultured for 5 days in FBM medium. Cells were viewed with an Olympus IX-80 inverted confocal microscope under 60X. (Upper Left) Cells were excited with a 488 nm argon laser. GFP maximum excitation is 488 nm and maximum emission is 507 nm. GFP= Green Fluorescent Protein (Upper Right) Cells were excited with a 543 nm green hene laser. DsRedFP maximum excitation is 558 nm and maximum emission is 583 nm. DsRedFP=Discisoma sp Red Fluorescent Protein (Lower Left) Cells in gray scale view. (Lower Right) Overlay view of upper left view and upper right view. **B** - Magnified Overlay view from**A.**

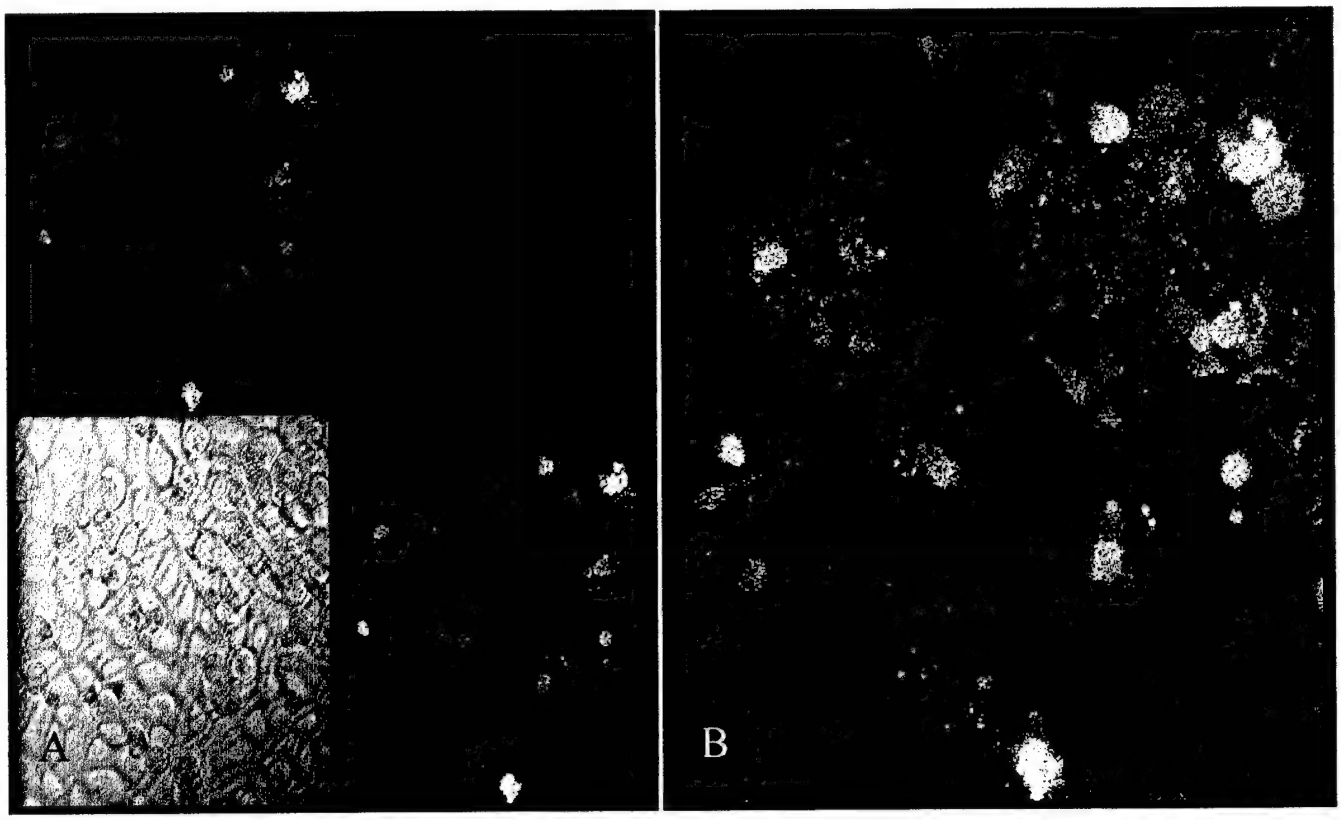


**Figure 5C. Co-culture of HME-EYFP and TTU1-DsRedFP cells**. 50K HME-EYFP and 3K TTU1-DsRedFP cells were plated on a 4-chamber slide (Lab-Tek II) and cultured for 5 days in FBM medium. Cells were viewed with an Olympus IX-80 inverted confocal microscope under 60X. (Upper Left) Cells were excited with a 488 nm argon laser or 543 green HeNe laser. EYFP maximum excitation is 513 nm and maximum emission is 527 nm. EYFP= Enhanced Yellow Fluorescent Protein (Upper Right) Cells were excited with a 543 nm green hene laser. DsRedFP maximum excitation is 558 nm and maximum emission is 583 nm. DsRedFP=Discisoma sp Red Fluorescent Protein (Lower Left) Cells in gray scale view. (Lower Right) Overlay view of upper left view and upper right view. **D-** Magnified Overlay view from figure 5C Lower Right

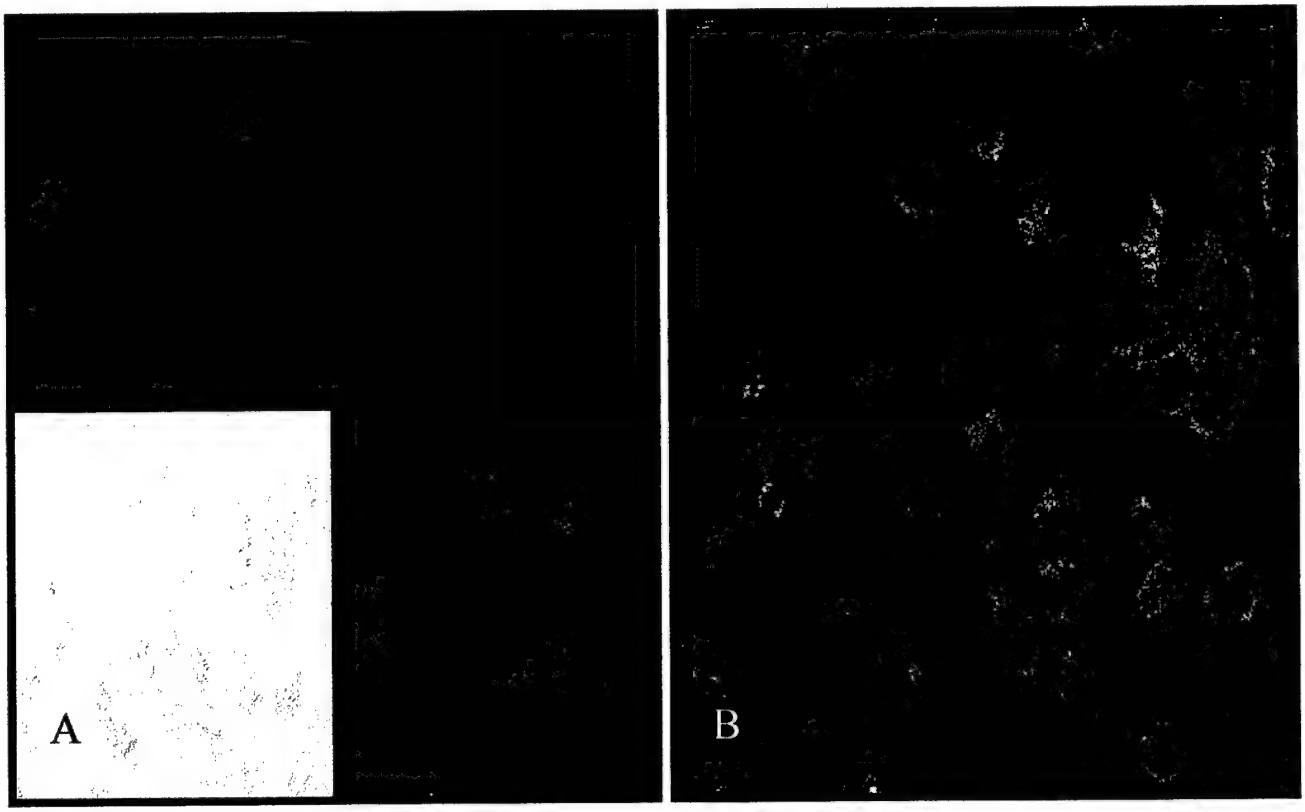


**Figure 6. Co-culture of HME-EYFP, HMS-GFP and TTU1-DsRedFP cells**. 50K HME-EYFP and 3K TTU1-DsRedFP cells were cultured for 5 days in a T75 in FBM medium and then 30Kof this co-culture was placed in a 4-chamber slide (Lab-Tek) and cultured for 5 days in FBM medium. Cells were viewed with an Olympus IX-80 inverted confocal microscope under 60X. (Upper Left) Cells were excited with a 488 nm argon laser or 543 green HeNe laser. EYFP maximum excitation is 513 nm and maximum emission is 527 nm. EYFP= Enhanced Yellow Fluorescent Protein (Upper Right) Cells were excited with a 543 nm green HNne laser. DsRedFP maximum excitation is 558 nm and maximum emission is 583 nm. DsRedFP=*Discisoma* sp Red Fluorescent Protein (Lower Left) Transmitted light of cells in gray scale view. (Lower Right) Overlay view of upper left view and upper right view. **B** - Enlarged Overlay view from figure 7A Lower Right.

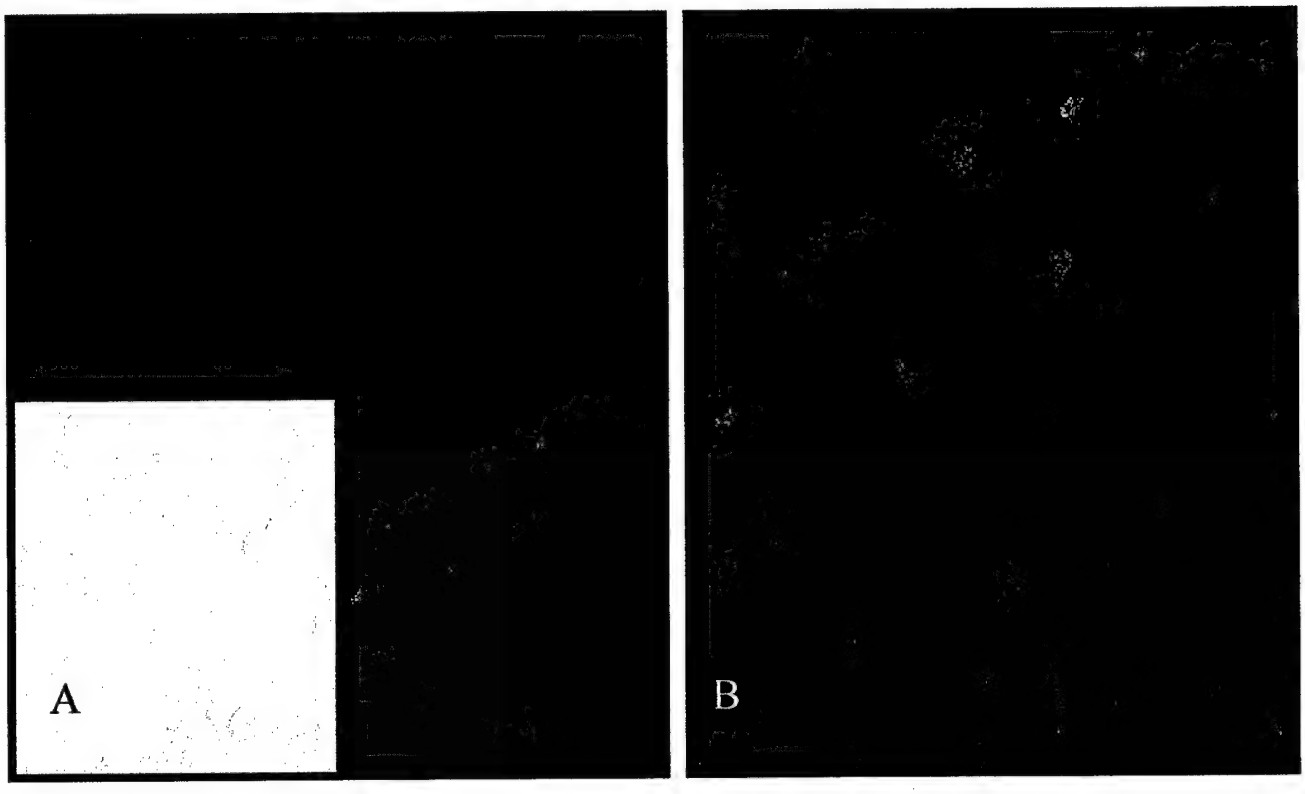


**Figure 6C. Co-culture of HMS-GFP,and TTU1-DsRedFP cells**. 50K HMS-GFP and 3K TTU1-DsRedFP cells were cultured for 5 days in a T75 in FBM medium and then 30Kof this co-culture was placed in a 4- chamber slide (Lab-Tek II) and cultured for 5 days in FBM medium. Cells were viewed with an Olympus IX-80 inverted confocal microscope under 60X. (Upper Left) Cells were excited with a 488 nm argon laser. GFP maximum excitation is 488 nm and maximum emission is 507 nm. GFP= Green Fluorescent Protein (Upper Right) Cells were excited with a 543 nm green HeNe laser. DsRedFP maximum excitation is 558 nm and maximum emission is 583 nm. DsRedFP=*Discisoma* sp Red Fluorescent Protein (Lower Right and Left) Overlay view of upper left view and upper right view. **D** - Enlarged Overlay view from C LowerLeft.

Task 1b. Determine the ratio of cell types in controlled and treated conditions using a fluorescent plate reader (Months 1-6).

The goal of these experiments was to determine the ratios of cell types in control and treated conditions using a fluorescent plate reader. Due to the difficulties encountered within the first six months of co-culturing, this task has not been directly addressed. However, we have indirectly addressed this task through the following method. Control and mixed populations of cells were plated onto 4-chamber slides to investigate growth patterns (Task 1a). These cells were digitally photographed through the confocal imaging software. Each slide consisted of 4 chambers. From each chamber, 4 random fields of vision were recorded. Cells from each of those areas were delineated by fluorescent protein emission and counted. Thus one 4-chamber slide yielded 16 counted fields of cells. These experiments were performed 4 times each. Figures 7-10 reflect the data for the cell counts.

These results reflect the interesting results reported in the growth pattern section. Namely that when the cells were placed at comparable densities, the tumor cells outgrew the normal cells and dominated the population. In addition, when the density was optimized for even cell growth among the cell types, the tumor cells initially grew quickly to that point, but did not continue to overgrow the population as previously observed. This phenomenon may be explained by the need for the normal cells to reach a specific density or establish themselves in culture (which occurs more slowly than the tumor cells due to slower cell cycle turnover) or establish HME-HMS interactions that signal the production and secretion of tumor inhibitory factors. We are currently addressing this issue by collecting media supernatant and screening it for the presence of known tumor inhibitor compounds such as TIMP, TGF β (Howard *et al.*, 1976; Lin *et al.*, 1995; Dong-Le Bourhis *et al.*, 1997).

We have now commenced the culturing in 24-well plates and 6-well plates for this series of experiments. Now that the initial tissue culture problems have been overcome, the other portions of the tasks are progressing rapidly. We expect to have most of the missed work from task 1b made up by September. In addition we expect that all the experiments described above will be completed with Taxol exposed cultures.

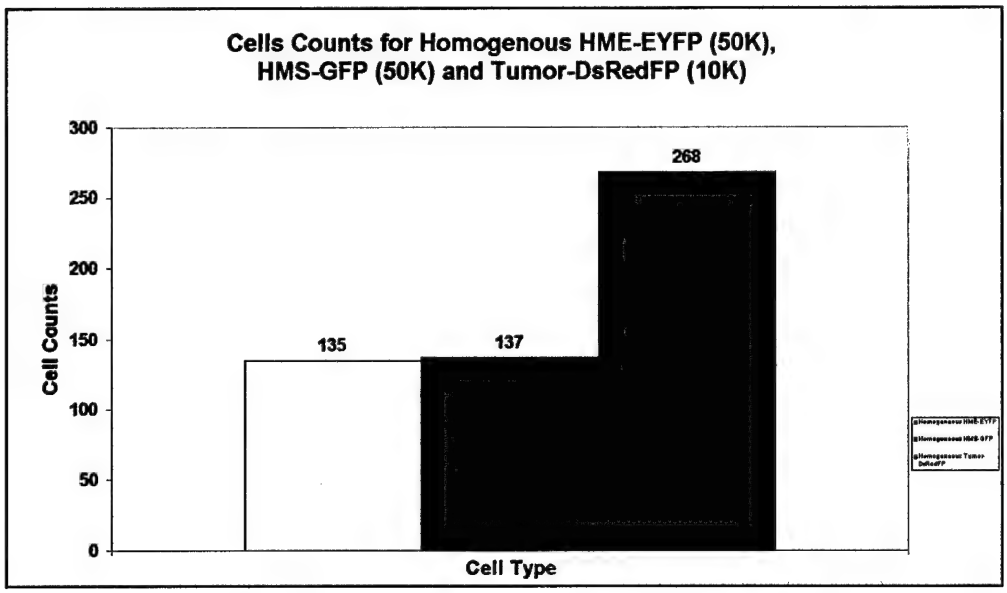


**Figure 7. Total Number of Cells Counted from Homogenous HME-EYFP (50K), HMS-GFP (50K), and Tumor-DsRedFP (10K) Populations.** Cells were plated on 4-chamber slides (Lab-Tek II) and cultured for 5 days in DMEM-XSG (HMS and Tumor) and SF-170 (HME) medium. Cells were viewed with an Olympus IX-80 inverted confocal microscope under 60X. Four random fields of view were counted per chamber per slide for each cell population.
EYFP= Enhanced Yellow Fluorescent Protein
GFP= Green Fluorescent Protein
DsRedFP=Discisoma sp Red Fluorescent Protein

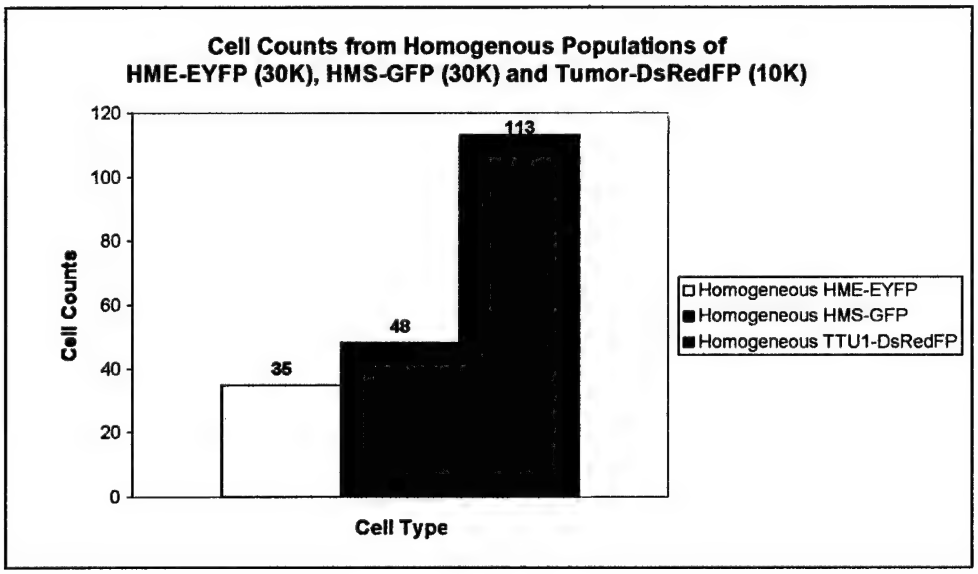


**Figure 8A. Cell Counts from Homogenous Populations of HME-EYFP (30K), HMS-GFP (30K) and Tumor-DsRedFP (10K).** Cells were plated on 4-chamber slides (Lab-Tek II) and cultured for 5 days in FBM media. Cells were viewed with an Olympus IX-80 inverted confocal microscope under 60X. Four random fields of view per chamber per slide were digitally photographed and cells counted.

EYFP= Enhanced Yellow Fluorescent Protein

GFP= Green Fluorescent Protein

DsRedFP=Discisoma sp Red Fluorescent Protein

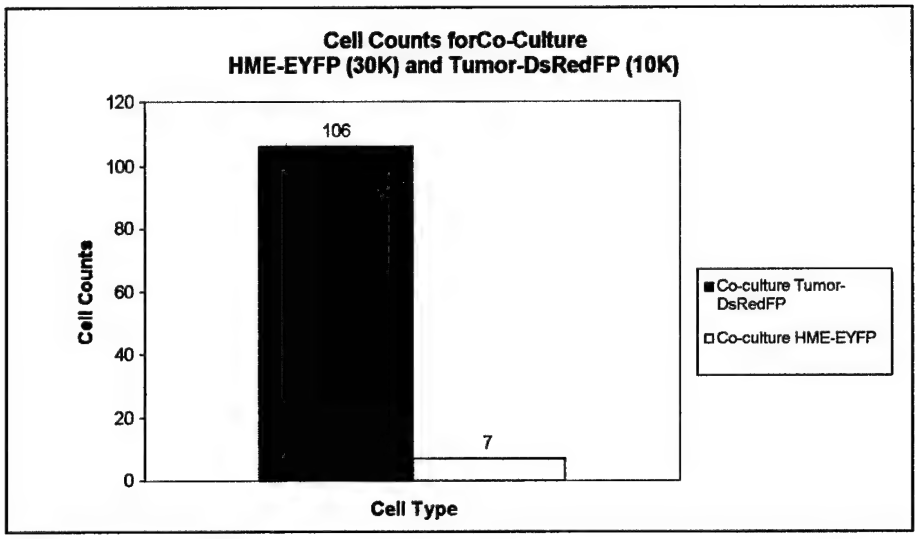


**Figure 8B. Cell Counts for Co-Culture HME-EYFP (30K) and Tumor-DsRedFP (10K).** Cells were plated on 4-chamber slides (Lab-Tek II) and cultured for 5 days in FBM media. Cells were viewed with an Olympus IX-80 inverted confocal microscope under 60X. Eight random fields of view were counted per chamber per slide for each cell type. EYFP= Enhanced Yellow Fluorescent Protein; *DsRedFP=Discisoma* sp Red Fluorescent Protein

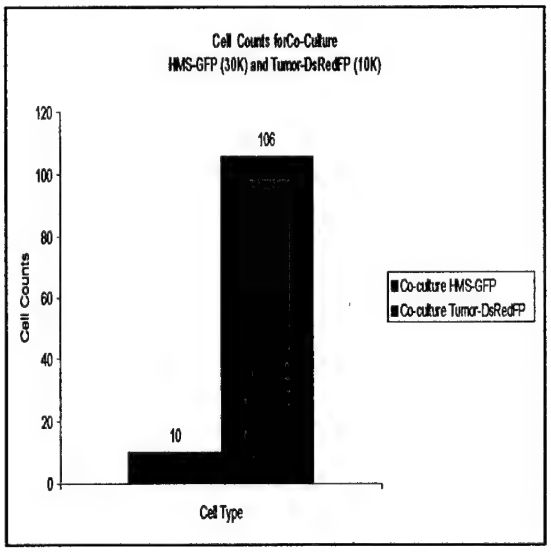


**Figure 8C. Cell Coumts from Co-Culture HMS-GFP (30K) and Tumor-DsRedFP (10K).** Cells were plated on 4-chamber slides (Lab-Tek II) and cultured for 5 days in FBM media Cells were viewed with an Olympus IX-80 inverted confocal microscope under 60X. Eight random fields of view were counted per chamber per slide for each cell type. GFP= Green Fluorescent ProteinDsRedFP=*Discisoma* sp Red Fluorescent Protein

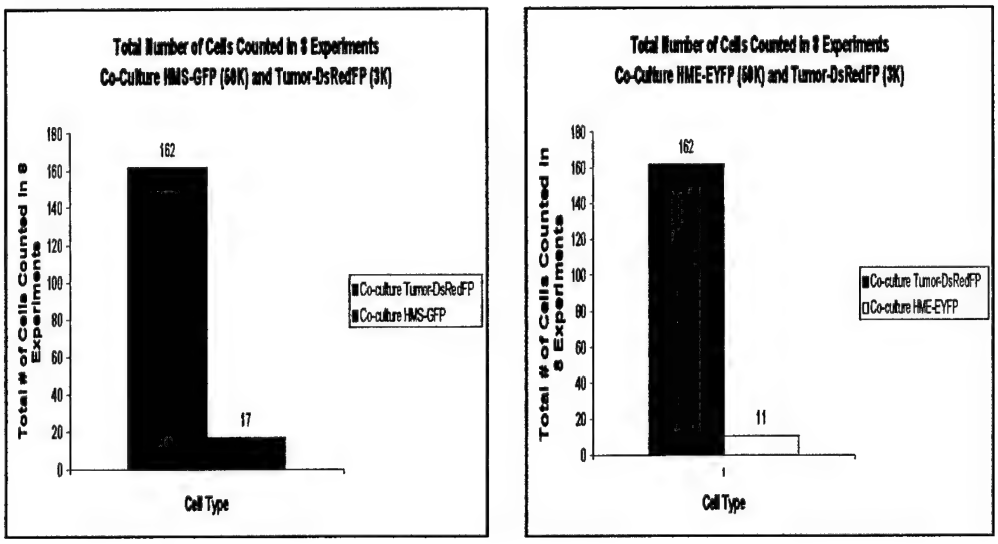


**Figure 9. Cell Counts from Co-Culture of HMS-GFP (30K) and Tumor-DsRedFP (10K) and HME-EYFP (30K) and Tumor-DsRedFP (10K).** Cells were plated on 4-chamber slides (Lab-Tek II) and cultured for 5 days in FBM media. Cells were viewed with an Olympus IX-80 inverted confocal microscope under 60X. Eight random fields of view were counted for each chamber on each clide. **A** - HMS-GFP (30K) and Tumor-DsRedFP (10K). **B** - HME-EYFP (30K) and Tumor-DsRedFP (10K). GFP= Green Fluorescent Protein, EYFP= Enhanced Yellow Fluorescent Protein, DsRedFP=Discisoma sp Red Fluorescent Protein.

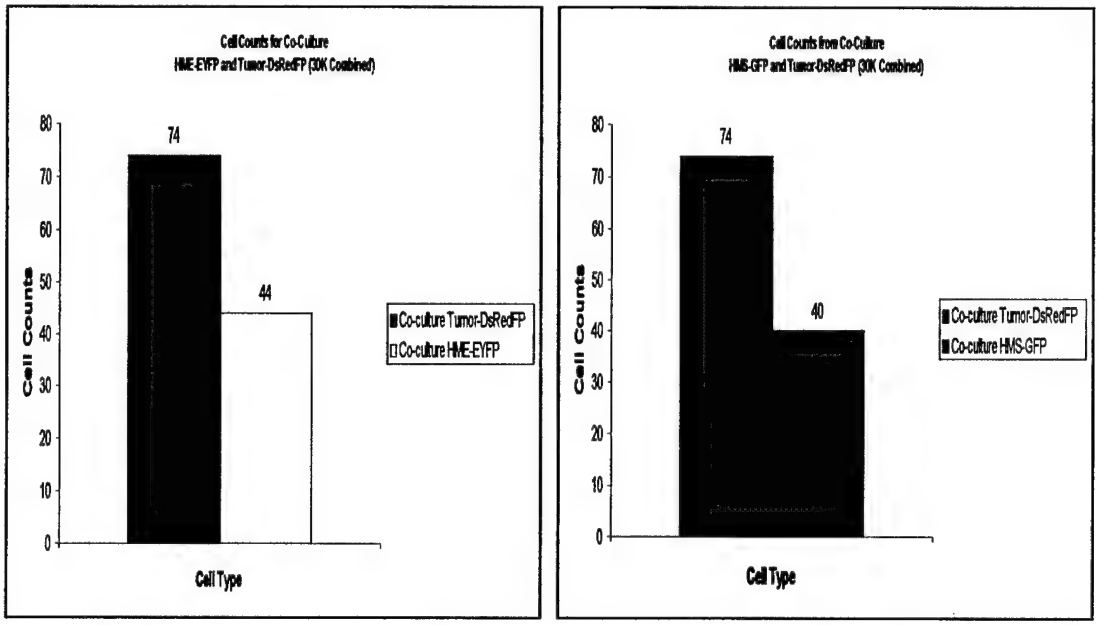


**Figure 10. Cell Counts from Co-Culture of HME-EYFP and Tumor-DsRedFP (30K Combined) and HMS-GFP and Tumor-DsRedFP (30K Combined).** 50K HME-EYFP, 50K HMS-GFP and 3K TTU1-DsRedFP cells were cultured for 5 days in a T75 in FBM medium and then 30Kof this co-culture was placed in 4- chamber slides (Lab-Tek II) and cultured for 5 days in FBM medium. Cells were viewed with an Olympus IX-80 inverted confocal microscope under 60X. Eight random fields of view for each chamber on each slide were digitally photographed and counted. EYFP= Enhanced Yellow Fluorescent Protein, GFP= Green Fluorescent Protein, DsRedFP=*Discisoma* sp Red Fluorescent Protein.

| Table 1. Summary of the cell counts per individual experiment | | | | | | | | | | |
|---|---|---|---|---|---|---|---|---|---|---|
| Experiment | Cell Type | Total | View 1 | View 2 | View 3 | View 4 | View 5 | View 6 | View 7 | View 8 |
| 1 | HME-EYFP | 135 | 43 | 41 | 20 | 31 | | | | |
| | HMS-GFP | 137 | 31 | 22 | 36 | 48 | | | | |
| | Tumor-DsRedFP | 268 | 61 | 85 | 56 | 66 | | | | |
| 2 | HME-EYFP | 35 | 7 | 8 | 14 | 6 | | | | |
| | HMS-GFP | 48 | 21 | 4 | 10 | 13 | | | | |
| | Tumor-DsRedFP | 113 | 29 | 25 | 32 | 27 | | | | |
| | Mix HME-EYFP | 7 | 3 | 1 | 0 | 0 | 1 | 2 | 0 | 0 |
| | Mix HMS-GFP | 10 | 7 | 0 | 0 | 2 | 1 | 0 | 0 | 0 |
| | MixTumor-DsRedFP | 106 | 9 | 10 | 13 | 9 | 17 | 21 | 14 | 13 |
| 3 | Mix HME-EYFP | 11 | 7 | 0 | 1 | 2 | 1 | 0 | 0 | 0 |
| | Mix HMS-GFP | 17 | 6 | 8 | 0 | 0 | 0 | 0 | 1 | 2 |
| | Mix Tumor-DsRedFP | 162 | 31 | 14 | 12 | 19 | 16 | 20 | 29 | 21 |
| 4 | Mix HME-EYFP | 44 | 6 | 7 | 1 | 3 | 8 | 5 | 4 | 10 |
| | Mix HMS-GFP | 40 | 5 | 4 | 6 | 5 | 3 | 6 | 4 | 7 |
| | Mix Tumor-DsRedFP | 74 | 8 | 16 | 7 | 9 | 6 | 5 | 11 | 12 |

*Task 1c. Determine the differential gene expression using FACsort analysis (Months 6-12).*

The goal of this series of experiments is to identify differential gene expression between cells from homogeneous parent populations and those in co-culture. Due to the length of time necessary to optimize cell co-culture conditions, this has not yet been addressed. However, we are scheduled to begin the FACsort runs in July. My graduate student is currently extracting RNA from the parent populations for (with and without hTERT) to establish baseline gene expression using GeneFilters from Research Genetics. She is also working through the procedure with small numbers of cells (<100,000) to insure her competence before handling the test cultures. We are also looking at alternate methods of lifting the cells from the plates that are not as damaging as Trypsin. This is in case Trypsin release demonstrates unforeseen results. One gene in which we are particularly interested given the work done to establish a valid transport procedure (Task 1d) is c-myc. It has been shown to be implicated in upregulation of GLUT-1 transport mechanism in tumor cells. (Osthus *et al.*, 2000). Thus it will be interesting to investigate the differences in gene expression of the tumor cells pre and post co-culture. The possibility exists that the normal cells may down-regulate c-myc through a dosage effect of p53. Alternatively, c-myc may exist in its growth suppression isoform c-myc –1 (Carter *et al.*, 1999) and as a result act as a dominant regulator of the c-myc 2 cell proliferation isoform. It will also be interesting to observe whether there is an upregulation of Mad, which would cause the dissociation of myc-max and slow cell proliferation. Finally, given the involvement of c-myc in the GLUT-1 transport mechanism, it will be interesting to observe whether there is a difference in the isoforms between the normal HME and HMS cells. If so, this would add to the growing data to explain the propensity of epithelial cells to progress to cancer in contrast to the fibroblast cells.

*Task 1d. Determine the differences between HME and HMS cells in the uptake and efflux transport characteristics for Taxol (Months 6-12).*

The goal of these experiments was to study the contribution of drug accumulation to Taxol resistance. The ability of tumor cells to efflux cytotoxic drugs like Taxol is a major cause of multidrug resistance in chemotherapy (Ambudkar et al., 1999; Krishna and Mayer, 2000). Typically, multidrug resistance results from the expression of ATP-dependent drug efflux transporters ("pumps") in the plasma membrane (Dean et al., 2001; Sauna et al., 2001). For example, meta-analysis of some 31 reports (from 1989-1996) found that 41% of breast tumors expressed one such pump, known as multidrug resistance protein 1 (MDR1) (Gottesman et al., 2002). MDR1 and several other transporters are capable of extruding Taxol (and a broad array of other antitumor drugs) from the cell, reducing its ability to kill the cancer cell (Parekh and Simpkins, 1997; Klein et al., 1999; Sharom, et al., 1999.

To measure Taxol accumulation in normal human mammary cells, we first carefully validated several critical transport and cell culture characteristics. These included 1) cell culture substrate, 2) shaking speed during the transport assay, 3) initial seeding density, 4) duration of cell growth prior to transport measurements, and 5) influence of growth factors on transport. These validation studies were extensive and time-consuming, but absolutely necessary. All

subsequent transport measurements will employ an optimal combination of experimental conditions based on these findings.

For the validation studies, we chose normal human mammary epithelial cells (HME 50) over equivalent strains because our stock of these cells was the most plentiful. Given that extensive experiments require large numbers of cells and our normal mammary cell lines can undergo only a limited number of population doublings, this choice was advantageous. In addition, because of numerous validation experiments, we chose to study glucose transport as a surrogate solute for Taxol uptake, for several reasons. First, the validation experiments were aimed at selecting cell culture conditions that optimized speed of cell growth, tolerance to the high shaking speeds used in the transport experiments, and expression of membrane transporters. Glucose uptake is a faithful reporter of cell viability, membrane integrity, and transporter differentiation, particularly when the transport assay measures influx mediated by glucose transporters (i.e., GLUT1), as our technique does (Karasov and Diamond, 1983). Second, breast tumor cells show increased expression of GLUT1 compared to normal cells (Brown et al., 1996), so that changes in glucose uptake may parallel the upregulation of other transporters (e.g., MDR1). Finally, the cost of radiolabeled glucose is only one-fifth that of labeled Taxol. Hence, it was prudent to reserve the more costly Taxol transport experiments for post-validation experiments.

To validate our transport assay for later measurements of Taxol uptake, it was essential to establish cell growth conditions that would enable the cells to withstand significant shaking speeds encountered in the transport assay. Why not simply eliminate shaking during the assay, preventing any chance of cells becoming detached or damaged? The absence of shaking produces unstirred layer effects, causing the solute concentrations in the bulk solution to differ significantly from that adjacent to the plasma membrane, owing to diffusional resistance. This results in a serious underestimation of solute uptake by several fold. For hydrophobic solutes like Taxol, the effect of unstirred layers is disproportionately large (i.e., unstirred-layer resistance becomes rate-limiting for highly permeant solutes). Unfortunately, previous studies of Taxol transport have typically failed to measure transport under conditions where unstirred layer effects were minimized (see Parekh et al., 1997; Walle and Walle, 1998; Letrent et al., 1999; Crowe, 2002). We aimed to avoid this error by analyzing the effects of stirring rates on solute uptake.

HME 50 cells were seeded at 50,000 cells/well in 24-well plates, grown to a confluent monolayer for 5 days directly on plastic substrate, with a low epidermal growth factor (EGF) concentration (10 ng/ml) in the medium. For the transport assay, the culture medium was replaced with transport buffer (37 °C) containing 50 mM D-glucose in the apical (milk) compartment, together with trace amounts of $^{14}$C-D-glucose as probe and $^{3}$H-L-glucose as marker. The cells were incubated for 15-min, then rinsed to reduce adherent fluid before lysis in NaOH. An aliquot of the lysate was reserved for protein determination and the remainder counted in a liquid scintillation spectrometer. Under these conditions, the resulting transport calculations represents initial rate influx through membrane glucose transporters (e.g., GLUT 1), having been corrected for both extracellular adherent fluid and simple diffusion of glucose.

Figure 1 shows the results for measuring glucose uptake at different shaking speeds. As shaking speed increases up to 900 rpm, there is a linear increase in nutrient uptake, as unstirred

layer effects are proportionately reduced. However, at the maximum speed tested (1200 rpm), membrane integrity or cell viability is dramatically reduced, as evidenced by the 80 % fall in glucose uptake.

Next, we examined how glucose uptake changed under different seeding densities, duration of cell culture post-seeding, and with shaking during cell growth. The last of these variables– shaking during cell growth– was included because in multi-well plates, some cells on a single plate may be assayed on different days and thus, subjected to shaking before the actual transport assay. We wish to know how this might affect transport, and the results are shown in Figure 2. With one exception (cells seeded at the lower density and shaken during culture), glucose uptake generally increases with time in culture after seeding. Higher seeding densities (which uses up more cells) produced greater uptake rates only in cells shaken during culture and only at the longest duration in culture (14 days). Accordingly, there was no significant advantage to using the higher seeding density. Although all cells were shaken during the transport assay, those that were subjected to a shaking episode during growth in culture clearly exhibited a glucose uptake pattern that was different and not desirable compared to those not shaken. Hence, growing cells for 7 - 10 days at the lower seeding density ($5 \times 10^4$) and not shaking them during culture appears the best compromise among the multiple conditions tested.

Optimal growth rates that rapidly produce differentiated cells with high transporter expression was another aim of these experiments. We tested the effects of adding at higher concentration EGF to achieve that result. For HME 50 cells grown on plastic wells for 7 days post-seeding, the higher EGF concentration gave unexpected results, as shown in Figure 3. Although the cells reached confluence faster, glucose uptake rates were depressed and essentially independent of stirring speeds, except at the highest speed tested (600 rpm). A possible explanation is that cells grown on plastic divide rapidly at the higher EGF concentration, but fail to differentiate and to express GLUT1 transporters at high levels. Alternatively, at higher cell division rates, a different substrate may be required to support adequate cell adhesion and transporter differentiation.

We tested how coating the wells with two different extracellular matrix proteins (ECMs) might influence transporter expression. Both fibronectin and laminin are ECMs found underlying mammary epithelial cell in normal breast tissue. When cells exposed to the higher EGF concentration were grown on fibronectin-coated wells, glucose uptake was significantly enhanced at all stirring speeds, compared to those grown on plastic at the same EGF concentration (Fig. 4). In contrast, growing cells on fibronectin, but adding a lower EGF concentration, resulted in depressed glucose uptake rates. Moreover, the transport rates no longer increased as a function of shaking speed. Thus, growing cells on fibronectin at high EGF concentrations produced the best combination of rapid cell growth and transporter expression.

We also examined whether growing cells on laminin might enhance glucose uptake rates. At the lower EGF concentration, cells grown on laminin did exhibit higher glucose uptake rates than those grown on fibronectin (Fig. 6). Nevertheless, when shaking speeds were raised moderately above 200 rpm, glucose uptake dropped precipitously. This indicates that the cells, although well differentiated, were adhering less tightly to their underlying substrate. We have not yet examined the remaining condition of growing cells on laminin at the higher EGF

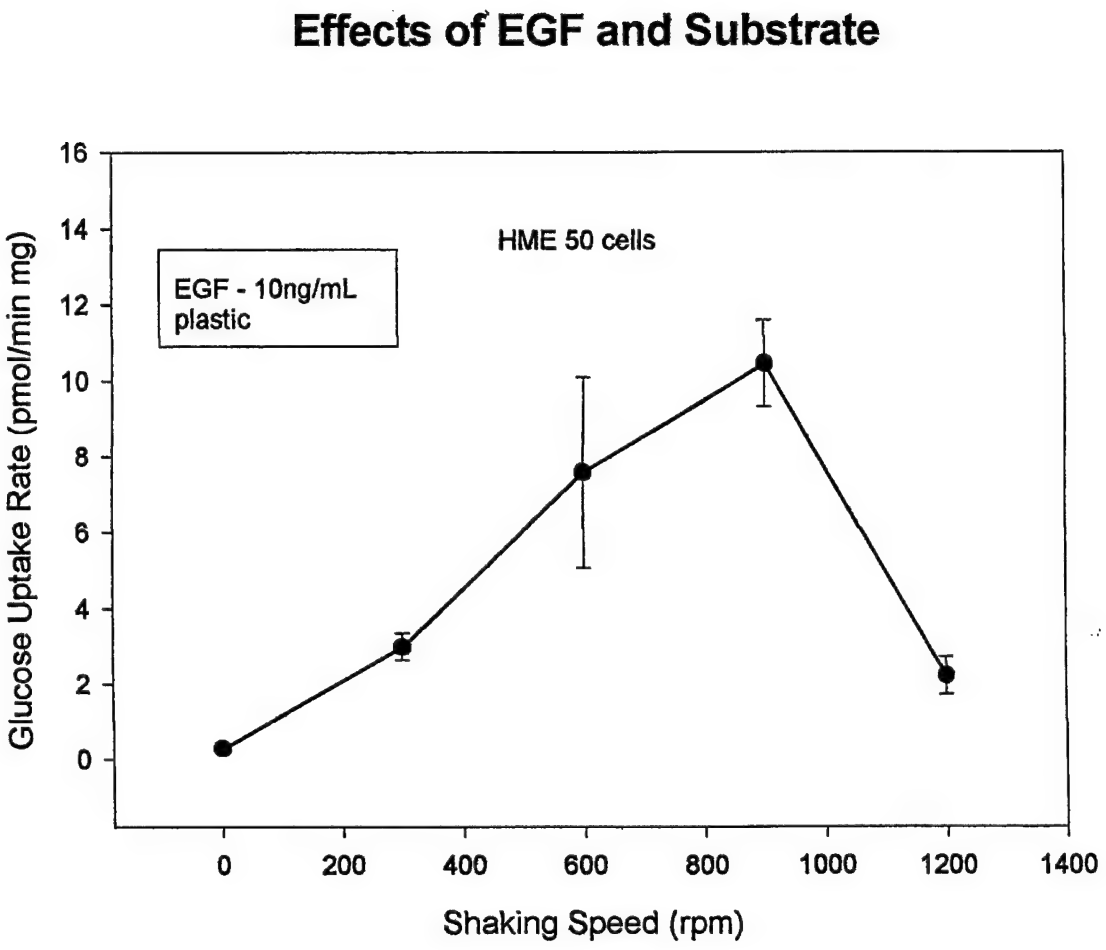


Fig. 1. Glucose uptake as an indicator of cell viability, membrane integrity, and epithelial differentiation in human mammary epithelial cells (HME 50). At low epidermal growth factor (EGF) concentrations (10 ng/ml), cells grown to confluence directly on a plastic substrate for 5 days show a linear increase in nutrient uptake as shaking speed increases. At the maximum speed tested (1200 rpm), membrane integrity or cell viability is dramatically reduced as evidenced by the 80 % fall in glucose uptake. Here and in subsequent graphs, cells were incubated for 15 min with 50 mM D-glucose in the apical (milk) compartment, together with trace amounts of $^{14}$C-D-glucose as probe and $^{3}$H-L-glucose as marker. Transport represents initial rate influx through membrane glucose transporters (e.g., GLUT 1), having been corrected for both extracellular adherent fluid and simple diffusion of glucose. Wells were seeded with $10^5$ cells. Values are mean ± S.E.M of four wells for each shaking speed.

## Effects of Seeding Density and Shaking During Growth

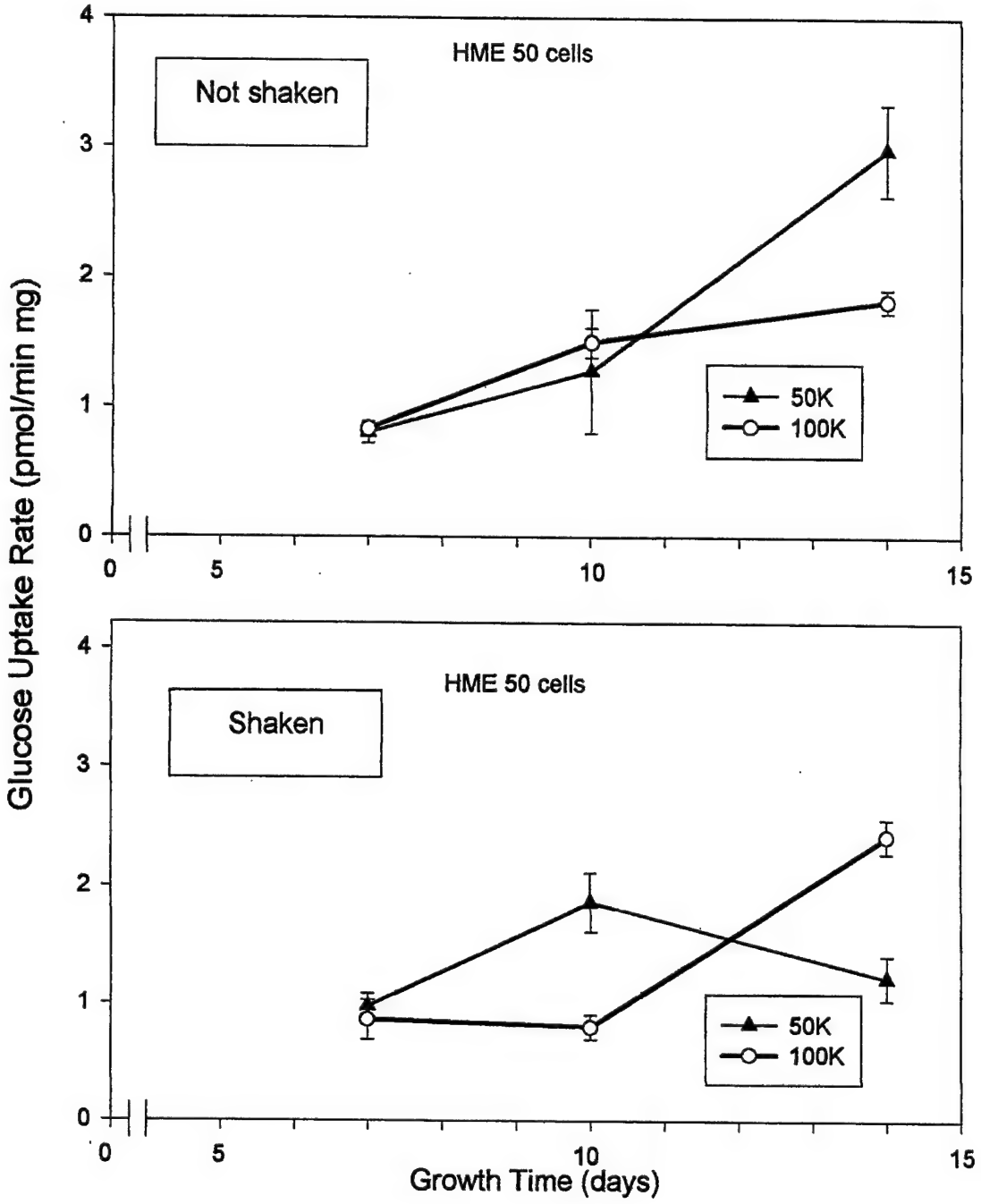


Fig. 2. Effects on glucose uptake of seeding density (50K vs. 100K), duration of cell culture after seeding, and shaking during cell growth. Overall, glucose uptake increases with time in culture after seeding, with one exception (cells seeded at the lower density and shaken during culture). Seeding cells at higher densities produced greater uptake rates only in cells shaken during culture and only after 14 days post-seeding. Cells that were shaken during growth (as opposed to during the uptake measurement) showed a pattern of glucose uptake with time in culture that was clearly different, though not superior to those not shaken. Thus, growing cells for 7 - 10 days at the lower seeding density ($5 \times 10^4$) and not shaking them during culture appears the best compromise among the multiple conditions tested. Other conditions were identical to those listed in Fig. 1 legend.

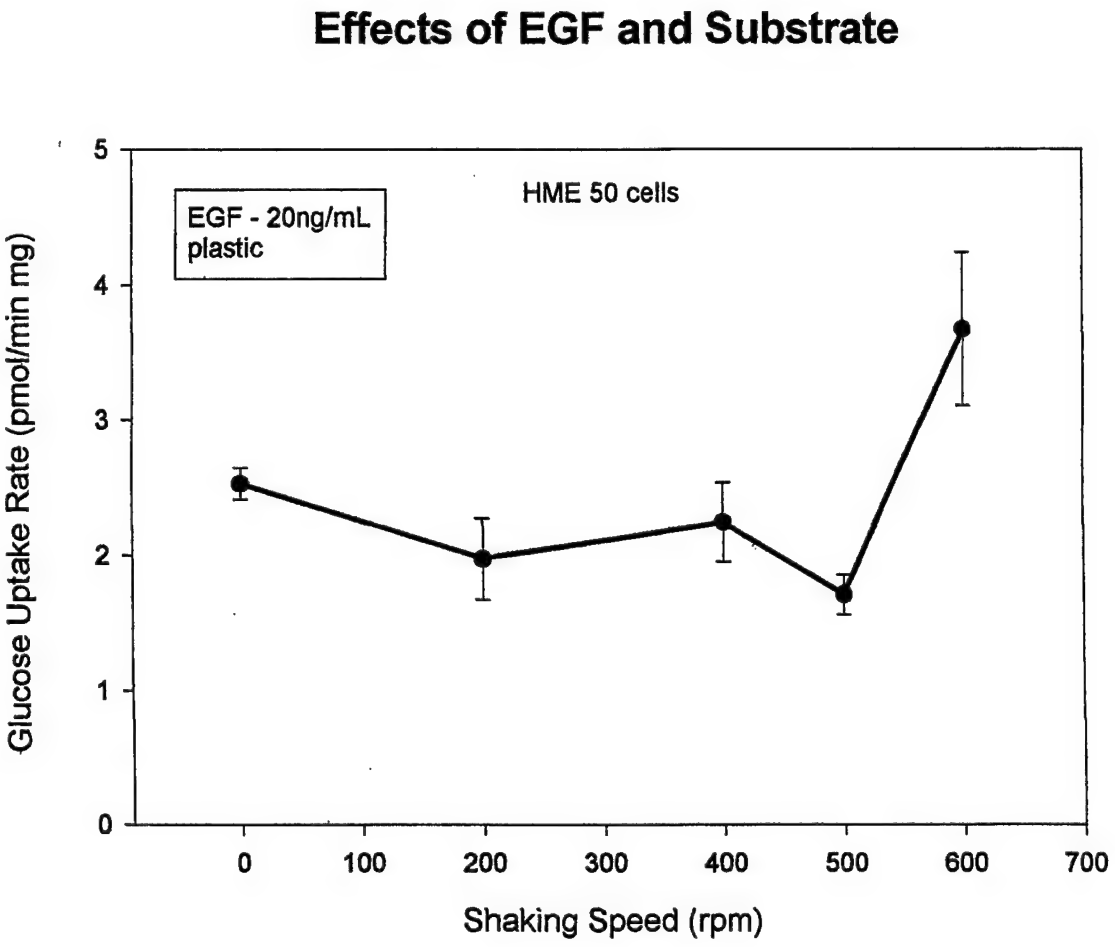


Fig. 3. Glucose uptake as a function of shaking speed in cells grown at a high EGF concentrations to accelerate growth. Although the mammary cells became confluent faster, glucose uptake rates were depressed and increased slightly only at high shaking speeds (600 rpm). Other conditions were identical to those listed in Fig. 1 legend.

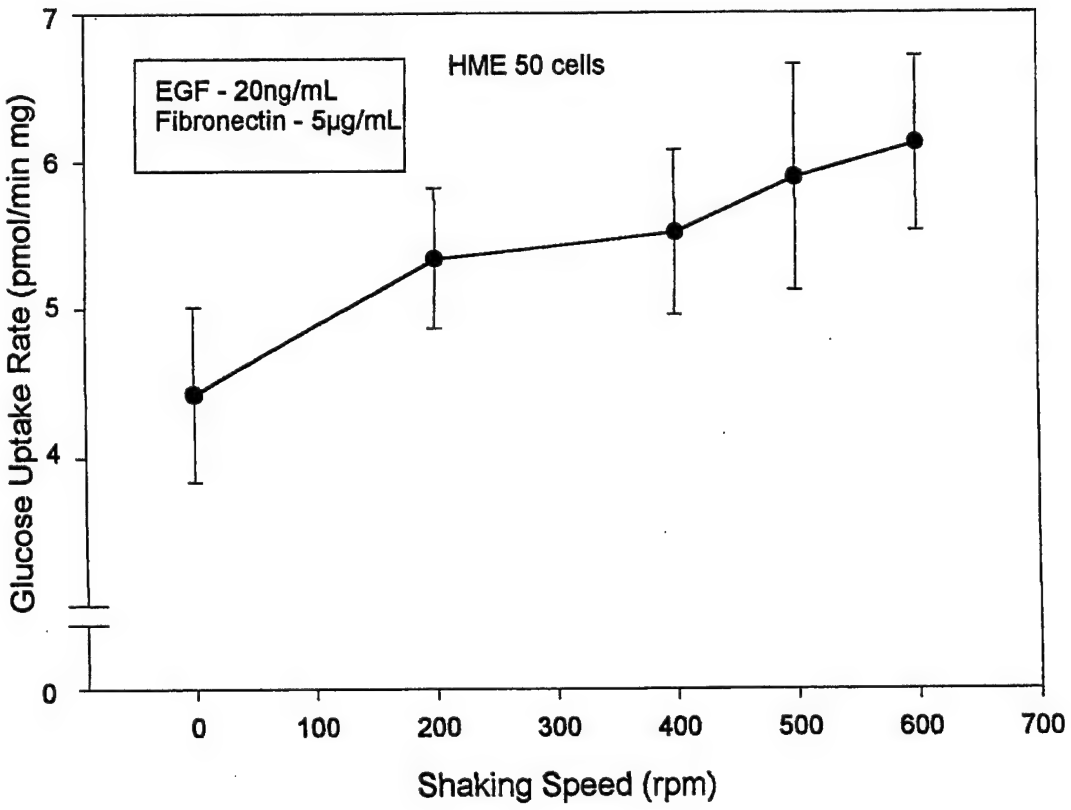


Fig. 4. Effects on glucose uptake of growing cells on a substrate coated with the extracellular matrix protein fibronectin. In contrast to mammary cells grown on plastic, those grown on fibronectin at high EGF concentrations show a linear increase in glucose uptake as shaking speed was raised to 600 rpm. See Figure 1 legend for other conditions.

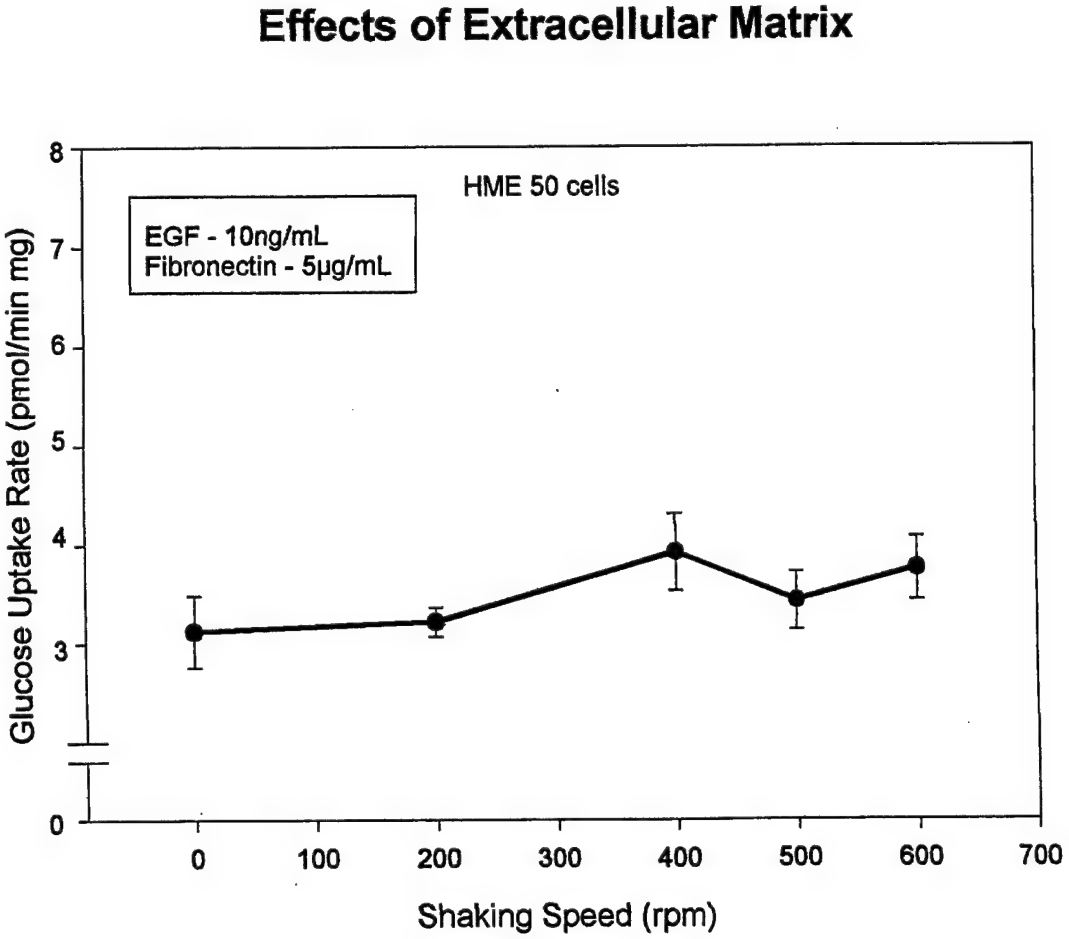


Fig. 5. Glucose uptake at low EGF concentrations grown on fibronectin. Unlike cells grown at high EGF, those grown at low EGF exhibit low glucose uptake despite the presence of fibronectin as the substrate. In addition, there is almost no dependence of transport on shaking speed. Thus, a combination of high EGF concentration and growing cells on fibronectin coated wells optimized growth rates and maintained good transporter expression and membrane integrity as shown by the glucose uptake rates.

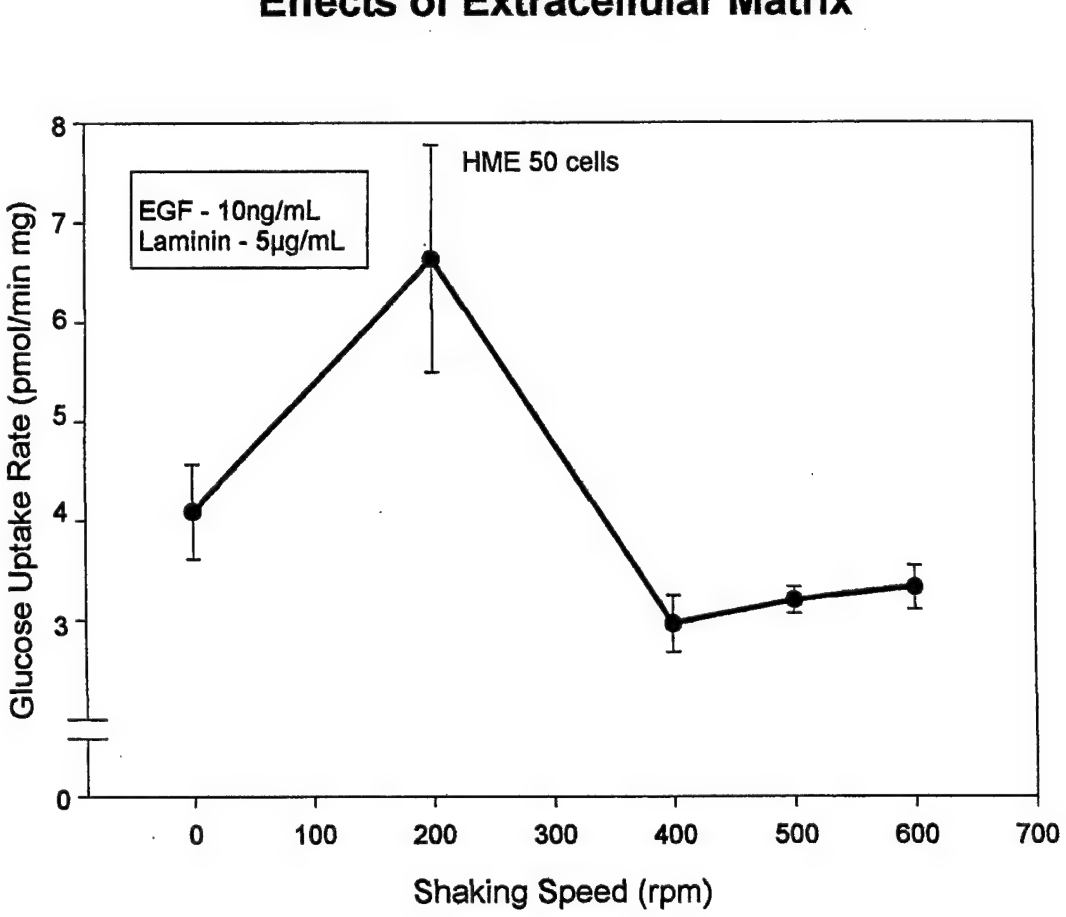


Fig. 6. Changes in glucose uptake as a function of shaking speed in cells grown on the extracellular matrix protein laminin. At low EGF concentrations, cells grown on laminin exhibit higher uptake rates compared to those grown on fibronectin. However, the cells appear more sensitive to increased shaking speeds, because glucose uptake falls rapidly at shaking speeds above 200 rpm.

concentration. When that test is completed, we will know whether growing cells at higher EGF concentrations elicits optimal glucose uptake when the underlying substrate is laminin or fibronectin.

With completion of these validation experiments, we will begin measuring Taxol uptake and efflux in human mammary epithelial cells. Parallel validation experiments for normal human mammary stromal (HMS) cells will also proceed rapidly, based on the findings from the above described experiments. Although we did not achieve our goal of completing Taxol transport assays in both HME and HMS cells in this reporting period, we believe our work will progress more rapidly in the coming year. We now have a full year of experience in growing cells under optimal conditions and in performing the transport assays efficiently. Our progress last year was less rapid than anticipated in part because the doctoral student expected to participate in the study was unable to do so. Fortunately, another Ph.D. student (Shailaja Srinagesh) has been recruited and will be trained this summer. In addition, a Howard Hughes Medical Institute undergraduate research fellow (David Keelen), with a year of experience working on the transport experiments, will continue working on this project.

**Key Research Accomplishments:**

- Optimized cell co-culture conditions for plate reader analysis and Facsorting
- Establishment of normal HME and HMS cell lines with unlimited replicative capability.
- Optimized conditions for confocal microscopy.
- Optimized cell culture conditions and transport assay procedures to permit accurate measurements of Taxol transport in human mammary epithelial cells.

**Reportable Outcomes**

None at this time.

**Conclusions**

Within the course of culturing the cells and combining them for co-culture purposes, we ran into a problem that caused us to adjust the co-culture methods. Serendipitously, this also made possible one of the most important observations concerning the growth patterns of these cells. Initial control growth curves showed the tumor cells to go through population doublings 2.5 times quicker than HMS and HME cells. During the first set of co-culture experiments, the cells were all plated from homogeneous parent populations at the same density. We observed that in culturing the cells following this method, the tumor cells quickly took over the population and the normal cells did not grow well. The phenotype of the normal cells was that of stressed cells with vacuolation, blebbing and very low cell counts. This phenotype is demonstrated in figures 1-5. Additionally, this stress may have affected the expression of the fluorescent proteins such that it was compartmentalized to a greater extent as a survival mechanism.

We address this problem by decreasing the number of tumor cells plated through a series of cell culture experiments. HME and HMS cells were kept at a constant density with the density of the tumor cells being varied. **We found that the optimal cell numbers to plate for each cell**

**type was HME and HMS at 50,000 cells; Tumor cells at 3000 cells.** In retrospect this is an important observation if the etiology of cancer development and progression is considered. Breast tumors have been shown to be primarily monoclonal in nature (Noguchi *et al.*, 1992; Feist *et al.*, 1997; Going *et al.*, 2001). They develop slowly. Thus the ratio of tumor cells to normal cells is extremely low. One of the reasons for this slow development has been speculated to be negative growth inhibiting paracrine factors secreted by adjacent cells. Such findings have been demonstrated in (Miller *et al.*, 1989; Adam *et al.*, 1994; Rossi *et al.*, 1994; Dong-Le Bourhis *et al.*, 1997; Wilson *et al.*, 1999; Rossi *et al.*, 2000). As the tumor cells become autonomous or are able to overcome these inhibitory growth signals, protease activity, constitutive cell division and a variety of upregulated transport mechanisms allow them to invade the surrounding tissue. Therefore, by plating the same number of all the cell types, we inadvertently gave the tumor cells a selective advantage over the normal cells. This also was less reflective of tumor etiology *in situ*, (i.e. a DNA mutation that is inherited and stable within the genome gives rise to cells carrying that same mutation that progress to a transformed phenotype – cancer.

Another important observation that came out of the cell culture experiments for cell growth patterns concerned the manner in which the cells were maintained prior to being plated on the glass chamber slides or the well plates for the ratio determinations. Initially, all the cells were maintained in homogeneous cell populations from which they were harvested and combined in chamber slides to investigate growth patterns. During a successive series of experiments, the tumor cells were observed to dominate the population as previously stated. While optimizing cell plating numbers, 50k of HME cells, 50k of HMS cells and 3 K of the tumor cells were mixed in a 15 cc tube and plated onto a T75. Several interesting observations were made from this mixed population. First, in comparison to the parent cells plated at a similar density, the HME and HMS cell types grew more quickly. In addition, all the cell types were observed to form small colonies while at low cell density within the flask. This could not be misconstrued as a result of adding the cell types at different times since they were resuspended in the medium prior to being placed into the T 75. As the cell populations increased, the colonies merged. There were no noticeable cell boundaries as is associated with the establishment of primary cell cultures (Shay *et al.*, 1995; Gollahon and Shay, 1996b; Gazdar *et al.*, 1998). These experiments are in the process of being repeated. Another concurrent observation was made regarding the tumor cells. They grew more slowly. Intrigued by these results, we utilized this culture as a source for the chamber slides. When these cells became 75-80% confluent, they were subcultured to a 4-chamber slide. These observations were confirmed by confocal microscopy. Cell counts and digital images under fluorescent conditions revealed that the overall cell numbers were much more evenly distributed suggesting that the tumor cells grew more slowly and therefore did not dominate the cell population. This series of experiments with the cell lines took approximately six months. Due to the nature of the cell growth and observations, the Taxol co-culture experiments were not started until April. We expect to move very quickly through this series of experiments and makeup lost time from Task 1a. One of the reasons is that there is an undergraduate research assistant who is working in the lab that has been assigned this portion of the project. Minesh Patel is a Howard Hughes Medical Institute Undergraduate Science Research Fellow who has worked in my lab for the past year. He has worked with Taxol on a parallel project and has now started these experiments. In addition, we will be utilizing the Deconvolution microscope to document growth patterns for the cells in homogeneous populations and mixed populations over the surface of a T75. This will confirm our observations of the cell patterns and cell distribution from initial

plating through to confluence. The Deconvolution microscope should also allow us to observe co-cultures of HME-HMS cells using HME cells with CFP.

**References**


Adam, L., Crepin, M., Lelong, J.C., Spanakis, E., and Israel, L. (1994). Selective interactions between mammary epithelial cells and fibroblasts in co-culture. Int J Cancer *59*, 262-268.

Ambudkar, S. V., Dey, S., Hrycyna, C. A., Ramachandra, M., Pastan, I., Gottesman, M. M. Biochemical cellular and pharmacological aspects of the multidrug transporter, Annu Rev Pharmacol Toxicol. 39: 361-98, 1999.

Brown, R. S., Leung, J. Y., Fisher, S. J., Frey, F. A., Ethier, S. P., Wahl, R. L. Intratumoral distribution of tritiated FDG in breast carcinoma: correlation between Glut1 expression and FDG uptake, J Nucl Med. 37: 1042-47, 1996.

Carter, P.S., Jarquin-Pardo, M., and De Benedetti, A. (1999). Differential expression of Myc1 and Myc2 isoforms in cells transformed by eIF4E: evidence for internal ribosome repositioning in the human c-myc 5'UTR. Oncogene *18*, 4326-4335.

Counter, C., Meyerson, M., Eaton, E., Ellisen, L., Caddle, S., Haber, D., and al., e. (1998). Telomerase activity is restored in human cells by ectopic expression of hTERT (hEST2), the catalytic subunit of telomerase. Oncogene *16*, 1217-1222.

Crowe, A. The influence of p-glycoprotein on morphine transport in caco-2 cells, comparison with paclitaxel, Eur J Pharm. 440: 7-16, 2002.

Dean, M., Rzhetsky, A., Allikmets, R. The human ABC transporter superfamily, Gen Res. 11: 1156-66, 2001.

Dong-Le Bourhis, X., Berthois, Y., Millot, G., Degeorges, A., Sylvi, M., Martin, P.M., and Calvo, F. (1997). Effect of stromal and epithelial cells derived from normal and tumorous breast tissue on the proliferation of human breast cancer cell lines in co-culture. Int J Cancer *71*, 42-48.

Feist, H., Lilischkis, R., Hallas, C., Aanesen, J.J., Gassel, A., Gallert, K.C., and Kreipe, H. (1997). [Clonal analysis in cells using PCR and laser microdissection]. Verh Dtsch Ges Pathol *81*, 339-342.

Gazdar, A.F., Kurvari, V., Virmani, A., Gollahon, L., Sakaguchi, M., Westerfield, M., Kodagoda, D., Stasny, V., Cunningham, H.T., Wistuba, II, Tomlinson, G., Tonk, V., Ashfaq, R., Leitch, A.M., Minna, J.D., and Shay, J.W. (1998). Characterization of paired tumor and non-tumor cell lines established from patients with breast cancer. Int J Cancer *78*, 766-774.

Gollahon, L.S., Kraus, E., Wu, T.A., Yim, S.O., Strong, L.C., Shay, J.W., and Tainsky, M.A. (1998). Telomerase activity during spontaneous immortalization of Li-Fraumeni syndrome skin fibroblasts. Oncogene *17*, 709-717.

Gollahon, L.S., and Shay, J.W. (1996a). Immortalization of human mammary epithelial cells transfected with mutant p53 (273his). Oncogene *12*, 715-725.

Gollahon, L.S., and Shay, J.W. (1996b). Immortalization of human mammary epithelial cells transfected with mutant p53 (273his). Oncogene *12*, 715-725.

Going, J.J., Abd El-Monem, H.M., and Craft, J.A. (2001). Clonal origins of human breast cancer. J Pathol *194*, 406-412.

Gottesman, M. M., Fojo, T., Bates, S. Multidrug resistance in cancer: role of ATP-dependent transporters, Nature. 2: 48-58, 2002.

Howard, E.F., Scott, D.F., and Bennett, C.E. (1976). Stimulation of thymidine uptake and cell proliferation in mouse embryo fibroblasts by conditioned medium from mammary cells in culture. Cancer Res *36*, 4543-4551.

Jiang, X.R., Jimenez, G., Chang, E., Frolkis, M., Kusler, B., Sage, M., Beeche, M., Bodnar, A.G., Wahl, G.M., Tlsty, T.D., and Chiu, C.P. (1999). Telomerase expression in human somatic cells does not induce changes associated with a transformed phenotype. Nat Genet *21*, 111-114.

Karasov, W. H., Diamond, J. M. A simple method for measuring intestinal solute uptake in vitro, J Comp Physiol. 152: 105-16, 1983.

Krishna, R., Mayer, L. D. Multidrug resistance in cancer, mechanisms, reversal suing modulators of MDR and the role of MDR modulators in influencing the pharmokinetics of anticancer drugs, Eur J Pharm Sci. 11: 265-83, 2000

Letrent, S. P., Polli, J. W., Humphreys, J. E., Pollack, G. M., Brouwer, K. R., Brouwer, L. R. P-glycoprotein mediated transport of morphine in brain capillary endothelial cells, Biochem Pharm. 58: 951-7, 1999.

Lin, Y.Z., Yao, S.Y., Veach, R.A., Torgerson, T.R., and Hawiger, J. (1995). Inhibition of nuclear translocation of transcription factor NF-kappa B by a synthetic peptide containing a cell membrane-permeable motif and nuclear localization sequence. J.Biol.Chem. Journal of Biological Chemistry *270*, 14255-14258.

McChesney, P.A., Aisner, D.L., Frank, B.C., Wright, W.E., and Shay, J.W. (2000). Telomere dynamics in cells with introduced telomerase: a rapid assay for telomerase activity on telomeres. Mol Cell Biol Res Commun *3*, 312-318.

Miller, F.R., McEachern, D., and Miller, B.E. (1989). Growth regulation of mouse mammary tumor cells in collagen gel cultures by diffusible factors produced by normal mammary gland epithelium and stromal fibroblasts. Cancer Res *49*, 6091-6097.

Morales, C.P., Holt, S.E., Ouellette, M., Kaur, K.J., Yan, Y., Wilson, K.S., White, M.A., Wright, W.E., and Shay, J.W. (1999). Absence of cancer-associated changes in human fibroblasts immortalized with telomerase. Nat Genet *21*, 115-118.

Noguchi, S., Motomura, K., Inaji, H., Imaoka, S., and Koyama, H. (1992). Clonal analysis of human breast cancer by means of the polymerase chain reaction. Cancer Res *52*, 6594-6597.

Osthus, R.C., Shim, H., Kim, S., Li, Q., Reddy, R., Mukherjee, M., Xu, Y., Wonsey, D., Lee, L.A., and Dang, C.V. (2000). Deregulation of glucose transporter 1 and glycolytic gene expression by c-Myc. J Biol Chem *275*, 21797-21800.

Parekh, H., Wiesen, K., Simpkins, H. Acquisition of taxol resistance via p-glycoprotein and non p-glycopreotein mediated mechanisms in human ovarian carcinoma cells, Biochem Pharm. 53: 461-70, 1997.

Parekh, H., Simpkins, H. The transport and binding of taxol, Gen Pharmac. 29: 167-72, 1997.
Rossi, L., Reverberi, D., Capurro, C., Aiello, C., Cipolla, M., Bonanno, M., and Podesta, G. (1994). Fibroblasts regulate the migration of MCF7 mammary carcinoma cells in hydrated collagen gel. Anticancer Res *14*, 1493-1501.

Rossi, L., Reverberi, D., Podesta, G., Lastraioli, S., and Corvo, R. (2000). Co-culture with human fibroblasts increases the radiosensitivity of MCF-7 mammary carcinoma cells in collagen gels. Int J Cancer *85*, 667-673.

Sauna, Z. E., Smith, M. M., Muller, M., Kerr, K. M., Ambudkar, S. V. The mechanism of action of multidrug resistance linked p-glycoprotein, J Bioenerg Biomem. 33: 481-91, 2001.

Sharom, F. J., Yu, X., Lu, P., Liu, R., Chu, J. W. K., Szabo, K., Muller, M., Hose, C. D., Monks, A., Varadi, A., Seprodi, J., Sarkadi, B. Interaction of the p-glycoprotein multidrug transporter (MDR1) with high affinity peptide chemosensitizers in isolated membranes, reconstituted systems, and intact cells, Biochem Pharm. 58: 571-86, 1999.
Shay, J.W., Tomlinson, G., Piatyszek, M.A., and Gollahon, L.S. (1995). Spontaneous in vitro immortalization of breast epithelial cells from a patient with Li-Fraumeni syndrome. Mol Cell Biol *15*, 425-432.

Takakura, M., Kyo, S., Kanaya, T., Hirano, H., Takeda, J., Yutsudo, M., and Inoue, M. (1999). Cloning of human telomerase catalytic subunit (hTERT) gene promoter and identification of proximal core promoter sequences essential for transcriptional activation in immortalized and cancer cells. Cancer Res *59*, 551-557.

Walle, U. K., Walle, T. Taxol transport by human intestinal epithelial caco-2 cells, Drug Met Disp. 26: 343-6, 1997.

Wilson, S.E., Liu, J.J., and Mohan, R.R. (1999). Stromal-epithelial interactions in the cornea. Prog Retin Eye Res *18*, 293-309.

MOLECULAR AND CELLULAR BIOLOGY, Jan. 1995, p. 425–432
0270-7306/95/$04.00+0
Copyright © 1995, American Society for Microbiology
Vol. 15, No. 1

# Spontaneous In Vitro Immortalization of Breast Epithelial Cells from a Patient with Li-Fraumeni Syndrome

JERRY W. SHAY,[1]* GAIL TOMLINSON,[2] MIECZYSLAW A. PIATYSZEK,[1] AND LAUREN S. GOLLAHON[1]

*Department of Cell Biology and Neurosciences[1] and Harold C. Simmons Comprehensive Cancer Center,[2] University of Texas Southwestern Medical Center at Dallas, Dallas, Texas 75235-9039*

Received 2 August 1994/Returned for modification 30 August 1994/Accepted 25 October 1994

**Individuals with germ line mutations in the p53 gene, such as Li-Fraumeni syndrome (LFS), have an increased occurrence of many types of cancer, including an unusually high incidence of breast cancer. This report documents that normal breast epithelial cells obtained from a patient with LFS (with a mutation at codon 133 of the p53 gene) spontaneously immortalized in cell culture while the breast stromal fibroblasts from this same patient did not. Spontaneous immortalization of human cells in vitro is an extremely rare event. This is the first documented case of the spontaneous immortalization of breast epithelial cells from a patient with LFS in culture. LFS patient breast stromal fibroblasts infected with a retroviral vector containing human papillomavirus type 16 E7 alone were able to immortalize, whereas stromal cells obtained from patients with wild-type p53, similarly infected with human papillomavirus type 16 E7, did not. The present results indicate a protective role of normal pRb-like functions in breast stromal fibroblasts but not in breast epithelial cells and reinforces an important role of wild-type p53 in the regulation of the normal growth and development of breast epithelial tissue.**

Familial cancer syndromes with germ line mutations, such as the dominantly inherited p53 mutations present in Li-Fraumeni syndrome (LFS), have helped to illustrate the important role of tumor suppressor genes in the development of human cancers (3, 30, 31, 35, 36, 37, 52). The p53 gene is presently considered to be one of the most frequently mutated genes in human cancer (19, 22, 28, 29, 47, 56, 58), and the functional effects of mutations in evolutionarily conserved regions of the p53 phosphoprotein are currently a subject of intense study (24, 25, 28, 43, 46, 59–63). While a complete understanding of wild-type p53 function is not yet known, it is generally believed that perturbations of wild-type p53 function may lead to genomic instability and permit the expansion of the pool of proliferating cells, which leads to a cascade of additional mutations, increasing the probability of neoplastic transformation. The discovery of the importance of the tumor suppressor gene p53, and the identification of germ line mutations in p53 in LFS-affected families, has led to a growing awareness of the cancer risk to such families. Even though rare bone and soft tissue sarcomas are relatively common in families affected by LFS, other, more frequently occurring forms of cancer other than breast cancer (such as colorectal carcinoma) are not overrepresented. Among women in families affected by LFS, breast tumors are the most prevalent cancer (afflicting at least 50%), with 28% of the breast cancers diagnosed before age 30 and 89% diagnosed before age 50 (21, 31, 37). A molecular explanation for the specifically increased incidence of breast cancer, particularly early-onset breast cancer, in families affected by LFS relative to other forms of cancer has not yet been elucidated (20, 41).

We and others have shown that spontaneous immortalization of human cells in vitro (a cell culture term for unlimited proliferative capacity of cells) is an extremely rare event (23, 32, 50) requiring alteration or mutations in several genes which are normally involved in the regulation of cellular senescence (16, 42, 57). It has been suggested that cellular immortalization is a critical and perhaps rate-limiting step in the development of most human cancers (18, 50). It has previously been reported (1, 2, 45, 49) that the expression of viral oncoproteins such as large T antigen of simian virus 40 (SV40) and E6/E7 of high-risk strains of human papillomavirus (HPV) can cause human breast epithelial cells to immortalize at a much higher frequency than fibroblasts. In cell culture, while the stromal fibroblasts require abrogation of both p53 and retinoblastoma (pRb)-like functions to become immortalization competent, human breast epithelial cells appear to require abrogation only of p53 (1, 2, 45, 49). In either case, alteration of p53 in breast epithelial cells or p53 and a pRb-like function in breast stromal cells is only the first of two stages that need to be altered for cells to become immortal. While abrogation of this first stage (mortality stage 1 [M1]) generally results in extension of the in vitro life span, a second step, referred to as crisis or mortality stage 2 (M2), represents a condition in which most cells cease proliferation again.

In normal human somatic cells there is a gradual loss of the ends of chromosomes (telomeres), a process known as the telomere end replication problem (8, 14, 17). The loss of telomeric repeats in vitro and in vivo continues during the period between M1 and M2 (8, 48, 49). At M2 the telomeres reach a critically short length, resulting in destabilization of chromosomes and cessation of cell proliferation. It has been proposed that only if telomerase is reexpressed (an enzyme activity that adds DNA hexameric TTAGGG sequences to telomeres) does an immortalized cell line arise out of M2 (8, 9, 26, 46). Once a cell overcomes crisis (M2), telomerase appears to stabilize telomere length and permit indefinite cell division.

This study addresses the molecular basis for the increased frequency of immortalization-competent human breast epithe-

* Corresponding author. Mailing address: Department of Cell Biology and Neurosciences, University of Texas Southwestern Medical Center at Dallas, 5323 Harry Hines Blvd., Dallas, TX 75235-9039. Phone: (214) 648-3282. Fax: (214) 648-8694. Electronic mail address: Shay@UTSW.SWMED.EDU.

lial cells, by testing the hypothesis that LFS patient breast epithelial cells containing a germ line p53 mutation would spontaneously immortalize at a relatively high frequency but fibroblasts from the same patient should only rarely immortalize (because of a pRb-like function preventing abrogation of M1). Previously, it was reported that skin fibroblasts derived from members of two separate LFS-affected families immortalized in cell culture at a very low frequency (4). However, efforts to reproduce these findings using the same primary fibroblasts were unsuccessful even though loss of the wild-type p53 allele occurred after long-term culture (33). In addition, Maclean et al. (34) originally were unable to observe spontaneous immortalization of fibroblasts obtained from other LFS-affected families, even though more recently they have succeeded (43a).

## MATERIALS AND METHODS

**Cells and culture.** Primary tumor and adjacent normal tissue samples were obtained from a 31-year-old LFS patient undergoing surgery for breast cancer. The normal breast tissue was enzymatically digested by a combination of hyaluronidase and collagenase to separate breast epithelial and ductal tissue (organoids) from stromal cellular components (primarily adipocytes) (55). After dispersion, organoid clusters were cultured in serum-free medium (53) (MEBM from Clonetics Corp., San Diego, Calif.) supplemented with 0.4% bovine pituitary extract (Hammond Cell Tech, Alameda, Calif.), 5 μg of insulin (Sigma, St. Louis, Mo.) per ml, 10 ng of epidermal growth factor (Collaborative Research, Bedford, Mass.) per ml, 0.5 μg of hydrocortisone (Sigma) per ml, 5 μg of transferrin per ml, and 25 μg of gentamicin (Sigma) per ml to select for growth of epithelial cells (HME50; Fig. 1a). The medium was changed every 2 to 3 days. To select for the growth of stromal fibroblasts (HMS50; Fig. 1b), cells were grown in a 4:1 mixture of Dulbecco modified Eagle medium and medium 199 containing 15% iron-supplemented calf serum (Hyclone Laboratories, Logan, Utah) supplemented with 5 μg of insulin per ml and 0.5 μg of hydrocortisone (Sigma) per ml. Epithelial cells were continuously subcultured when near or at confluence, and the cumulative population-doubling level was recorded. Epithelial cells with a typical cobblestone morphology grew out of the organoids in MEBM and expressed cytokeratin 14 (a basal cell marker), cytokeratin 18 (a luminal cell marker), and involucrin (a marker associated with keratinizing squamous epithelium) (55). The epithelial cells growing in these conditions appeared to be from a stem cell population capable of differentiating into a number of different pathways. Breast epithelial cells obtained from milk appear to have more of a luminal cell phenotype (expressing cytokeratin 19), as is the case for the majority of breast tumors, with only a small subset showing some evidence of basal markers (54).

**Retroviral vectors and transfection.** Retroviral vectors consisted of the parent vector pLXSN (obtained from A. D. Miller) or pLXSN containing the genes for HPV type 16 (HPV16) E6, HPV16 E7, or both (designated HPV16 E6/E7) under the transcriptional regulation of the Moloney murine leukemia virus promoter-enhancer sequences (obtained from D. Galloway). These vectors also contain the gene conferring neomycin resistance under the transcriptional regulation of the SV40 promoters. Recombinant viruses were generated in the amphotrophic packaging line PA317 according to previously described procedures (38). Plasmid DNA was transfected into Psi-2 or PE501 cells by calcium phosphate precipitation. Viral supernatants derived from the Psi-2 cells were used to infect PA317 cells to generate clones containing unrearranged proviral copies of pLXSN, HPV16 E6, HPV16 E7, or HPV16 E6/E7. PA317 clones which had viral titers of approximately $3 \times 10^4$ to $5 \times 10^4$ PFU/ml (15) were selected on G418 (1 mg/ml). Medium containing released viruses produced from confluent dishes of each clone was filtered (0.4-μm pore size) and used to infect human mammary epithelial cells and stromal cells as previously described (49). In brief, cells growing in 100-mm-diameter plates were approximately 30 to 50% confluent the day prior to infection. On the day of infection, the medium was removed and replaced with medium containing helper-free viral supernatant (preventing further spread of the vector after initial infection) in the presence of 2 to 4 μg of Polybrene (Gibco/BRL, Gaithersburg, Md.) per ml. After 12 to 16 h the medium was replaced with fresh medium lacking viral supernatant. The next day the cells were split in a series of dilutions into several plates for isolation of clones and then selected on G418 for approximately 2 weeks (Gibco/BRL). Breast stromal cells were selected on 600 to 800 μg of G418 per ml in medium containing serum, while breast epithelial cells, which are more sensitive to G418, were selected on 50 to 100 μg of G418 per ml in serum-free medium. Infection frequencies of 10 to 25% were common, and donor age did not appear to alter this result as long as the cells were replication competent. These frequencies were determined by dividing the number of G418-resistant colonies by the number of colonies growing in the absence of selection.

**Mutation analysis.** Single-strand conformation polymorphism (SSCP) analysis (40) was used to screen for mutations of the p53 gene in cells and tissues from the proband and other patients. Exons 5 to 9 of p53 were PCR amplified with primers flanking coding regions (6). [$\alpha$-$^{32}$P]dCTP was incorporated into the PCR in order to obtain radiolabeled PCR products. Amplified products were treated with formamide, heated to 95°C, subjected to electrophoresis through 5% polyacrylamide gels, and visualized by direct autoradiography. A shift in electrophoretic mobility, suggestive of a change in conformation due to sequence variation, was confirmed by cloning the amplified fragments into M13 vectors and DNA sequencing.

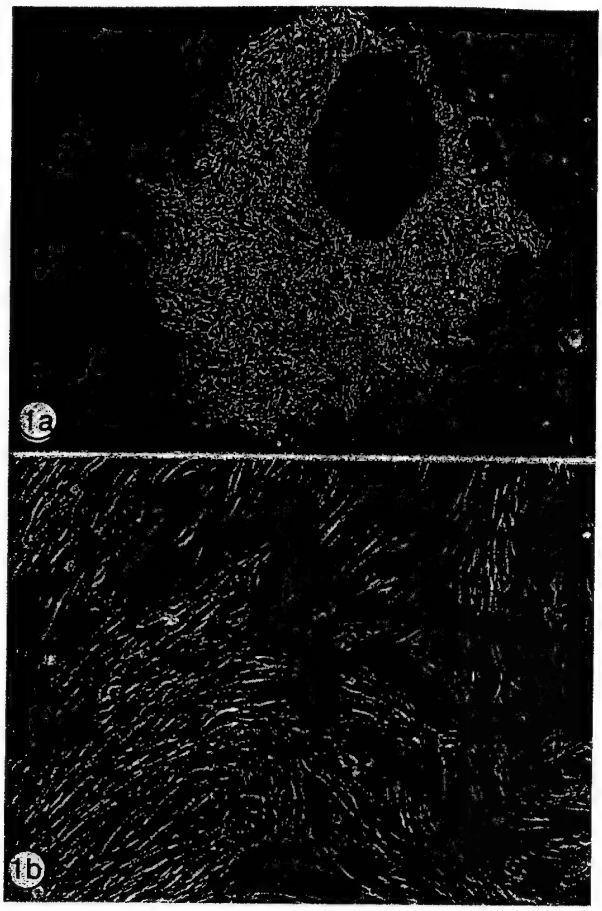


FIG. 1. The breast organoids obtained by overnight digestions with enzymes consist of epithelial, myoepithelial, stromal, and stem cells which are placed either in MCDB170 medium to select for the growth of mammary epithelial cells (a) or in Dulbecco modified Eagle medium-medium 199 with iron-supplemented bovine calf serum to select for the growth of stromal cells (b). Initially all types of cells grow in defined growth medium, but with continuous cell culture the epithelial cells predominate. The ductules of the human mammary gland are lined by a layer of luminal epithelial cells surrounded by a layer of basal or myoepithelial cells. The epithelial cells which grow out from the organoids have a cuboidal, cobblestone-like appearance (a) and are keratin positive (data not shown; see reference 55), whereas the stromal cells (b) are more fusiform, elongated, and vimentin positive (data not shown; see reference 55).

**Telomerase assays.** The one-tube PCR-based telomerase assay is schematically presented in Fig. 2 and is based on the technique as originally described (26). The assay is performed in two steps: (i) telomerase-mediated extension of an oligonucleotide primer (TS), which serves as a substrate for telomerase, and (ii) PCR amplification of the resultant product (an incremental 6-nucleotide single-stranded DNA ladder) with the oligonucleotide primer pair TS (forward) and CX (reverse).

Details of the method are as follows. For cells in culture, pellet 100,000 cells ($3,000 \times g$ in a 1.5-ml microcentrifuge tube for 6 min [Eppendorf centrifuge]) in culture medium. Carefully remove the supernatant, and quickly store the pellet at −80°C. Washing the pellet is not necessary. Lyse the cells with 200 μl of ice-cold lysis buffer consisting of 0.5% 3-[(3-cholamidopropyl)-dimethyl-ammonio]-1-propanesulfonate (CHAPS), 10 mM Tris-HCl (pH 7.5), 1 mM $MgCl_2$, 1 mM ethylene glycol-bis(β-aminoethyl ether)-*N,N,N',N'*-tetraacetic acid (EGTA), 10% glycerol, 5 mM β-mercaptoethanol, 0.1 mM AEBSF [4-(2-aminoethyl)-benzenesulfonyl fluoride] (ICN Biomedical Inc., Aurora, Ohio), and leave them

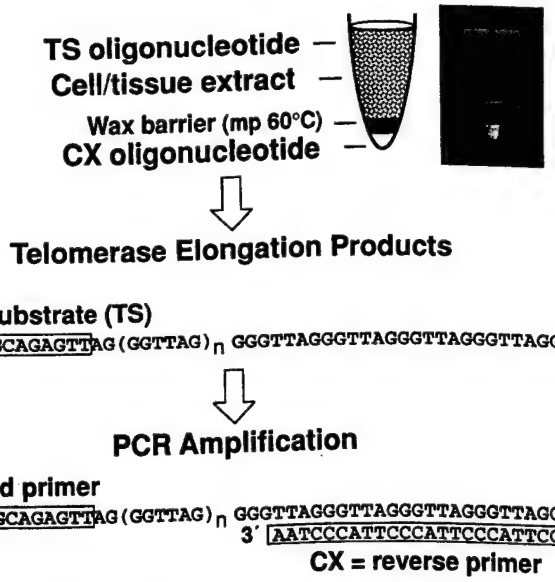


FIG. 2. Diagram of the PCR-based telomerase assay. PCR amplification of telomerase extension products is as detailed by Kim et al. (26). Telomerase synthesizes telomeric repeats [$(TTAGGG)_n$] onto the nontelomeric oligonucleotide (TS) which serves as a telomerase substrate. Such telomerase products are specifically amplified by PCR using the downstream primer CX [5′-$(CCCTTA)_3$CCCTAA-3′] and the upstream primer TS. As is illustrated in this figure, a single-tube assay is accomplished by initially separating the CX primer from the rest of the reaction mix by a wax barrier. The CX primer in the photograph in this figure was labelled at the 5′ end with fluorescein to illustrate its sequestration below the wax barrier.

on ice for 30 min. Centrifuge the lysate at 16,000 × *g* for 20 min at +4°C. Collect 160 μl of supernatant into an Eppendorf tube, making sure that no traces of cell debris from pellet are withdrawn; flash-freeze the supernatant in liquid nitrogen; and then store it at −80°C. Generally 2 μl of each lysate is analyzed, which is equivalent to approximately 1,000 cells. Modifications of this procedure are required for analysis of primary tumor material. Each tissue sample of 50 to 100 mg of frozen (−80°C) tissue is first washed in ice-cold washing buffer (10 mM HEPES [*N*-2-hydroxyethylpiperazine-*N*′-2-ethanesulfonic acid]-KOH [pH 7.5], 1.5 mM $MgCl_2$, 10 mM KCl, 1 mM dithiothreitol) and then homogenized in 200 μl of ice-cold lysis buffer in Kontes tubes with matching disposable pestles (VWR, Vineland, N.J.) rotated at 450 rpm by a drill. After 25 min of incubation on ice, the lysate is centrifuged at 16,000 × *g* for 20 min at 4°C, and the supernatant is rapidly frozen in liquid nitrogen and stored at −80°C. The concentration of protein is measured with the bicinchoninic acid protein assay kit (Pierce Chemical Co., Rockford, Ill.), and an aliquot of the extract containing 6 μg of protein is used for each telomerase assay.

An appropriate amount of extract is assayed in 50 μl of reaction mixture containing 50 μM each deoxynucleoside triphosphate, 344 nM TS primer (5′-AATCCGTCGAGCAGAGTT-3′), 0.5 μM T4 gene 32 protein (U.S. Biochemicals, Cleveland, Ohio), [α-$^{32}$P]dCTP, [α-$^{32}$P]TTP, and 2 U of *Taq* polymerase (Gibco/BRL) in a 0.5-ml tube which contains the CX primer (5′-CCCTTAC CCTTACCCTTACCCTAA-3′) at the bottom sequestered by a wax barrier (Ampliwax; Perkin-Elmer, Foster City, Calif.). After 30 min of incubation at room temperature for telomerase-mediated extension of the TS primer, the reaction mixture is heated at 90°C for 90 s to inactivate telomerase and subjected to 31 PCR cycles of 94°C for 30 s, 50°C for 30 s, and 72°C for 45 s (Fig. 2). As a control, 5 μl of extract is incubated with 1 μg of RNase (5Prime→3Prime, Boulder, Colo.) for 20 min at 37°C prior to the telomerase assay. The PCR products are electrophoresed on a 10% acrylamide gel as previously described (26). Since human telomerase is processive, during the initial 30 min of incubation in the presence of the TS primer, various numbers of hexameric repeats are added to it and when subsequently amplified yield a 6-bp DNA incremental ladder. Extracts from tissues not containing telomerase do not extend the TS primer (26).

**Gel electrophoresis and immunoblotting.** Cell extracts were prepared according to published protocols (11) and analyzed for protein concentration (bicinchoninic acid protein assay; Pierce). Proteins were separated in one dimension by sodium dodecyl sulfate (SDS)-polyacrylamide gel electrophoresis on 8% gels with 4% stacking gels using a minigel apparatus (Mini Protean II System; Bio-Rad, Richmond, Calif.). Immunoblotting, incubation, and developing procedures followed the protocol for chemiluminescence detection of proteins (5) as modified by Gillespie and Hudspeth (13). Briefly, after electrophoresis, gels were transferred to charged nylon (Nytran from Schleicher & Schuell, Keene, N.H.) or polyvinylidene difluoride membranes (Immobilon P from Millipore, Bedford, Mass.) and incubated with a primary antibody (anti-p53 clone PAb1801; Oncogene Science Inc., Manhasset, N.Y.) followed by a secondary antibody conjugated to alkaline phosphatase. The blot was then placed in an assay buffer containing methoxyspiroyl phenyl phosphate for 5 min, blotted on filter paper, and exposed to X-ray film.

Immunoprecipitation procedures were modified from those of Zhang et al. (62, 63). Briefly, treated cells were washed with phosphate-buffered saline (PBS), incubated for 2 to 4 h in methionine- and cysteine-free medium, and then metabolically labelled with 200 μCi of [$^{35}$S]methionine per ml for 4 h at 37°C in a 5% $CO_2$ incubator. Cells were rinsed with PBS, placed for 1 h at 4°C in lysis buffer (150 mM NaCl, 0.5% Nonidet P-40, 5 mM EDTA, 20 mM Tris-HCl [pH 8.0], 10 mM dithiothreitol, and 2.5 mM phenylmethylsulfonyl fluoride [Sigma]), and immunoprecipitated with anti-p53 antibodies, PAb240, PAb1620, and PAb1801 (Oncogene Science Inc.). Lysates were precleared with Protein-G Plus agarose and immunoprecipitated overnight at 4°C. Samples were then run on an SDS–10% acrylamide gel, dried, and exposed to Fuji X-ray film.

**Metaphase spread analysis.** Cultures were incubated with 0.01 μg of colcemid (Gibco/BRL) per ml for 4 h. After collection, cells were incubated for 1 h at 37°C in 0.067 M KCl and then fixed in 3:1 methanol-glacial acetic acid. Cell suspensions were dropped onto slides, and the resulting chromosome spreads were stained in 4% Giemsa stain (Sigma). Chromosomes were counted from 25 randomly chosen spreads per clone.

**Fluctuation analysis.** The frequency of escape from crisis (i.e., immortalization frequency of HME50 clones and HMS50 clones expressing HPV16 E7) was estimated by an approach based on what is essentially a fluctuation analysis as previously described (45, 48). Clones were expanded several population doublings before crisis into multiple series in several sizes of culture vessels at a constant cell density. Each series was subsequently maintained as a separate culture, so that at the end of the experiment the fraction of each series that gave rise to an immortal cell line could be determined. Using different sizes of vessels permitted setup of series which contained a different number of cells per dish while maintaining a constant culture environment (cells per square centimeter). Cultures were split at or just prior to confluence. Once cells reached crisis, they were split at least once every 3 weeks until virtually no surviving cells remained or the culture had immortalized. Stromal fibroblast clones were subcultivated at 6,667 cells per $cm^2$, and mammary epithelial cells were subcultivated at 5,000 cells per $cm^2$. When too few cells were obtained, all of the cells were put back into culture in a single dish. Mammary epithelial and stromal fibroblasts were considered immortal if they expressed telomerase or if vigorous growth occurred after crisis during two subcultivations in which 1,000 cells were seeded into a 50-$cm^2$ dish and allowed to proliferate for 3 weeks for each cycle.

Immortalization is expressed as the number of immortal lines per number of culture series. Frequency is expressed as the probability of obtaining an immortal cell line based on the total number of cells plated at each passage (not per cell division) and is calculated by dividing the total number of independent immortalization events by the total number of cells plated. For example, if one maintained nine series at a minimum population size of $10^6$ cells per dish, for a total pool size of $9 \times 10^6$, and three immortalization events were observed, this would yield a frequency of 3 divided by $9 \times 10^6$, or $3.3 \times 10^{-7}$.

TABLE 1. Spontaneous immortalization of breast epithelial cells obtained from a patient with LFS containing a mutant p53 allele (HME50) but not in breast epithelial cells (HME31 and HME32) containing wild-type p53[a]

| Clone (*n*) | p53 alleles | No. of immortalized clones expressing: | | | |
|---|---|---|---|---|---|
| | | pLXSN (vector only) | HPV16 E6 | HPV16 E7 | HPV16 E6/E7 |
| HME50 (9) | +/− | 4 | ND[b] | ND | ND |
| HME31 (24) | +/+ | 0 | 4 | 0 | 7 |
| HME32 (6) | +/+ | 0 | 1 | 0 | 2 |
| HMS50 (6) | +/− | 0 | 0 | 2 | 3 |
| HMS31 (6) | +/+ | 0 | 0 | 0 | 2 |
| HMS32 (6) | +/+ | 0 | 0 | 0 | 2 |

[a] Five of the six HMS50 stromal fibroblasts senesced around population doubling 40 to 50, while one clone exhibited extended growth but then senesced at population doubling 68. This extended in vitro growth was not observed in HMS31 and HMS32 stromal fibroblasts. Immortalization occurred in LFS patient HMS50 cells expressing HPV16 E7 and containing mutant p53 but not in HPV16 E7-expressing HMS31 and HMS32 cells which contain wild-type p53.
[b] ND, not done.

## RESULTS

The frequency of in vitro spontaneous immortalization of an LFS patient's normal epithelial cells (HME50; Fig. 1a) was compared with that of breast stromal fibroblast cells (HMS50; Fig. 1b) derived from the same patient (Table 1). Both LFS-affected (HMS50) and normal (HMS31 and HMS32) stromal cells were infected shortly after isolation with the defective retrovirus (pLSXN) expressing HPV16 E6/E7 (as a positive control for immortalization), HPV16 E7 alone (15), or HPV16 E6 alone or the control vector pLXSN (38) lacking HPV16 inserted sequences (as a negative control) and cultured along with control (untransfected) populations of LFS patient stromal fibroblasts.

The results of these experiments confirmed our hypothesis that breast epithelial cells from a patient with LFS can spontaneously immortalize (Table 1). While no spontaneous immortalization of the LFS patient control fibroblasts HMS50 (zero of six clones), HMS31 (zero of six clones), and HMS32 (zero of six clones) was observed, we did observe spontaneous immortalization of LFS patient breast epithelial cells (HME50) in cell culture (four of nine cultures) which followed a period of crisis (analyzed positively by the telomerase activity assay; Fig. 2). Breast epithelial cells containing wild-type p53 (HME31 and HME32) did not spontaneously immortalize (0 of 24 and 0 of 6 clones, respectively). Additionally, the immortalization of LFS patient HMS50 fibroblasts expressing HPV16 E7 alone was observed (two of six clones), but that of HPV16 E7-expressing normal breast stromal cells (HMS31, zero of six clones; HMS32, zero of six clones) was not. In these experiments, after infection of the retroviral vector and G418 selection, individual clones were isolated and maintained separately to determine if immortalization occurred. All immortalized clones were thus likely to be of independent origin. While most clones did not immortalize under these experimental conditions, the clones that did immortalize went through a period of crisis that varied in time for each of the individual clones (in some instances lasting several months). The probability of obtaining an immortalization event (in immortalization-competent clones) is generally proportional to the number of cells maintained at the time of crisis.

Figure 3a illustrates the LFS-affected family pedigree along with SSCP data (Fig. 3b) from the primary breast tumor demonstrating a p53 alteration. DNA sequencing (data not shown) confirmed that this alteration was a codon 133 mutation (Met to Thr [M133T]). This same p53 mutation was previously reported (27) in a large LFS-affected family pedigree also characterized by the frequent occurrence of very early-onset breast cancer. It has been reported that while some p53 mutations do not affect the wild-type p53 protein conformation, the p53 mutation M133T does (27, 52). SSCP analysis of DNA from

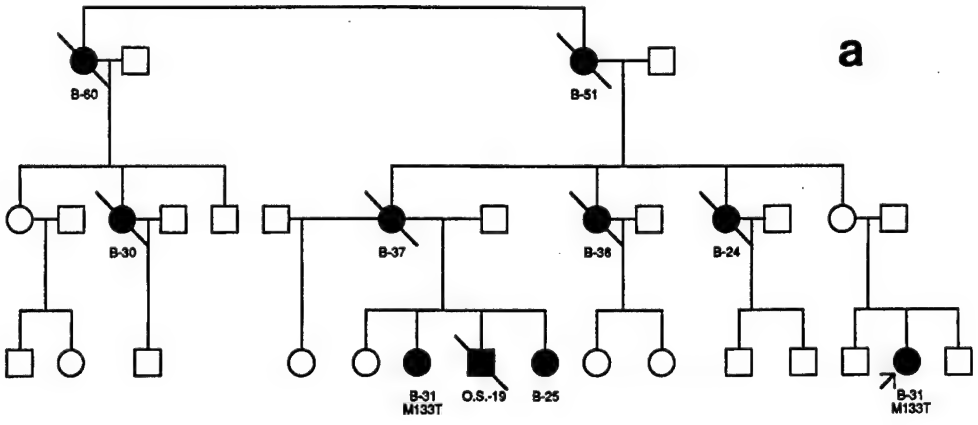


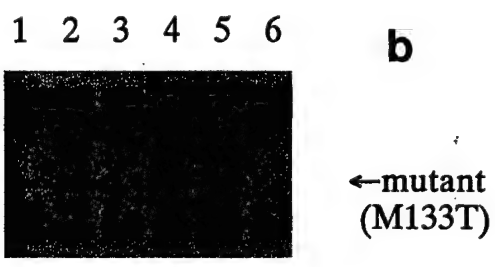


FIG. 3. (a) Pedigree of an LFS-affected family. The arrow indicates the 31-year-old proband from which breast tissue was obtained to establish epithelial and stromal cell cultures. This family has at least three generations of transmission of breast cancer (B) and one individual with osteogenic sarcoma (O.S.). Circles, females; squares, males. Numbers indicate the ages at which individuals presented with cancer (solid symbols); slashes indicate death from the cancer. (b) SSCP analysis of peripheral blood mononuclear cells obtained from the proband in panel a (lane 2). Sequence analysis of PCR-amplified fragments of p53 using primers flanking exon 5 indicate that there is an alteration at codon 133 of the p53 gene. Other, unrelated breast cancer patients (lanes 1, 3, 5, and 6) do not have the p53 alteration, but an additional member of this family does (lane 4).

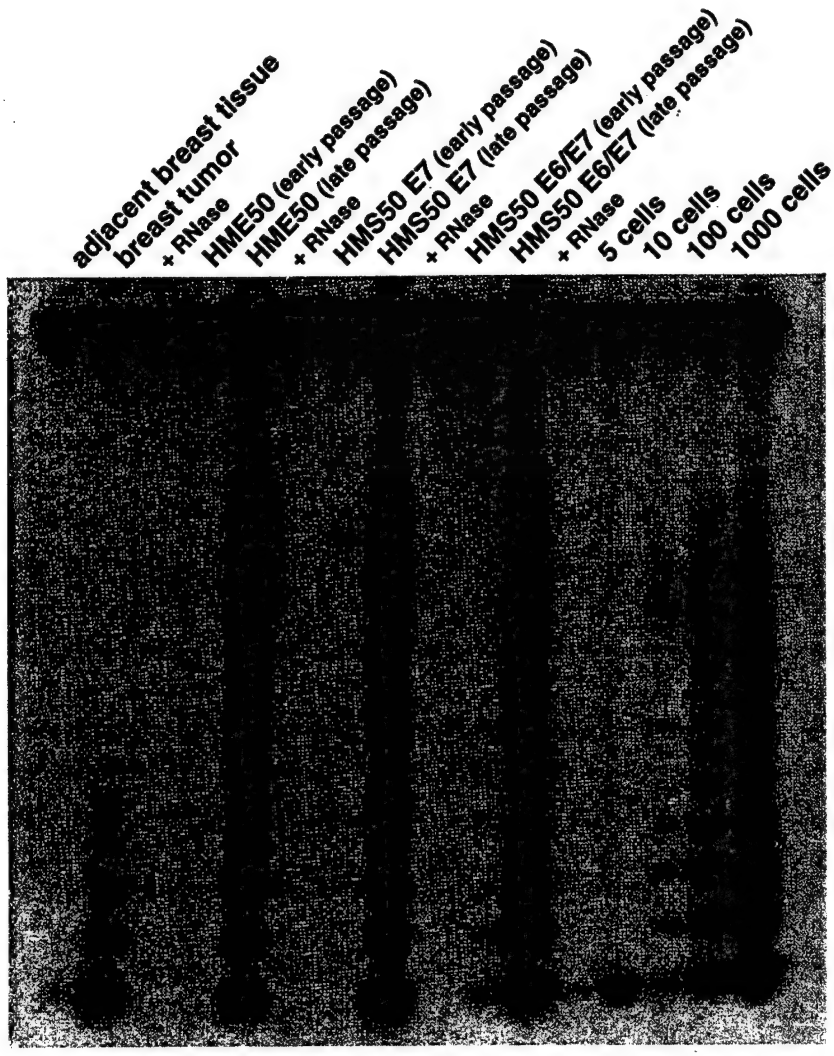


FIG. 4. An assay of telomerase activity using a PCR-based modification of the conventional assay indicates that the normal tissue obtained from this patient does not have detectable telomerase activity (lane 1) whereas the tumor tissue was telomerase positive (lane 2) and RNase sensitive (lane 3). Normal organoid primary explant cultures of both epithelial cells (HME50) and stromal cells expressing HPV16 E7 or E6/E7 (HMS50) were initially negative for telomerase activity (early-passage lanes). After growth in cell culture for several months and escape from crisis, telomerase activity was present (late-passage lanes) and was RNase sensitive (+RNase lanes). The four rightmost lanes are assays of cell equivalents from an established breast tumor cell line.

peripheral blood mononuclear cells (Fig. 3b, lane 4) from affected relatives in this family indicates that this p53 mutation is likely to underlie the high frequency of early-onset breast cancer in this family. Cancer incidence in this family was traced through three generations. Nine of eighteen women presented with breast cancer (the majority before age 40), and one male who presented with osteogenic sarcoma died at the age of 19.

The breast tumor and adjacent normal tissue were analyzed for telomerase activity (an indicator of immortalization) (8–10, 26, 51). Telomerase activity strongly correlates with immortalization events in both cell culture and primary tumors (9, 26). Using a PCR modification (Fig. 2 and reference 26) of the conventional telomerase activity assay (8, 9, 14, 39, 44), we observed that the primary tumor was telomerase positive whereas the normal breast tissue (consisting of both epithelial and stromal cells) was not (Fig. 4). The specificity of this activity is demonstrated by the presence of the hexanucleotide ladder and sensitivity of telomerase to RNase treatment of extracts prior to assay. The organoid explants (both epithelial and stromal) derived from the normal breast tissue of this patient were telomerase negative (indicating that immortal cells are unlikely to preexist in this normal tissue).

Of nine breast epithelial organoid cultures initially isolated, four have continued to proliferate in culture. All nine cultures underwent a decrease in growth rate resembling crisis in virally transfected cells. The four cultures that escaped crisis continue to grow and express telomerase activity and an increased amount of p53 protein. The frequency of immortalization was approximately $5 \times 10^{-7}$ for two of the organoid cultures and $1 \times 10^{-6}$ for the other two organoid cultures. The frequency of escape from crisis was estimated by a fluctuation analysis approach described previously (45, 48).

Initially, all the stromal fibroblasts (i.e., control and pLXSN, HPV16 E6, HPV16 E7, and HPV16 E6/E7 infected) were telomerase negative. After 5 months in cell culture, most of the control stromal cell clones (five of six) slowed down in growth rate between population doublings 40 and 50, appeared to senesce, and remained telomerase negative (Table 1). One of

the stromal cell clones grew until population doubling 68, did not express telomerase, and did not immortalize. However, two of the six HPV16 E7-expressing and three of the six HPV16 E6/E7-expressing HMS50 stromal cell clones immortalized with a frequency of approximately $3 \times 10^{-7}$ continue to grow vigorously (>100 population doublings) and most have acquired the ability to express telomerase activity (immortalized) that is RNase sensitive. Interestingly, one clone of HMS50 stromal cells expressing HPV16 E7 is presently beyond population doubling 130 and does not express telomerase. Similar results have been observed in some SV40 large T antigen immortalized human fibroblasts (26), but at present we do not have a molecular understanding of this phenomenon. The breast stromal fibroblasts obtained from patients undergoing mammoplasty for hypermastia (HMS32) and for prophylactic mastectomy (HMS31) neither spontaneously immortalized nor immortalized when expressing HPV16 E7 (Table 1). However, they did immortalize when expressing HPV16 E6/E7 (Table 1) or SV40 large T antigen (45, 55).

While it is difficult to accurately quantitate relative telomerase activity levels in each sample, we analyzed extracts from different numbers of cell equivalents of a telomerase-positive breast tumor cell line. The final three lanes of Fig. 4 illustrate that we can detect telomerase activity from as few as 10 to 100 cell equivalents (1 to 10% [by volume] of an extract of $10^3$ cells). The primary breast tumor (second lane), though positive for telomerase, has a slightly less processive hexanucleotide ladder than the late-passage immortalized stromal and epithelial cell lines illustrated in Fig. 4. This could be explained by the fact that the primary breast tumor is a mixture of stromal cells (telomerase negative) and epithelial carcinoma cells (telomerase positive). In addition, during the early passages after an immortalization event has occurred in cell culture, there is often a weak telomerase signal which generally increases within several passages (data not shown). While it is possible that expression of telomerase activity increases with time, we believe that it is much more likely that in the early stages after immortalization there are still many mortal (telomerase-negative) cells mixed in the population with a few immortalized (telomerase-positive) cells.

Results of Western blot (immunoblot) analysis of protein extracts from representative epithelial and stromal cells probed with antibodies (recognizing both wild-type and mutant p53 [PAb1801]) are illustrated in Fig. 5. Protein extracts of breast tumor tissue from this LFS patient express more p53 than do those of the adjacent normal breast tissue. The organoid breast epithelial cultures (HME50) initially express low levels of p53 but appear to increase in total p53, a change which is presumed to be due to an increase in the abundance of mutant conformation of p53 as part of the immortalization process in cell culture (as previously reported [12, 33]). This indicates that while the HME50 breast epithelial cells in culture initially contain both mutant and wild-type p53 alleles, the allele containing the wild-type p53 appears to become inactivated (perhaps by mutation of the endogenous wild-type allele, by the loss of the wild-type p53 alleles, or by ectopic expression of a dominant-negative p53 allele). The breast stromal cells (HMS50) transfected with HPV16 E7 also initially express low levels of p53, but similarly to the breast epithelial cells, as part of the immortalization process in cell culture, the mutant p53 protein levels increase. Thus, loss of wild-type p53 function likely permits increased cell proliferation, ultimately resulting in immortalization. With time, the mortal cells stop dividing and/or die while the immortalized cells increase and dominate the population, leading to a stronger telomerase activity signal.

We are not sure that there is a second p53 mutation in the primary tumor, since by SSCP analysis the wild-type p53 signal is still present. This is likely due, in part, to the presence of connective tissue stromal cells mixed in with the primary tumor. In order to determine if wild-type p53 was expressed in the immortalized epithelial cells, we metabolically labelled HME50 cells pre- and postimmortalization with [$^{35}$S]methionine and then immunoprecipitated them using p53 antibodies that recognize wild-type p53 conformation (PAb1620), mutant p53 conformation (PAb240), or both the mutant and wild-type p53 conformations (PAb1801) (7, 61–63). While we could detect both a wild-type and mutant p53 conformation in early-passage HME50 cells (population doubling 22), only a stronger mutant conformation signal in late passage (population doubling >55) cells was detected (data not shown). This indicates that the mutant conformation of p53 increases as part of the immortalization process but does not exclude the possibility that a small amount of wild-type p53 remained undetectable by immunoprecipitation.

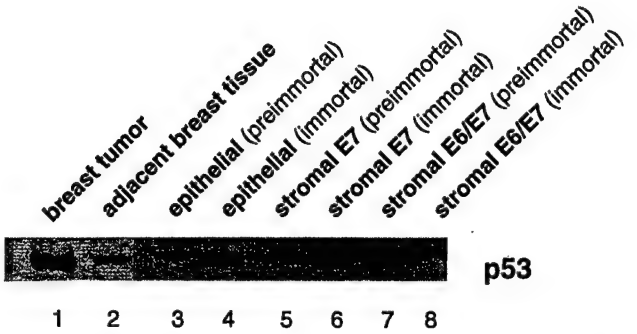


FIG. 5. Western blot analysis of p53 in protein extracts from the tissue and cells obtained from an LFS patient by using PAb1801 antibody, which recognizes both wild-type and mutant conformations of p53. Levels of p53 in the tumor are much higher than in the adjacent normal tissue from which epithelial and stromal cells were obtained. LFS patient epithelial and stromal cells in early passage also have low levels of expression of p53, while the epithelial cells that spontaneously immortalized and the stromal cells expressing HPV16 E7 that immortalized have increased expression of p53. The stromal cells that immortalized with HPV16 E6/E7 do not have increased expression of p53, since the E6 protein of HPV16 facilitates degradation of p53.

From our previous studies (45), we predicted that those clones which were able to remain near diploid were the most likely to immortalize. Chromosome analysis of metaphase spreads indicated that there was a higher fraction of breast epithelial clones remaining near diploid in three clones that spontaneously immortalized compared with three clones that did not spontaneously immortalize (Table 2). This was also true for the LFS patient breast stromal cells expressing HPV16 E7 and E6/E7 (Table 2).

## DISCUSSION

This is the first report documenting spontaneous immortalization of human breast epithelial cells obtained from patients with LFS, although it has been reported that skin fibroblast cells from LFS patients can spontaneously immortalize (4). Even though we did not observe spontaneous immortalization of LFS patient stromal cells in the present study, we did observe immortalization of LFS patient stromal cells expressing HPV16 E7. These results indicate that wild-type p53 is important in regulating cellular senescence in breast epithelial cells and also suggest an important role for both p53 and a pRb-like function in the regulation of senescence of breast stromal cells.

Previously it has been reported that LFS patient skin fibroblast cells immortalize spontaneously at a very low frequency

TABLE 2. Chromosome analysis of human mammary epithelial (HME) and human mammary stromal (HMS) cells from an LFS patient

| Clone name | Immortalized | Range of chromosomes/metaphase[a] | Median no. of chromosomes | % Diploid metaphases |
|---|---|---|---|---|
| HME50-5 | Yes | 44–123 | 47 | 60 |
| HME50-8 | Yes | 38–101 | 46 | 68 |
| HME50-9 | Yes | 41–107 | 49 | 55 |
| HME50-3 | No | 42–99 | 59 | 42 |
| HME50-6 | No | 32–155 | 75 | 20 |
| HME50-7 | No | 37–174 | 78 | 36 |
| HMS50-E7-5 | Yes | 41–113 | 47 | 72 |
| HMS50-E7-pop | Yes | 38–102 | 46 | 84 |
| HMS50-E6/E7-2 | Yes | 40–133 | 46 | 68 |

[a] Based on counts from 25 metaphase spreads.

(4), but this work has been difficult to confirm (33, 34). In a yet unpublished study (43a), stromal fibroblasts of an LFS patient appeared to senesce at 42 population doublings, but after several months of maintenance in the senescent state, cell proliferation which was associated with a loss of the wild-type p53 allele recommenced. One of these clones appeared to spontaneously immortalize even though after an additional 30 population doublings the rest of the clones again ceased proliferation (similar to crisis in SV40-transformed cells) and did not immortalize. These results and those in the present report suggest that wild-type p53 is important in maintenance of DNA stability and that loss of wild-type p53 function may be associated with a breakdown in cell growth control (loss of cellular homeostasis), causing increased proliferation ultimately resulting in immortalization, generally by the reactivation of telomerase activity. While our studies indicate that loss of p53 function may be sufficient to allow breast epithelial cells to immortalize, in the fibroblast lineages loss of p53 function alone may not be sufficient to obtain immortalization, and it is only after the additional loss of a pRb-like function that these cells become immortalization competent. Irrespective, loss of p53 function in breast epithelial cells or p53 and pRb-like function in stromal cells is only the first of two stages that must be overcome for cells to immortalize (46, 50). Thus, it is not surprising that fibroblasts obtained from LFS patients are difficult to immortalize and that even with the complete loss of wild-type p53 immortalization was not observed (33).

The implications of these findings are potentially important, not only because they concern LFS patients' risks of developing cancer but also because they indicate the important role of normal p53 in protecting human breast epithelial cells from immortalizing and progressing to malignant carcinoma. These studies may also provide one reason for the high frequency of breast cancer in LFS-affected families. While alterations in p53 appear to be a central factor for the development of breast cancer in LFS patients, tissue-specific changes (perhaps related to differentiation) are also likely to be important, since LFS-affected families do not have a high incidence of sporadic colorectal cancer although such cancers are associated with a high prevalence of p53 mutations (22). Finally, the spontaneously immortalized breast epithelial cell lines obtained in the present study may be useful in the elucidation of additional critical steps in the development of breast cancer.

## ACKNOWLEDGMENTS

This study was supported by research grants CA50195 and CA64871 from the National Institutes of Health (J.W.S.); USAMR grant DAMD-94-J-4077 (J.W.S.); Geron Corp., Menlo Park, Calif. (J.W.S.); the Children's Cancer Research Fund (G.T.); the American Society of Clinical Oncology (G.T.); and the Susan G. Komen Breast Cancer Foundation (G.T. and J.W.S.).

We thank Woodring Wright, Joe Goldstein, Jennifer Cuthbert, John Minna, Arnold Levine, and Curtis Harris for valuable discussions.

## REFERENCES

1. **Band, V., S. Dalal, L. Delmolino, and E. J. Androphy.** 1993. Enhanced degradation of p53 protein in HPV-6 and BPV-1 E6-immortalized human mammary epithelial cells. EMBO J. **12**:1847–1852.
2. **Band, V., J. A. De Caprio, L. Delmolino, V. Kulesa, and R. Sager.** 1991. Loss of p53 protein in human papillomavirus type 16-immortalized human mammary epithelial cells. J. Virol. **65**:6671–6676.
3. **Birch, J. M., A. L. Hartley, K. J. Tricker, J. Prosser, A. Condie, A. M. Kelsey, M. Harris, P. H. M. Jones, A. Binchy, D. Crowther, A. W. Craft, O. B. Eden, D. G. R. Evans, E. Thompson, J. R. Mann, J. Martin, E. L. D. Mitchell, and M. F. Santibanez-Koref.** 1994. Prevalence and diversity of constitutional mutations in the p53 gene among 21 Li-Fraumeni families. Cancer Res. **54**:1298–1304.
4. **Bischoff, F. Z., S. O. Yim, S. Pathak, G. Grant, M. J. Siciliano, B. C. Giovanella, L. C. Strong, and M. A. Tainsky.** 1990. Spontaneous abnormalities in normal fibroblasts from patients with Li-Fraumeni cancer syndrome: aneuploidy and immortalization. Cancer Res. **50**:7979–7984.
5. **Bronstein, I., J. C. Voyta, K. G. Lasseri, O. Murphey, B. Edwards, and L. J. Kricka.** 1990. Rapid and sensitive detection of DNA in Southern blots with chemiluminescence. BioTechniques **8**:310–314.
6. **Buchman, V. L., P. M. Chumakov, N. N. Ninkina, O. P. Samarina, and G. P. Georgiev.** 1988. A variation in the structure of the protein-coding region of the human p53 gene. Gene **70**:245–252.
7. **Chen, J.-Y., W. D. Funk, W. E. Wright, J. W. Shay, and J. D. Minna.** 1993. Heterogeneity of transcriptional activity of mutant p53 proteins and p53 DNA target sequences. Oncogene **8**:2159–2166.
8. **Counter, C. M., A. A. Avilion, C. E. LeFeuvre, N. G. Stewart, C. W. Greider, C. B. Harley, and S. Bacchetti.** 1992. Telomere shortening associated with chromosome instability is arrested in immortal cells which express telomerase activity. EMBO J. **11**:1921–1929.
9. **Counter, C. M., H. W. Hirte, S. Bacchetti, and C. B. Harley.** 1994. Telomerase activity in human ovarian carcinoma. Proc. Natl. Acad. Sci. USA **91**:2900–2904.
10. **deLange, T.** 1994. Activation of telomerase in a human tumor. Proc. Natl. Acad. Sci. USA **91**:2882–2885.
11. **Dunbar, B. S.** 1987. Two-dimensional electrophoresis and immunological techniques, p. 335–341. Plenum Press, New York.
12. **Frebourg, T., M. Sadelain, Y.-S. Ng, J. Kassel, and S. H. Friend.** 1994. Equal transcription of wild-type and mutant p53 using bicistronic vectors results in the wild-type phenotype. Cancer Res. **54**:878–881.
13. **Gillespie, P. G., and A. J. Hudspeth.** 1991. Chemiluminescence detection of proteins from single cells. Proc. Natl. Acad. Sci. USA **88**:2563–2567.
14. **Greider, C. W.** 1990. Telomeres, telomerase and senescence. Bioessays **12**: 363–369.
15. **Halbert, C. L., G. W. Demers, and D. A. Galloway.** 1992. The E6 and E7 genes of human papillomavirus type 6 have weak immortalizing activity in human epithelial cells. J. Virol. **66**:2125–2134.
16. **Hara, E., H. Tsurui, A. Shinozaki, S. Nakada, and K. Oda.** 1991. Cooperative effect of antisense-Rb and antisense-p53 oligomers on the extension of life span in human diploid fibroblasts. Biochem. Biophys. Res. Commun. **179**:528–534.
17. **Harley, C. B., A. B. Futcher, and C. W. Greider.** 1990. Telomeres shorten during aging of human fibroblasts. Nature (London) **345**:458–460.
18. **Harris, C. C.** 1987. Human tissues and cells in carcinogenesis research. Cancer Res. **47**:1–10.
19. **Harris, C. C.** 1993. p53: at the crossroads of molecular carcinogenesis and risk assessment. Science **262**:1980–1981.
20. **Harris, J. P., M. E. Lippman, and V. Veronesi.** 1992. Breast cancer. N. Engl. J. Med. **327**:319–328.
21. **Hartley, A. L., J. M. Birch, H. B. Marsden, and M. Harris.** 1986. Breast cancer risk in mothers of children with osteosarcoma and chondrosarcoma. Br. J. Cancer **54**:819–823.
22. **Hollstein, M., D. Sidransky, B. Vogelstein, and C. C. Harris.** 1991. p53 mutations in human cancers. Science **253**:49–53.
23. **Huschtscha, L. I., and R. Holiday.** 1983. Limited and unlimited growth of SV40-transformed cells from human diploid MRC-5 fibroblasts. J. Cell Sci. **63**:77–99.
24. **Kastan, M. B., Q. Zhan, W. S. El-Deiry, F. Carrier, T. Jacks, W. V. Walsh, B. S. Plunkett, B. Vogelstein, and A. J. Fornace.** 1992. A mammalian cell cycle checkpoint pathway utilizing p53 and GADD45 is defective in ataxia-telangiectasia. Cell **71**:587–597.
25. **Kern, S. E., J. A. Pietenpol, S. Thiagalingam, A. Seymour, K. W. Kinzler, and B. Vogelstein.** 1992. Oncogenic forms of p53 inhibit p53-regulated gene expression. Science **256**:827–830.
26. **Kim, N.-W., M. A. Piatyszek, K. R. Prowse, P. Ho, G. Coviello, C. Harley,**

**M. D. West, W. E. Wright, S. Weinrich, and J. W. Shay.** Specific association of human telomerase activity with immortal cells and cancer. Science, in press.
27. **Law, J. C., L. C. Strong, A. Chidambaram, and R. E. Ferrell.** 1991. A germ line mutation in exon 5 of the p53 gene in an extended cancer family. Cancer Res. **51**:6385–6387.
28. **Levine, A. J.** 1993. 11th Ernst Klenk Lecture. The p53 tumor suppressor gene and product. Biol. Chem. **374**:227–235.
29. **Levine, A. J., J. Momand, and C. A. Finlay.** 1991. The p53 tumor suppressor gene. Nature (London) **351**:49–53.
30. **Li, F. P., and J. F. Fraumeni, Jr.** 1969. Soft tissue sarcomas, breast cancer, and other neoplasms. A familial syndrome. Ann. Intern. Med. **71**:747–752.
31. **Li, F. P., J. F. Fraumeni, Jr., J. J. Mulvihill, W. A. Blattner, M. G. Dreyfus, M. A. Tucker, and R. W. Miller.** 1988. A cancer family syndrome in twenty-four kindreds. Cancer Res. **48**:5358–5362.
32. **Linder, S., and H. Marshall.** 1990. Immortalization of primary cells by DNA tumor viruses. Exp. Cell Res. **191**:1–7.
33. **Livingstone, L. R., A. White, J. Sprouse, E. Livanos, T. Jacks, and T. D. Tlsty.** 1992. Altered cell cycle arrest and gene amplification potential accompany loss of wild-type p53. Cell **70**:923–935.
34. **Maclean, K., E. M. Rogan, N. J. Whitaker, A. C.-M. Chang, P. B. Rowe, L. Dalla-Pozza, G. Symonds, and R. R. Reddel.** 1994. In vitro transformation of Li-Fraumeni syndrome fibroblasts with SV40 large T antigen mutants. Oncogene **9**:719–725.
35. **Malkin, D.** 1990. p53 and the Li-Fraumeni syndrome. Cancer Genet. Cytogenet. **66**:83.
36. **Malkin, D., K. W. Jolly, N. Barbier, A. T. Look, S. H. Friend, M. C. Gebhardt, T. I. Anderson, A. L. Borresen, F. P. Li, J. Garber, et al.** 1992. Germline mutations of the p53 tumor-suppressor gene in children and young adults with second malignant neoplasms. N. Engl. J. Med. **326**:1309–1315.
37. **Malkin, D., F. P. Li, L. C. Strong, J. F. Fraumeni, C. E. Nelson, D. H. Kim, J. Kassell, M. A. Gryka, F. Z. Bischoff, M. A. Tainsky, and S. H. Friend.** 1990. Germ line p53 mutations in a familial syndrome of breast cancer, sarcomas, and other neoplasms. Science **250**:1233–1238.
38. **Miller, A. D., and G. J. Rosman.** 1989. Improved retroviral vectors for gene transfer and expression. BioTechniques **7**:980–990.
39. **Morin, G. B.** 1989. The human telomere terminal transferase is a ribonucleoprotein that synthesizes TTAGGG repeats. Cell **59**:521–529.
40. **Orita, M., H. Iwahana, H. Kanazawa, K. Hayashi, and T. Sekiya.** 1989. Detection of polymorphisms of human DNA by gel electrophoresis as single-strand conformation polymorphisms. Proc. Natl. Acad. Sci. USA **86**:2766–2770.
41. **Osteen, R. T., and K. H. Karnell.** 1994. The National Cancer Data Base report on breast cancer. Cancer **73**:1994–2000.
42. **Radna, R. L., Y. Caton, K. K. Jha, P. Kaplan, G. Li, F. Traganos, and H. L. Ozer.** 1989. Growth of immortal simian virus 40 *tsA*-transformed human fibroblasts is temperature dependent. Mol. Cell. Biol. **9**:3093–3096.
43. **Raycroft, L., H. Y. Wu, and G. Lozano.** 1990. Transcriptional activation by wild-type but not mutants of the p53 antioncogene. Science **249**:1049–1051.
43a. **Reddell, R. (Children's Medical Research Institute, Westmead, New South Wales, Australia).** Personal communication.
44. **Shay, J. W., D. Brasiskyte, M. Ouellete, M. A. Piatyszek, H. Werbin, Y. Ying, and W. E. Wright.** 1994. Methods for analysis of telomerase and telomeres. Methods Mol. Genet. Genes Chromosome Anal. Part C **5**:263–280.
45. **Shay, J. W., B. A. Van der Haegen, Y. Ying, and W. E. Wright.** 1993. The frequency of immortalization of human fibroblast and mammary epithelial cells transfected with SV40 large T-antigen. Exp. Cell Res. **209**:45–52.
46. **Shay, J. W., and H. Werbin.** 1993. Toward a molecular understanding of the onset of human breast cancer: a hypothesis. Br. Cancer Res. Treat. **25**:83–94.
47. **Shay, J. W., H. Werbin, W. Funk, and W. E. Wright.** 1992. Cellular and molecular advances in elucidating p53 function. Mutat. Res. **277**:163–171.
48. **Shay, J. W., and W. E. Wright.** 1989. Quantitation of the frequency of immortalization of normal diploid fibroblasts by SV40 large T-antigen. Exp. Cell Res. **184**:109–118.
49. **Shay, J. W., W. E. Wright, D. Brasiskyte, and B. A. Van Der Haegen.** 1993. E6 of human papilloma virus 16 can overcome the M1 stage of immortalization in human mammary epithelial cells but not in human fibroblasts. Oncogene **8**:1407–1413.
50. **Shay, J. W., W. E. Wright, and H. Werbin.** 1991. Defining the molecular mechanisms of human cell immortalization. Biochim. Biophys. Acta **1072**: 1–7.
51. **Shay, J. W., W. E. Wright, and H. Werbin.** 1993. Loss of telomeric DNA during aging may predispose cells to cancer. Int. J. Oncol. **3**:559–563.
52. **Srivastava, S., S. Wang, Y. A. Tong, K. Pirollo, and E. H. Chang.** 1993. Several mutant p53 proteins detected in cancer-prone families with Li-Fraumeni syndrome exhibit transdominant effects on the biochemical properties of the wild-type p53. Oncogene **8**:2449.
53. **Stampfer, M. R., R. C. Hallowes, and A. J. Hackett.** 1980. Growth of normal human mammary cells in culture. In Vitro (Rockville) **16**:415–425.
54. **Taylor-Papadimitriou, J., F. Berdichevsky, B. D'Souza, and J. Burchell.** 1993. Human models of breast cancer. Cancer Surv. **16**:59–78.
55. **Van Der Haegen, B. A., and J. W. Shay.** 1993. Immortalization of human mammary epithelial cells by SV40 large T-antigen involves a two-step mechanism. In Vitro Cell. Dev. Biol. **29**:180–182.
56. **Vogelstein, B., and K. W. Kinzler.** 1992. p53 function and dysfunction. Cell **70**:523–526.
57. **Wright, W. E., O. M. Pereira-Smith, and J. W. Shay.** 1989. Reversible cellular senescence: a two-stage model for the immortalization of normal human diploid fibroblasts. Mol. Cell. Biol. **9**:3088–3092.
58. **Wright, W. E., and J. W. Shay.** 1992. Telomere positional effects and the regulation of cellular senescence. Trends Genet. **8**:193–197.
59. **Yin, Y., M. A. Tainsky, F. Z. Bischoff, L. C. Strong, and G. M. Wahl.** 1992. Wild-type p53 restores cell cycle control and inhibits gene amplification in cells with mutant p53 alleles. Cell **70**:937–948.
60. **Zambetti, G. P., J. Bargonetti, K. Walker, C. Prives, and A. J. Levine.** 1992. Wild-type p53 mediates positive regulation of gene expression through a specific DNA sequence element. Genes Dev. **6**:1143–1152.
61. **Zauberman, A., Y. Barak, N. Ragimov, N. Levy, and M. Oren.** 1993. Sequence-specific DNA binding by p53: identification of target sites and lack of binding to p53-MDM2 complexes. EMBO J. **12**:2799–2808.
62. **Zhang, W., W. D. Funk, W. E. Wright, J. W. Shay, and A. B. Deisseroth.** 1993. DNA binding and transcriptional activation by mutant p53 proteins. Oncogene **8**:2555–2559.
63. **Zhang, W., J. W. Shay, and A. Deisseroth.** 1993. Inactive p53 mutants may enhance the transcriptional activity of wild-type p53. Cancer Res. **53**:4772–4775.

Oncogene (1996) 12, 715-725
© 1996 Stockton Press All rights reserved 0950-9232/96 $12.00

# Immortalization of human mammary epithelial cells transfected with mutant p53 ($273^{his}$)

Lauren S Gollahon and Jerry W Shay

*The University of Texas Southwestern Medical Center at Dallas, Department of Cell Biology and Neurosciences, 5323 Harry Hines Boulevard, Dallas, Texas 75235-9039, USA*

**Normal human breast epithelial cells were transfected with expression vectors containing the p53 gene mutated at either codon 143, 175, 248 or 273, or by infection with a recombinant retroviral vector containing the p53 gene mutated at codons 143, 175, 248, or 273. The breast epithelial cells were monitored for extension of *in vitro* lifespan and immortalization. Expression of some, but not all, p53 mutants resulted in an extension of *in vitro* lifespan. Experiments with the p53 temperature sensitive mutant $143^{ala}$ revealed that at 32°C, the nonpermissive temperature, the growth of breast epithelial cells was inhibited. At 37°C, the mutant conformation, there was increased proliferation of cells, resulting in extension of *in vitro* lifespan. Breast epithelial cells expressing p53 mutant $273^{his}$ maintained DNA binding and transcriptional activities and one clone immortalized after a period of growth arrest (crisis). The progression of this immortalization event was characterized by the reactivation of telomerase using the telomeric repeat amplification protocol (TRAP), and terminal restriction fragment analysis (TRF). This is the first reported immortalization of human mammary epithelial cells transfected with a mutant 53.**

**Keywords:** telomerase; telomeres; senescence; life'span

## Introduction

Both normal human fibroblasts and epithelial cells maintained in cell culture undergo cellular senescence and do not spontaneously immortalize. A model involving a two stage mechanism for regulating cellular senescence or aging has been previously reported (Shay and Wright, 1989; Wright *et al.*, 1989; Wright and Shay, 1992a). In this model, the first stage or mortality stage 1 (M1) leads to normal cellular senescence. In order for cells to grow past this stage, the M1 mechanism must be overcome. This may be accomplished by interaction of mutant p53 with activated oncogenes such as Ha-*ras* (Eliyahu *et al.*, 1984) or by the activity of DNA tumor virus gene products such as human papilloma virus type 16 E6/E7, adenovirus 5 E1A/E1B or SV40 large T antigen (Linzer and Levine, 1979; Sarnow *et al.*, 1982; DeCaprio *et al.*, 1988; Huange *et al.*, 1988; Shay *et al.*, 1989; Werness *et al.*,1990; Shay *et al.*, 1993a, b; Demers *et al.*, 1994), presumably by inactivation of the tumor suppressor gene products pRb and p53. However, these DNA virus proteins fail to directly immortalize human cells. Cells overcoming M1 continue to proliferate in an 'extended lifespan' period until an independent second mortality stage (M2) mechanism is activated (crisis), and only if a critical M2 gene becomes inactivated can a rare cell escape crisis and become immortal.

The p53 tumor suppressor gene product and the retinoblastoma gene product (pRb) or a retinoblastoma-like activity appear to be important in regulating the M1 stage in most human cell types (Hara *et al.*, 1991; Shay *et al.*, 1991, 1993a,b; Gotz and Montenarh, 1995). In normal mammary epithelial cells the p53 levels remain constant throughout their lifespan in culture (this paper) in contrast to human diploid fibroblasts which showed an increase in levels of p53 as cells reached senescence (Kulju and Lehman, 1995). The pRb levels in HME cells, decrease significantly as the cells approach senescence (this paper). The p53 tumor suppressor gene is one of the most commonly mutated genes in human cancer (Harris and Hollstein, 1992), with approximately 50% of primary breast tumors containing alterations involving the p53 gene (Callahan and Campbell, 1989; Hollstein *et al.*, 1991; Harris and Hollstein, 1992; Moll *et al.*, 1992). Prompted by the findings of Band *et al.*, (1990, 1991), that human mammary epithelial cells may occasionally immortalize when expressing HPV 16 or HPV 18 plasmids defective in pRb binding but normal for the E6 function of p53 abrogation, we infected human mammary epithelial cells (HME) with defective retroviruses expressing HPV 16 E6, E7 or E6/E7 (Shay *et al.*, 1993a). The results showed that HME cells expressing either HPV 16 E6/E7 or E6 alone were capable of overcoming M1 and in some instances M2. Direct support for this was recently obtained when it was demonstrated that breast epithelial cells but not breast stromal cells obtained from a patient with Li-Fraumeni Syndrome (containing a germline mutation in p53) spontaneously immortalized in cell culture (Shay *et al.*, 1995). That breast epithelial cells immortalize more easily than stromal cells is also supported by the epidemiological findings that the annual incidence of epithelial cell carcinomas such as breast cancer, are at least 100 times higher than the annual incidence of soft tissue sarcomas (Pollock, 1992). Tissue specific lineages are likely to have different regulatory mechanisms which may influence their ease of escape from senescence followed by immortalization. This does not necessarily indicate that bypassing M1 is less frequent in fibroblasts, since Bond *et al.* (1994) have been able to successfully abrogate p53 function in

Correspondence: JW Shay
Received 18 September 1995; revised 6 November 1995; accepted 6 November 1995

human diploid fibroblasts with the introduction of mutant p53 $143^{ala}$. This tissue specific lineage may help explain the apparently different roles that p53 and pRb have in cellular senescence for epithelial versus human mammary stromal cells (Shay *et al.*, 1993a,b).

Inactivation of M2 most likely involves recessive events consistent with the observations that a limited proliferative capacity is restored in hybrids between immortal and mortal cells (Pereira-Smith, 1987). Mutational inactivation of one allele followed by the elimination of the remaining wild-type allele by nondisjunctional or chromosomal conversions (Rew, 1994), selective growth advantage for the mutant (Harvey *et al.*, 1995) or possibly telomere shortening as theorized by Wynford-Thomas *et al.* (1995), are all likely mechanisms for escape from M2. However, the gene product regulating the M2 stage still remains to be determined. One possibility is that it may involve a gene in the telomerase repression pathway (Shay and Werbin, 1993). The ribonucleoprotein enzyme, telomerase, is involved in maintaining the stability of telomeres at the ends of chromosomes (Counter *et al.*, 1992). The end replication problem described by Watson (1972) would lead to progressive telomere shortening in normal cells since the mechanism of DNA replication in linear chromosomes is different for each of the two strands (e.g., leading and lagging). This progressive loss of telomeres (simple tandem repeats of the sequence TTAGGG) at the ends of human chromosomes may be a molecular mechanism that determines the time of onset of cellular senescence (Olovnikoff, 1973; Harley, 1990).

Telomerase, an enzyme expressed in germ line cells, stem cells and cancer cells (Greider and Blackburn, 1985, 1989; Morin, 1989; Counter *et al.*, 1994; Kim *et al.*, 1994; Hiyama *et al.*, 1995; Piatyzsek *et al.*, 1995) contains its own RNA template and thus extends the overhanging G-rich telomeric strand by direct polymerization of deoxynucleotides into tandem TTAGGG repeats. This extended G-rich strand is now used as the template for synthesizing the C-rich complementary strand. Telomerase therefore stabilizes the telomeric length in immortal and cancer cells by compensating for the end replication problem. The absence of telomerase in normal somatic cells results in loss of 50–200 bp/cell from telomeres per round of replication (Harley *et al.*, 1990; Allsopp *et al.*, 1992). Bypassing M1 does not reactivate telomerase and telomeres continue to shorten during the period of extended lifespan (Counter *et al.*, 1992; Shay *et al.*, 1993c). The immortal cells that overcome M2 almost always re-express telomerase activity and are capable of maintaining stable telomere lengths (Counter *et al.*, 1992; Wright and Shay, 1992b; Shay *et al.*, 1993b,c). Escape from M2 may thus represent the abrogation in the repression pathway of telomerase activity in somatic cells (Counter *et al.*, 1992; Wright and Shay, 1992a; Shay *et al.*, 1993a,c; Piatyszek, 1995).

In the present study we sought to determine if the M1 mechanism in HME cells could be directly overcome by the introduction of p53 mutants implicated in a variety of human cancers. While some of the p53 mutants inserted into normal human mammary epithelial cells resulted in extension of *in vitro* lifespan, one clone expressing p53 mutant $273^{his}$ immortalized.

## Results

### *Cell culture*

In culture, using defined medium supplemented with growth factors, normal human mammary epithelial cells (HME) vary in their proliferative capacities, ranging from 25–50 population doublings and then undergo morphological changes associated with finite lifespan (Shay *et al.*, 1993a; Van Der Haegen and Shay, 1993). Young HME cells initially display high proliferative capabilities, but as they approach M1 (the first stage of cellular senescence), the proliferation rate slows down until the cells cease to divide. Normally HME cells can remain in a senescent, growth arrested state for several months if nutrients are replaced frequently.

### *Transfection/infection of mutant p53 constructs*

p53 'hot spot' mutants were introduced into normal HME 31 cells at PDL 28 and into HME 32 at PDL 15 either by lipofectin transfection of expression vectors, or by infection of recombinant retroviruses, containing p53 mutants. Since these cell strains were previously characterized by our laboratory for *in vitro* lifespan (Van Der Haegen and Shay, 1993), extension of lifespan is determined as a cell strain proliferating greater than 10 PDL past their oldest observed senescence point. Of 123 total clones obtained, 34 (28%) were able to bypass the M1 stage of cellular senescence and continue proliferating exhibiting an 'extended lifespan' (summarized in Table 1a). Table 1b shows the range of extended lifespan for those clones able to bypass M1 and the mean PDL of extended lifespan *in vitro*. Lipofectin transfection yielded more clones capable of extension of lifespan than did defective retroviral infections (Figure 1a). HME 31 cells had 24% of lipofectin transfected clones with extended lifespan in culture in comparison to 7.7% of infected clones (Figure 1a). Figure 1b summarizes the relative efficiencies of the promoters driving the mutant p53 constructs used in this study to overcome M1. Clones with extension of lifespan were more readily obtained via lipofectin transfection with a CMV promoter from HME 32 compared to HME 31 and one clone was able to bypass the M2 stage and immortalize (Figure 1c).

Table 2 summarizes the extension of lifespan of HME 31 and 32 for each mutant p53 introduced. HME cells were transfected with the expression plasmid (pRc/CMV) containing the p53 mutations at either codon $143^{ala}$, $175^{his}$, $248^{trp}$ or $273^{his}$ respectively, or infections with defective retroviral construct pZipneo SV(X) containing $143^{ala}$, $175^{his}$, $248^{trp}$, or $273^{his}$ respectively. The two most frequently observed p53 mutations in human cancers, e.g., $248^{arg}$ and $273^{his}$ (Hollstein *et al.*, 1991), demonstrated extended lifespan in all clones isolated from HME 32 and in one instance an immortalized clone was obtained (HME 32 (273)-1). Introduction of the expression vectors without p53 mutants did not result in extension of lifespan or spontaneous immortalization in any instance (Table 2).

### *Analysis of mutant p53 proteins by Western blot*

Western blot analysis of protein extracts from HME cells expressing transfected p53 mutants with mono-

clonal antibody PAb DO-1 revealed p53 overexpression in the 143, 175, 248 and some but not all of the 273 clones. Overexpression was not observed however in the immortalized clone, HME 32(273)-1, nor HME 32 (273)-6, another 273 clone that did not immortalize (Figure 2a). Figure 2b shows protein levels of p53 and pRb in young and senescent HME cells and reveals that pRb levels decrease in both senescent HME 31 and 32 cells and may explain the 100-fold greater frequency of immortalization of mammary epithelial cells versus stromal cells (Pollock, 1992). Western analysis of the MDM2 protein revealed no overexpression of this known p53 transcription target (data not shown). Experiments were then undertaken to determine if the overexpression of the temperature sensitive mutant p53 $143^{ala}$ could repress cell growth when the wild-type conformation of p53 was expressed (32°C). While the cells continued to proliferate when the mutant conformation was expressed (37°C), the cells markedly decreased proliferation within 24 h when shifted to 32°C (wild-type p53 conformation) in both HME 31 and 32. This was evidenced by cell counts taken at 12, 24, 36 and 48 h after temperature shift to 32°C. For the clones containing the $143^{ala}$ p53 mutant, the decrease in the total cell count was 43% of the control cells. By 48 h in culture, cell counts were 28% of the control counts. Three weeks in culture revealed the mean percentage of HME 31 (143)-1 and HME 32 (143)-1 cells to be 13% of their respective controls. Thus overexpression of the wild-type p53 without DNA damage induction (Smith *et al.*, 1995) inhibits HME growth irrespective of the age of the cells.

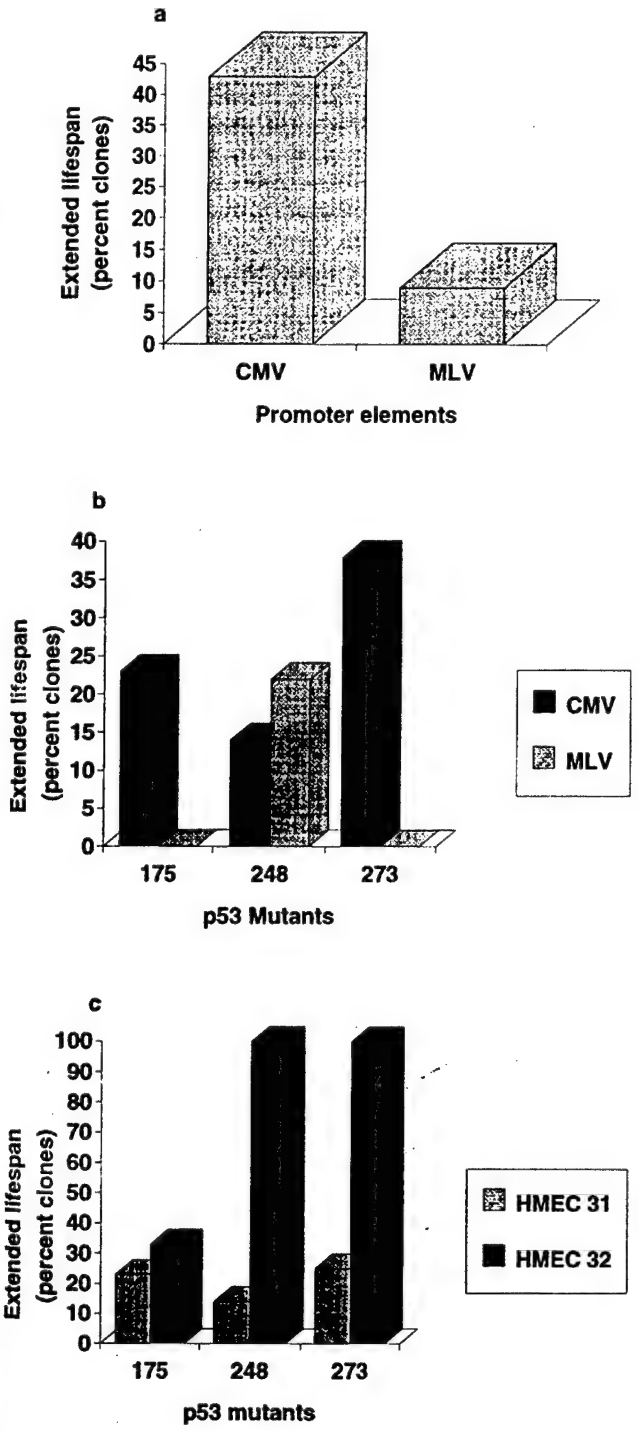


**Figure 1** (a) The relative efficiency of the promoters used to introduce mutant p53 into the cells in this study to bypass M1 and induce extension of lifespan. CMV: cytomegalovirus promoter; MLV: Moloney murine leukemia virus promoter-enhancer sequences. (b) Comparison of the p53 mutants introduced via each vector and their ability to extend lifespan in culture. p53 mutants are: $175^{his}$, $248^{trp}$, $273^{his}$. (c) Variability between cell strains is illustrated by comparing the efficiency of bypassing M1 and extending *in vitro* lifespan

*Analysis of the temperature sensitive mutant p53 $143^{ala}$*

To determine relative levels of mutant $143^{ala}$ p53 expression, immunoprecipitations were performed (Zhang *et al.*, 1992). HME 32 cells expressing p53 mutant $143^{ala}$ were immunoprecipitated with monoclonal antibodies PAb 240, PAb 1620 and PAb DO-1 at both the permissive and nonpermissive temperatures (Figure 3). While a strong signal using PAb 240 was observed, detection with PAb 1620 yielded weak signal at 37°C. However, at 32°C, there was a significant decrease in the expression of mutant p53 and correspondingly, an increase in signals exhibited by PAb DO-1 and PAb 1620.

Control HME 31 and HME 32 cells were cultured at both temperatures to determine growth rates as well as to observe morphological alterations. Figure 4 shows, as expected, normal cells at 32°C grow much slower. Photomicrographs representative of the morphologies observed from these cells are illustrated in Figure 5. Normal cells at 32°C and 37°C and p53 $143^{ala}$ mutant transfected cells at 37°C share the same phenotype in culture whereas the mutant transfected cells at 32°C (wild-type conformation) become large and flat.

*Analysis of immortalization of HME 32 with p53 mutant $273^{his}$*

HME 32 transfected with the 'hot spot' p53 mutant $273^{his}$ were able to bypass the M1 stage and after an extended crisis period also escaped from the M2 stage. Characterization of the immortalization process was followed by several techniques including terminal telomere restriction fragment (TRF) analysis, telomerase activity assays using the telomeric repeat amplifica-

tion protocol (TRAP), p53 DNA binding reporter assays, chromosome counts, number of population doublings in culture, as well as Western blot analysis with several p53 reactive antibodies. The presence of the original mutant p53 vector introduced was confirmed by PCR amplification of a 347 bp fragment from the CMV promoter region while the presence of the mutant within the genomic p53 gene was confirmed by SSCP (G Tomlinson, personal communication).

The frequency of immortalization was calculated by determining the total number of cells plated and collected using what is essentially a fluctuation analysis (Shay *et al.*, 1993a). From this number, the likelihood of the single HME 32 (273)-1 clone escaping from crisis (e.g. M2) was estimated to be $2 \times 10^{-7}$. This figure is consistent with the range previously determined for human fibroblasts (Shay *et al.*, 1993a) but lower than that for HME cells expressing human papillomavirus 16 E6/E7 or SV40 T antigen (Shay *et al.*, 1993a).

Western blot analysis showed that the mutant p53 $273^{his}$ protein product was not overexpressed in the immortalized clone. Levels of p53 remained comparable at all PDLs examined (Figure 6).

In order to verify the expression of mutant p53 $273^{his}$ protein products and the lack of wild-type p53 in the immortal cells, transient transfections were performed by cotransfection of a LacZ reporter construct containing either the p53 consensus sequence or RGC consensus sequence and a luciferase reporter gene. The p53CON and ribosomal gene cluster (RGC) are DNA sequences that had been identified by their ability to bind wild-type p53 either alone (RGC) or as part of a nuclear complex (p53CON) (Kern *et al.*, 1992; Funk *et al.*, 1992). Chen *et al.* (1993) previously showed that transcriptional activation by $273^{his}$ of the p53con sequence is comparable to wild-type activity, while little transcriptional activity is observed with the RGC consensus sequence. Figure 7 illustrates that while wild-type HME transactivation is high for both p53CON and RGC, the immortalized HME cells containing the $273^{his}$ mutant exhibit minimal transactivational activation of the RGC consensus but strong activity to the p53CON sequence.

PCR amplification using primers custom synthesized for the pRc/CMV promoter sequence revealed the presence of the construct in the HME 32 (273)-1 clone and the pRc/CMV 273 positive control but not in the parental HME 32 cell strain (Figure 8).

TRF results are illustrated in Figure 9. Normal HME 32 have an average length of approximately 7–8 kb at population doubling 20 (PDL 20). The HME 32(273)-1 cells at PDL 60 show a significant decrease in average telomere length to approximately 3–4 kb (nearly 100 bp of the telomeres are lost per doubling). By PDL 80 there is no further shortening and telomere length has stabilized at about 2 kb. Additional TRF analysis at PDL 225 showed no change in the telomere length from that observed at PDL 80 and 100 (data not shown).

A PCR based assay for the measurement of telomerase activity (Kim *et al.*, 1994; Piatyszek *et al.*,

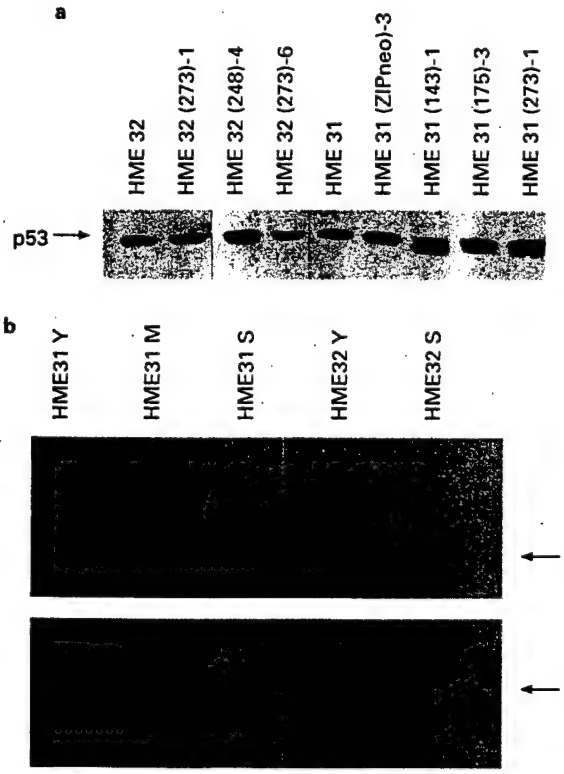


**Figure 2** (a) p53 expression levels are illustrated from representative p53 mutant clones. Each lane contains 40 $\mu$g of protein and p53 was detected using anti-p53 monoclonal antibody PAb 1801. All clones shown were lipofectin transfected for the p53 mutants. (b) Relative levels of endogenous p53 and pRb are shown for young and senescent normal HME. p53 levels were detected using PAb 1801. Monoclonal antibody MAb-1 was used to detect levels of pRb

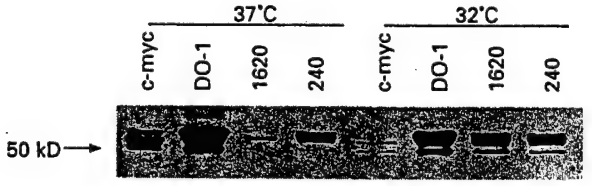


**Figure 3** Immunoprecipitation results for the p53 conformation of the p53 temperature sensitive mutant $143^{ala}$ p53 was immunoprecipitated with the indicated antibodies at 37°C and 32°C from HME 32 cells transfected with the $143^{ala}$ p53 mutant as described in the Methods section. An antibody against c-myc was used as a negative control. KDa: molecular weight protein markers sizes

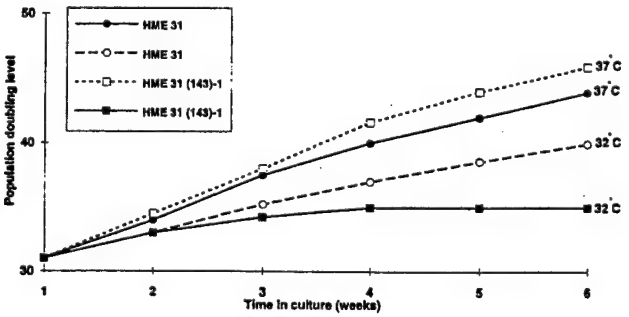


**Figure 4** Growth of HME at 32°C and 37°C. Cultures at 32°C were approximately 3–4 PDL slower than those at 37°C. Proliferation was markedly decreased by 24 h in culture after temperature shift to 32°C. By 3 weeks, cell counts in the transfected cells were 10% that of the control cells

1995) was performed (Figure 10). The parent cells at PDL 20, and precrisis HME 32(273)-1 cells PDL 41 had no detectable telomerase activity while from PDL 60 on, HME 32 (273)-1 did. This is consistent with a rare telomerase positive clonal population emerging around PDL 50–60 and quickly predominating the population of cells which were initially heterogeneous with a population of normal cells undergoing crisis and continuing to shorten their telomeres. Co-amplification of a genomic internal DNA standard (ITAS) indicated that there were not PCR inhibitors present in the extracts which could yield false negatives. Quantitation against this standard also revealed that there was no significant increase in the activity of telomerase with increasing PDL.

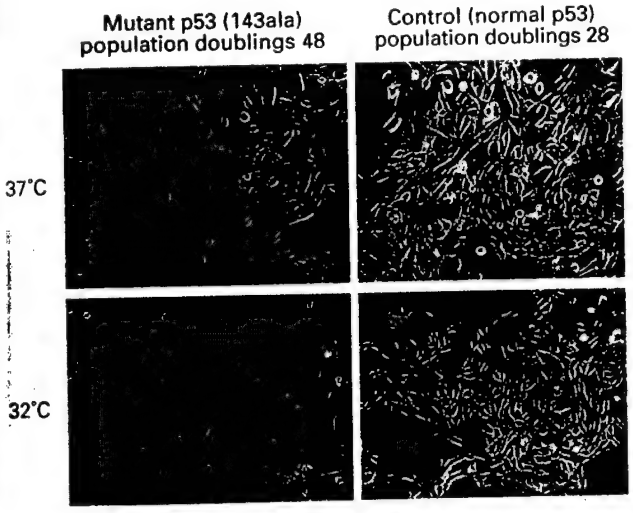


**Figure 5** Photomicrographs representative of temperature effects on the conformation of the p53 mutant $143^{ala}$ introduced into HME cells. Morphologically there was no difference in cell appearance for control and $143^{ala}$ expressing cells at 37°C nor for the control cells at 32°C. At 32°C however, there was a marked change in the morphology toward a senescent-like phenotype. At 37°C, $143^{ala}$ has a mutant conformation and no DNA transactivation activity. At 32°C the mutant exists in a wild-type conformation, resulting in overexpression of wild-type p53, cell enlargement and inhibition of cell proliferation

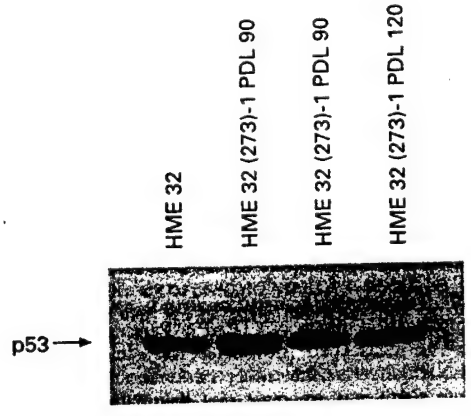


**Figure 6** Western blot analysis of the p53 expression levels for HME 32 and HME 32 (273)-1 at different times in culture. Extracts were detected using the PAb DO-1 antibody (20 $\mu$g were loaded per lane). No significant increase in p53 expression was observed

Metaphase spreads were counted on HME 32(273)-1 cells after 150 PDLs in culture. Analysis consisted of counting 27 random metaphase spreads. Of the spreads counted, a range of 62–139 chromosomes was observed. The median chromosome spread value was 81. Eleven percent of the population was pseudotetraploid, 22% were triploid, with the remaining 67% aneuploid.

## Discussion

The onset of breast cancer is generally associated with increased aging except in cases of Li-Fraumeni Syndrome and familial breast cancers (Li *et al.*, 1988; Malkin *et al.*, 1990; Kessler, 1992; Smith *et al.*, 1992; Malkin, 1993). Previously, it has been reported that abrogation of normal p53 function may be important in the immortalization of HME cells (Band *et al.*, 1991; Shay *et al.*, 1993a,b). The present study illustrates that

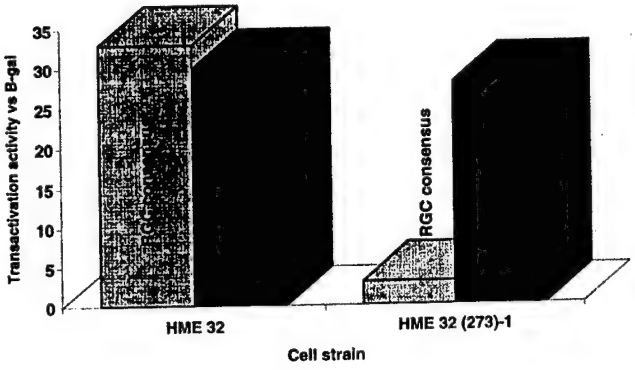


**Figure 7** Luciferase activity analysis. The transactivation activity of HME 32 and HME 32 (273)-1 was standardized against $\beta$-galactosidase activity electroporated into both parental cells HME 32 and the clone HME 32 (273)-1. The transactivation activity refers to the luciferase activity as measured against basal $\beta$-gal activity in the control cells. Immortal cells were tested at PDL 250, normal cells at PDL 18

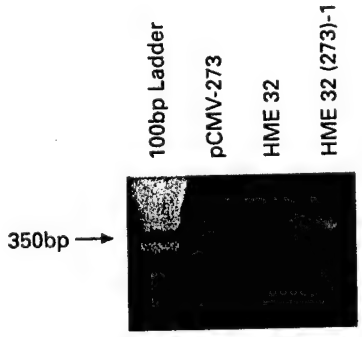


**Figure 8** Polymerase chain reaction analysis to detect the presence of the pRc/CMV construct within the immortalized clone. DNA from the originally transfected construct was used as a positive control. Normal HME 32 cells were tested at PDL 18. As shown, the presence of the construct is confirmed in the clone but not the parental cell strain. A 347 bp fragment of the CMV promoter region is the product from the PCR reaction

some but not all p53 mutants can neutralize the M1 mechanism of cellular senescence in human mammary epithelial cells (HME) in culture. Previous studies have shown that for most human cells to abrogate the M1 stage of cellular senescence both p53 and an Rb-like function must be overcome (Munger *et al.*, 1989; Woodworth *et al.*, 1989; Watanabe *et al.*, 1989; Band *et al.*, 1990). While HPV16 E6 only gives partial extension of lifespan in IMR90 fibroblasts as does HPV16 E7, combinations of the two result in the full extension of lifespan (Shay *et al.*, 1993a). Thus, for cells to reach the M2 stage and have the potential to immortalize, the cellular mechanisms involved in the M1 mechanism must be fully overcome. It has been shown that for HME cells, abrogation of only p53 is required to fully overcome the M1 stage. HPV16 E6 results in most HME cells reaching M2 and then a relatively rare cell in the population immortalizes (Shay *et al.*, 1993a). In addition, we recently reported the spontaneous immortalization of HME from a patient with Li-Fraumeni Syndrome (germline mutation in p53). Wazer *et al.* (1995) recently showed immortalization of distinct mammary epithelial cell types by HPV 16 E6 or E7 while Tsutsui *et al.* (1995) demonstrated extension of *in vitro* lifespan with the carcinogen aflatoxin B1. The present study extends these observations further to demonstrate that expression of mutant p53 into normal HME can also result in immortalization. The clone HME 32 (273)-1 was observed to have telomeres that continued to shorten with progressive subculturing as well as the reactivation of telomerase upon overcoming M2. PCR revealed the presence of the p53 mutant construct within the cells, SSCP showed the presence of the mutant allele (G Tomlinson, personal communication), while continuous subculturing has the cells currently at PDL 300. These observations taken together provide evidence for the immortalization of HME 32 by p53 mutant $273^{his}$.

We observed different relative efficiencies of expression vectors carrying mutant p53 to extend lifespan of the HME cells. The CMV expression vectors containing p53 mutants were more efficient in extending lifespan and abrogating wild-type p53 function (as indicated by immunoblotting and immunoprecipitations) but less so than HPV16 E6 (which degrades p53) in which over 90% of the clones had extension of lifespan (Shay *et al.*, 1993a). The p53 mutants carried in the defective retroviral vectors were not only less effective in inducing extension of lifespan but also did not give rise to any immortal clones. Thus,

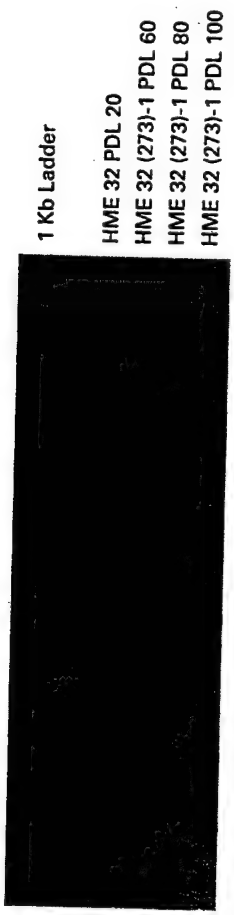


**Figure 9** TRF analysis by Southern blot. Immortal cells at PDL 60, 80 and 100 were analysed for decreasing telomere length *vs* normal, parent cells at PDL 23. A 24-mer, $(TTAGGG)_4$, was used as a probe. Telomeres stabilized to approximately 2.5 kb in length

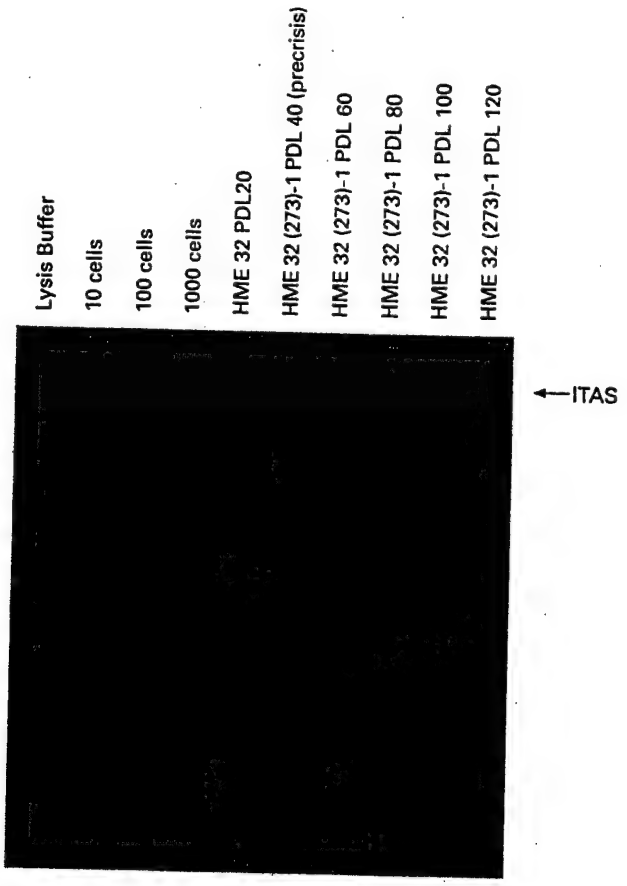


**Figure 10** Telomerase activity analysed using the telomeric repeat amplification protocol (TPAP). Parental cells (PDL 20) and precrisis cells had no detectable telomerase activity. Telomerase activity was first observed at about PDL 60 with no subsequent significant increase in telomerase activity with increasing passage as measured against the internal telomerase amplification standard (ITAS) as described in the Methods. Controls consisted of lysis buffer, dilutions of 10 cell, 100 cell and 1000 cell equivalents of a telomerase expressing cell line immortalized with HPV 16 E6/E7 mixed with normal cells from the original parent strain

telomeric probe $(TTAGGG)_4$ for 12 h followed. After washing three times in 0.1 × SSC at room temperature (7 min each), the gel was either exposed to X-ray film or analysed on a phosphorimaging device (Phosphors/Imager, Molecular Dynamics, Sunnyvale, CA).

*Telomerase assays*

A one tube PCR-based telomerase assay was performed as originally described (Kim *et al.*, 1994) with some modifications (Wright *et al.*, 1995). The assay was performed in two steps: (1) Telomerase mediated extension of an oligonucleotide primer (TS), which serves as a substrate for telomerase; and (2) PCR amplification of telomerase activity product (an incremental 6 nt ssDNA ladder) with the oligonucleotide primer CX in a competitive amplification reaction with a 150 bp fragment encoding aa 97–132 of rat myogenin as an internal telomerase amplification standard (ITAS).

Details of the method are as follows: For the cells in culture, $10^5$ cells were pelleted in culture medium. The supernatant was removed and the dry pellet stored at −80°C. The cells were lysed with 20 μl of ice cold lysis buffer consisting of 0.5% CHAPS, 10 mM Tris-HCl (pH 7.5), 1 mM $MgCl_2$,1 mM EGTA, 10% glycerol, 5 mM beta-mercaptoethanol, 0.1 mM AEBSF and left on ice for 30 min. The lysate was centrifuged at 14 000 r.p.m. for 20 min at 4°C, and 160 μl of supernatant was collected into an Eppendorf tube making sure that no traces of the pellet were withdrawn; flashfrozen in an EtOH-dry ice bath and then stored at −80°C. Generally 2 μl of each lysate was analysed containing the equivalent of approximately 1000 cells. In some instances the concentration of the protein in the extract was measured using the BCA protein assay kit (Pierce Chemical Company, Rockford, IL) and an aliquot of the extract containing approximately 6 μg of protein used for each telomerase assay.

Specificity of the processive 6 nt ladder is demonstrated by RNAse treatment. For RNAse controls, 5 μl of extract is incubated in 1 μg of RNAse (5′–3′, Boulder, CO) for 20 min at 37°C. A 2 μl aliquot of extract is then assayed in 50 μl of reaction mixture containing 50 μM each dNTP, 344 nM of TS primer (5′-AATCCGTCGAGCAGAGTT-3′), and 0.5 μM of T4 gene 32 protein (USB, Cleveland, OH), [α32P]dCTP, 5 attograms ITAS and 2 units of Taq polymerase (Gibco/BRL, Gaithersburg, MD) in a 0.5 ml tube which contained the CX primer (5′-CCCTTACCCTTACCCTTACCCTAA-3′) at the bottom sequestered by a wax barrier (Ampliwax™, Perkin-Elmer, Foster City, CA). After 30 min of incubation at room temperature for telomerase mediated extension of the TS primer, the reaction mixture is heated to 90°C for 90 s for inactivation of telomerase, and then subjected to 31 PCR cycles of 94°C for 30 s, 50°C for 30 s, and 72°C for 45 s. The PCR products were electrophoresed on a 10% acrylamide gel as previously described (Kim *et al.*, 1994). Since human telomerase is processive, during the initial 30 min of incubation, in the presence of the TS primer, varying numbers of hexameric repeats are added to the primer and when subsequently amplified yield a 6 bp DNA incremental ladder. Extracts from the samples not containing telomerase do not extend the TS primer (Kim *et al.*, 1994).

*Metaphase spread analysis*

Methods for obtaining metaphase spreads were described previously (Aldaz *et al.*, 1989). Cultures were incubated with 0.01 μg/ml Colcemid (Gibco/BRL, Gaithersburg, MD) in fresh medium for 4 h. After collection by trypsinization, cells were incubated for 1 h at 37°C in a 0.067 M KCl hypotonic solution then fixed in 3:1 methanol:glacial acetic acid, rinsed and spun 2× for 5 min each at 1200 r.p.m. After resuspension in 1–2 ml of fix, pellets were dropped onto precleaned microscope slides and stained with Giemsa Stain (Sigma Chemical Company, St. Louis, MO). Chromosomes were counted from >25 randomly chosen metaphase spreads.

*Fluctuation analysis*

The frequency of escape from crisis (e.g. immortalization frequency) was estimated using an approach based on what is essentially a fluctuation analysis previously described (Shay *et al.*, 1993a). Clones were expanded several population doublings before crisis into multiple series in several sizes of culture dishes at a constant cell density. Each series was subsequently maintained as a separate culture, so that at the end of the experiment the fraction of each series that gave rise to an immortal cell line could be determined. Using different size dishes permitted series to be set up which contained a different number of cells per dish while maintaining a constant culture environment (cells/cm²). Cultures were split at or just prior to confluence. Once cells reached crisis, they were split (at least once every 3 weeks) until only a few surviving cells remained or the culture had immortalized. Immortalization was expressed as the number of immortal lines per number of culture series. Frequency is expressed as the probability of obtaining an immortal cell line based on the total number of independent immortalization events and dividing by the total number of cells plated.

**Acknowledgements**

We thank Dr John Minna (Hamon Center, UT Southwestern Medical Center, Dallas, TX) for providing the mutant p53 expression constructs; and Dr Curtis Harris (National Cancer Institute, Bethesda, MD), for the retroviral vectors. In addition we thank JF Train, JP Suits and I Dac-Korytko for technical assistance and Drs SE Holt and WE Wright for helpful suggestions. This study was supported by USAMR research grant DAMD-94-J-4077 and postdoctoral support from USAMR, DAMD17-94-J-4023.

**References**

Aldaz CM, Trono D, Larcher F, Slaga TJ and Conti CJ. (1989). *Carcinogenesis*, **2**, 22–26.

Allsop RC, Vazirir H, Patterson C, Goldstein S, Younglai EV, Futcher AB, Greider CW and Harley CB. (1992). *Proc. Natl. Acad. Sci. USA*, **89**, 10114–10118.

Band V, Zajchowski D, Kulesa V and Sager R. (1990). *Proc. Natl. Acad. Sci. USA*, **87**, 463–467.

Band V, De Caprio JA, Delmolino L, Kulesa V and Sager R. (1991). *J. Virol.*, **65**, 6671–6676.

Bond JA, Wyllie FS, Wynford-Thomas D. (1994). *Oncogene*, **9**, 1885–1889.

Callahan R and Campbell G. (1989). *J. Natl. Cancer Inst.*, **81**, 780–786.

Chen J-Y, Funk WD, Wright WE, Shay JW and Minna JD. (1993). *Oncogene*, **8**, 2159–2166.

Cho Y, Gorina S, Jeffrey PD and Pavelitch NP. (1994). *Science*, **265**, 346–355.

Counter CM, Avilion AA, LeFeuvre CE, Stewart NG, Greider CW, Harley CB and Bacchetti S. (1992). *EMBO J.*, **11**, 1921–1929.

Counter CM, Hirte HW, Bacchetti S and Harley CB. (1994). *Proc. Natl. Acad. Sci. USA*, **91**, 2900–2904.

Oncogene (1998) 17, 709–717
© 1998 Stockton Press All rights reserved 0950–9232/98 $12.00
http://www.stockton-press.co.uk/onc

# Telomerase activity during spontaneous immortalization of Li-Fraumeni syndrome skin fibroblasts

Lauren S Gollahon[1,5], Eliyahu Kraus[2], Tian-Ai Wu[2], Sun O Yim[2], Louise C Strong[3,4], Jerry W Shay[1] and Michael A Tainsky[2]

*[1]Department of Cell Biology and Neuroscience, UT Southwestern Medical Center, 5323 Harry Hines Blvd., Dallas, Texas 75235-9039; [2]Department of Tumor Biology; [3]Department of Experimental Pediatrics; [4]Department of Molecular Genetics, The University of Texas, MD Anderson Cancer Center, 1515 Holcombe Blvd., Houston, Texas 77030, USA*

**Li-Fraumeni Syndrome (LFS) is characterized by heterozygous germline mutations in the p53 gene. Accompanied by genomic instability and loss or mutation of the remaining wild type p53 allele, a low frequency of spontaneous immortalization in LFS fibroblasts occurs. It is believed that the loss of p53 wild type function contributes to immortalization of these LFS fibroblasts, but it is not clear if this is sufficient. Because stabilization of telomere length is also thought to be a necessary step in immortalization, telomerase activity, expression of the telomerase RNA component (hTR) and telomere length were analysed at various passages during the spontaneous immortalization of LFS skin fibroblasts. One LFS strain which immortalized, MDAH087 (087), had no detectable telomerase activity whereas another LFS strain which immortalized, MDAH041 (041), had detectable telomerase activity. In preimmortal cells from both strains, hTR was not detected by *in situ* hybridization. Immortal 087 cells remained negative for hTR, while immortal 041 cells demonstrated strong hTR *in situ* hybridization signals. 087 cells had long and heterogenous telomeres whereas telomeres of 041 cells had short, stable telomere lengths. Tumorigenicity studies in nude mice with *ras*-transformed 087 and 041 cells resulted in both cell lines giving rise to tumors and retaining telomerase status. Overall these results suggest that strain specificity may be important in telomerase re-activation and that both abrogation of p53 function and a mechanism to maintain telomeres are necessary for immortalization.**

**Keywords:** p53; telomeres; ALT pathway; senescence; cell hybrids

## Introduction

Cellular immortalization is thought of as the capacity for normal diploid cells to escape cellular senescence. There appear to be two discrete stages, Mortality stage 1 (M1) and Mortality stage 2 (M2), that need to be overcome for human cells to bypass normal senescence programming before immortalizing (Wright *et al.*, 1989; Wright and Shay, 1992). Cells may be immortalized through the introduction of viral and cellular oncogenes such as SV40 large T-antigen (Huschtscha and Holliday, 1983; Mayne *et al.*, 1986; Shay *et al.*, 1993a; Van Der Haegen and Shay, 1993), adenovirus E1A/E1B (Graham and Smiley, 1977; Ross *et al.*, 1978; Sarnow *et al.*, 1982), high risk strains of human papillomavirus (Band *et al.*, 1993; Scheffner *et al.*, 1990; Shay *et al.*, 1991a, 1993b; Watanabe *et al.*, 1993; Werness *et al.*, 1990), mutant p53 (Eliyahu *et al.*, 1984b; Gao *et al.*, 1996; Gollahon and Shay, 1996; Rogan *et al.*, 1995; Slingerland *et al.*, 1993; Wyllie *et al.*, 1993), various human oncogenes such as c-*myc*, H-*ras* (Avery *et al.*, 1944; Bischoff *et al.*, 1991; Eliyahu *et al.*, 1984a; Gutman and Wasylyk, 1991; Lemoine *et al.*, 1990), and rarely, spontaneously (Bischoff *et al.*, 1990; Rogan *et al.*, 1995; Shay *et al.*, 1995). Fibroblast cells appear to immortalize less frequently than epithelial cells (Shay *et al.*, 1993a), suggesting that the frequency of immortalization may be cell lineage specific (Gao *et al.*, 1996; Gollahon and Shay, 1996; Hsiao *et al.*, 1997; Huschtscha and Holliday, 1983; Rainey *et al.*, 1994; Shay *et al.*, 1993a; Van Der Haegen and Shay, 1993; Wazer *et al.*, 1995; Wright *et al.*, 1989; Wyllie *et al.*, 1993). The requirements to overcome the M1/M2 cellular senescence program appear to be more stringently regulated in fibroblasts than in epithelial cells (Bischoff *et al.*, 1990, 1991; Mayne *et al.*, 1986; McCormick and Maher, 1988; Shay *et al.*, 1993a,b; Wright *et al.*, 1989) although a molecular explanation for this has not been determined.

Complementation studies of somatic cell hybrids (Pereira-Smith and Smith, 1988) have demonstrated that some immortal × immortal cell fusions may still senesce depending on the cell combinations used and that all mortal × immortal hybrids senesce suggesting that mortality is a dominant trail (Karlsson *et al.*, 1996; Wright *et al.*, 1996). In addition, several studies of cellular senescence induced by microcell chromosome mediated fusion have been reported (Barrett, 1993; Ohmura *et al.*, 1995; Saski *et al.*, 1994). One study demonstrated that the specific introduction of chromosome 3 but not other chromosomes into an immortal human renal cell carcinoma line expressing telomerase resulted in the downregulation of telomerase activity, progressive loss of telomere length, and eventual inhibition of cell growth (Ohmura *et al.*, 1995).

The ribonucleoprotein enzyme telomerase has been shown to be active in 85% of primary human tumors tested (Bacchetti and Counter, 1995; Shay and Bacchetti, 1997) and in over 90% of tumor-derived and experimentally immortalized cell lines (Avilion *et al.*, 1996; Bacchetti and Counter, 1995; Shay and Bacchetti, 1997; Shay and Wright, 1996). The proposed

Correspondence: LS Gollahon
[5]Current address: Department of Biological Sciences, PO Box 43131, Texas Tech University, Lubbock, Texas, 79409-3131, USA
Received 20 October 1997; revised 19 March 1998; accepted 19 March 1998

function of telomerase is thought to be in the maintenance of telomeric length in immortal cells. Telomeric repeats (TTAGGG) are lost with each successive cell division since DNA polymerase cannot completely replicate the end of a DNA duplex (Blackburn, 1991, 1994; Greider, 1991; Harley and Villaponteau, 1995; Olovnikov, 1973; Watson, 1972). This 'end replication problem' is considered an important biological timing mechanism (clock) that may determine the replicative capacity of all somatic cells which lack or have low levels of telomerase (Harley, 1991). The upregulation or reactivation of telomerase appears to correlate with unlimited proliferation potential of a cell, and telomere stability (Shay *et al.*, 1991b).

Telomeres are also important in the maintenance of chromosomal stability (Counter *et al.*, 1992; Murnane *et al.*, 1994). In cells that bypass the normal cellular senescence pathway (Shay *et al.*, 1991b), the reactivation of telomerase occurs when the telomeres have reached a critically shortened length (Harley *et al.*, 1990). Currently, there are no reports of telomerase-negative tumor-derived cell lines with short telomeres (<8 kb) (Avilion *et al.*, 1996; Harley *et al.*, 1994; Shay and Bacchetti, 1997). However, several examples of experimentally immortalized cultured cell lines have been reported that proliferate indefinitely with long, heterogenous telomere lengths, without the presence of detectable telomerase activity (Bryan *et al.*, 1995; Duncan *et al.*, 1993; Mayne *et al.*, 1986; Murnane *et al.*, 1994; Wright *et al.*, 1989; Wright and Shay, 1992).

The present report demonstrates that the ability to re-activate telomerase or to utilize the ALT pathway to immortalization may be strain-specific in fibroblasts derived from individuals with LFS. Our results indicate that in LFS 087 (tel−) fibroblasts, immortalization appears to correlate with p53 status but not telomerase reactivation, whereas in the 041 (tel+) LFS fibroblasts, loss of functional p53 and telomerase reactivation appear to occur at approximately the same time. However, spontaneous immortalization of telomerase negative LFS fibroblasts appears to retain telomere lengths greater than a preprogrammed, specific critical length. Additionally, this is the first report of human tumor formation in nude mice by a telomerase negative cell line (087), suggesting that telomerase activity is not always requisite for tumorigenesis.

## Results

### *LFS cell growth characteristics*

Normal skin fibroblasts from Li-Fraumeni patients heterozygous for a germline p53 mutation only rarely evolve into immortal cell lines. The molecular mechanism of immortalization is not well understood but is a long process often involving many months of cell culture to obtain a rare clone that immortalizes. In culture, LFS fibroblasts enter a growth crisis period at approximately 25–35 population doublings (PD) characterized by the cells only rarely dividing and mostly dying. During this crisis period, the chromosomes in these cells are highly unstable (Bischoff *et al.*, 1990). After a considerable amount of time (6–12 months), a rare cell in the population reinitiates slow growth until approximately 65 PD at which time the growth rate progressively increases (Bischoff *et al.*, 1990).

### *Telomerase activity and p53 status in 087 and 041 cells*

Li-Fraumeni fibroblasts from two patients were studied. The 087 fibroblasts contain a p53 allele with a missense point mutation at amino acid 248. The 041 fibroblasts contain a p53 allele with a point deletion at amino acid 184. This generates the translation of 60 amino acids from the resulting frameshift that are not normally in the p53 protein followed by a premature stop codon (Table 1). In order to determine whether the loss of wild type p53 is sufficient for the reactivation of telomerase activity, DNA prepared from LFS fibroblasts was analysed at various passages for p53 mutations by single strand conformational polymorphism (SSCP) and protein extracts for telomerase activity (Figure 1). In all LFS fibroblasts examined, the remaining wild type p53 allele was lost (041 cells) or replaced with a mutant p53 allele (087 cells) by PD 67 and absent from all subsequent PD (data not shown). Cell protein extracts from these fibroblasts were analysed for the presence of telomerase activity at various PD during their growth in culture and for loss of p53 protein by Western blot. We

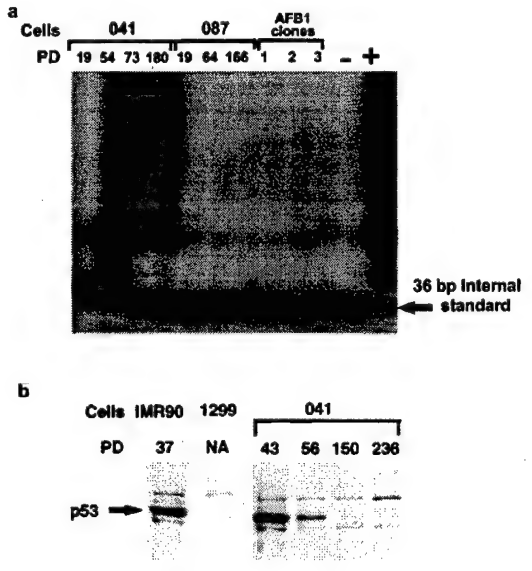


**Figure 1** Telomerase activity in 041 and 087 cells and p53 protein expression levels in 041 cells. (**a**) TRAP gel showing results of telomerase activity in 041 and 087 cells precrisis (PD 19) and postcrisis (PD 54 and 64, respectively). Aflatoxin B1 (AFB1) clones were obtained from AFB1 induced immortalization of 087 cells. These AFB1 clones were analysed after 100 PD in culture. Negative control (−) is lysis buffer only and positive control (+) is a cell extract obtained from HT1080 cells. (**b**) p53 immunoblot showing the levels of p53 in 041 cells (p53 null) precrisis (PD 43) and postcrisis (>PD 56). Note that there appears to be lower levels of p53 in 041 cells at PD 56 perhaps indicating selection for the p53 null, telomerase positive cells. Control cells: IMR90, normal diploid lung fibroblasts; 1299, non-small cell lung carcinoma derived; telomerase positive, p53 null immortal cell line. NA – not applicable

observed that at PD 19, 26, 30 and 35, 041 cells had no telomerase activity and p53 was still present. Between PD 54 and PD 67, 041 fibroblasts had lost p53 protein (Figure 1b) and gained detectable telomerase activity that was continuously maintained (Figure 1). Since 041 fibroblasts prior to PD 54 did not have detectable telomerase and lost p53 protein at approximately the same time as telomerase reactivation (Figure 1a), the direct loss of the remaining functional wild type p53 allele appears to correlate with reactivation of telomerase activity.

The spontaneous immortalization of the 087 cells was reproduced consistently, (this study and Bischoff *et al.*, 1990), and therefore represented a good strain to study the frequency of telomerase activation in immortalization. In addition, it has been reported (Tsutsui *et al.*, 1995) that enhancement of the immortalization frequency of 087 cells could be obtained by treatment of cells with aflatoxin B1 (AFB1) and X-ray treatment, (Tsutsui *et al.*, 1997). The 087 cell lines never developed detectable telomerase activity (Figure 1a) in eight of eight independent immortalization experiments including three immortalized by AFB1 (Tsutsui *et al.*, 1995), one immortalized by X-ray irradiation (Tsutsui *et al.*, 1997) and in four spontaneous immortalization events, (present study and Bischoff *et al.*, 1990). From that immortalization study cells were derived from 087+AFB1 and of these, cells capable of indefinite proliferation were also found to be telomerase negative (Figure 1a).

At the time of immortalization, DNA extracts from these cells were examined by SSCP and were found to be homozygous for the p53 mutation at codon 248 (data not shown). Mixing cellular extracts from telomerase negative (087) cells with an extract from a telomerase positive cell line (HT1080) did not result in inhibition of telomerase activity (data not shown) indicating that 087 cells did not contain a diffusable telomerase inhibitor. These data (summarized in Table 1) indicate that the reactivation of telomerase activity during the immortalization of LFS skin fibroblasts may be cell strain-specific.

**Table 1** Summary of mutation analysis of endogenous p53 in fibroblast skin cells obtained from patients with LFS

| *Cell strain* | *p53 mutation* | *Population doubling* | *Telomerase activity* |
|---|---|---|---|
| 041 | 184FS | <36 | − |
| 041 | 184FS | >54 | + |
| 087[a] | R248W | 19–166 | − |
| 087ras[b] Tum$^-$ | R248W | 59 | − |
| 087ras[b] Tum$^+$ | R248W | 104 | − |

[a]Six independent immortalization events. [b]Two independent transfectants

### *TRF analysis*

The telomere lengths in the LFS skin fibroblasts were estimated using TRF (terminal restriction fragment) analysis (Shay *et al.*, 1994) to determine if reactivation of telomerase activity in 041 cells resulted in telomere length stabilization, as well as to determine the telomere dynamics of the telomerase negative 087 cells (Figure 2). In the 041 cells, a progressive loss of telomeric DNA from 9 kb (PD 21) was observed up to the time of detection of telomerase activity (PD 54), followed by stabilization of telomere length at 4 kb

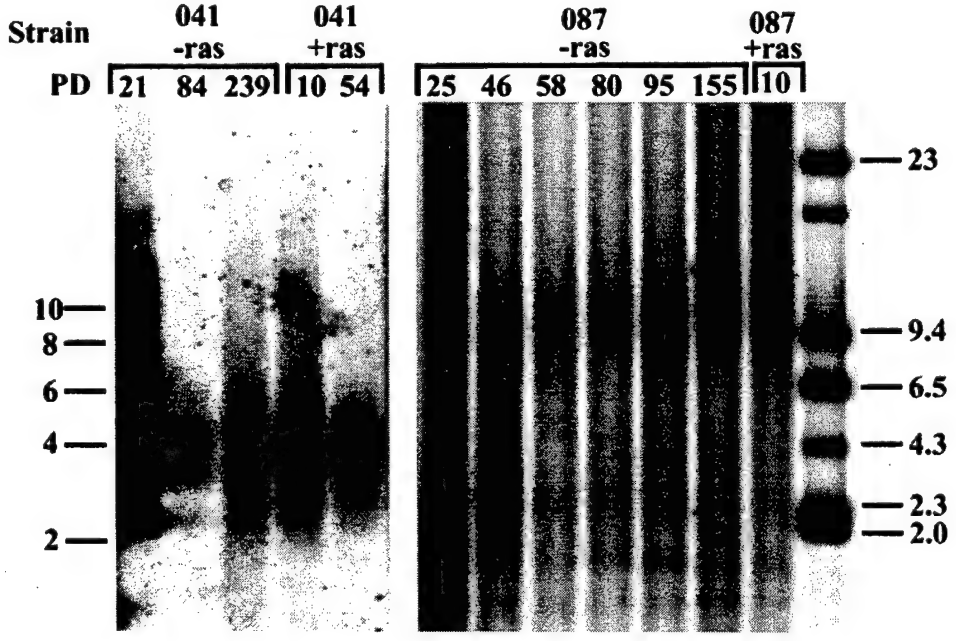


**Figure 2** TRF analysis of 041 cells and 087 cells during increasing PD. The pattern of telomeric signal is similar in the spontaneously immortalized cell lines (−*ras*) as well as the *ras*-induced immortalized cell lines (+*ras*). The initial precrisis 041 cells exhibit 2 major telomere subpopulations (9 kb and 4 kb). The larger is lost and it is a shorter subpopulation that determines the stabilized telomeric lengths. The 087 cells retain 2 primary subpopulations of distinct telomeric lengths (10 kb and 2.5 kb)

(PD 84). In the telomerase negative 087 cells, TRF analysis showed two not very prominent populations of telomere lengths at approximately 10 kb and 2.5 kb. No major fluctuations were observed in telomere lengths analysed over approximately 100 PD in culture.

*The RNA component of telomerase is enhanced in immortal 041 but not 087 cells*

In order to determine whether the RNA component of the telomerase correlates with enzyme activity, telomerase RNA expression levels were determined by *in situ* hybridization for both 041 (tel+) and 087 (tel−) cell precrisis (<30 PD) and postcrisis (<60 PD). A probe specific for the telomerase RNA component was used (Feng *et al*., 1995). As expected for both 041 and 087 preimmortal/precrisis cell strains, the telomerase RNA signal was not above background (Figure 3a and c). Postcrisis/immortal (PD 236), 041 (tel+) exhibited strong telomerase RNA signal (Figure 3b) corresponding with detectable telomerase activity which was maintained at the same levels with continuous passage. In contrast, low or no telomerase RNA signal was observed up to PD 166 for 087 cells (Figure 3d).

*Correlation of telomerase activity with p53 levels*

Introduction of wild type p53 utilizing an inducible tet-repressor into TR-9 cells (gift of G Stark and A Agarwal) was performed in order to explore the possibility of a direct correlation between p53 and telomerase activity. TR-9 cells are immortal 041 fibroblasts that were transfected with a wild type p53 cDNA driven by a tetracycline repressible promoter (Gossen and Bujard, 1992). Concurrently, parallel cultures were exposed to serum at both normal growth concentrations (10%) and low concentrations (0.75%). The rationale for low serum levels was to observe the effects of induced quiescence on telomerase activity and compare this to the effects of p53 induction over time. The inhibition of telomerase by p53 expression was evident after 48 h. In contrast, low serum produced comparable effects on telomerase activity after approximately 2 weeks. As seen in Figure 4a, when tetracycline is removed from the media, p53 is strongly induced and cell growth is arrested. Telomerase activity decreased tenfold over a 7 day period (Figure 4b). These data are consistent with previous observations (Holt *et al*., 1996b, 1997) demonstrating that telomerase competent cells exiting the cell cycle results in downregulation of telomerase activity.

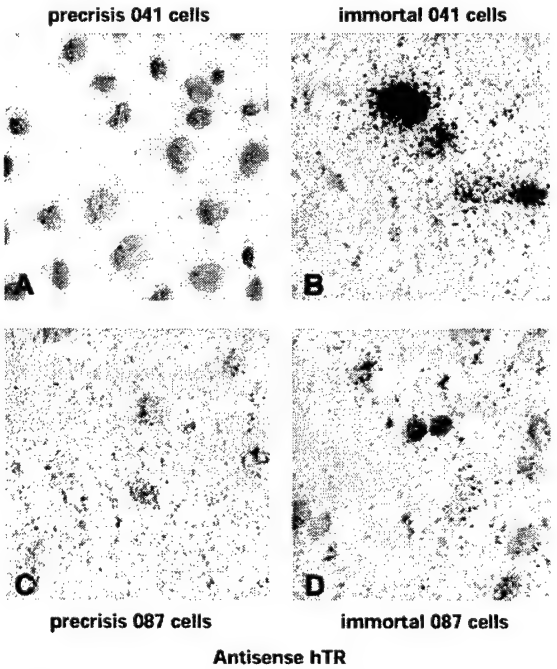


**Figure 3** Composite of representative telomerase RNA (hTR) signal in 041 cells and 087 cells precrisis and postcrisis hybridized with an antisense probe for hTR. 041 cells and 087 cells precrisis showed no telomerase RNA signal above background levels (**a** and **c**). **b** and **d** are 041 cells and 087 cells postcrisis, respectively. Note the intense hybridization signal (arrow) for 041 immortal cells (**b**). In contrast, the 087 RNA signal is comparable to that of the preimmortal cells (**d**)

*Tumorigenicity studies of 041 and 087 cells in nude mice*

Another property of immortalized 041 (tel+) and 087 (tel−) fibroblasts is their susceptibility to *ras* oncogene transformation (Bischoff *et al*., 1991). In order to determine if over-expression of *ras* and/or tumorigenic potential influenced telomerase activation, 041 (tel+) and 087 (tel−) cells at PD 54 and 56, respectively, were transfected with pSV2-neo-H-*ras* (val 12) and control pSV2-neo plasmids. Clonally derived cell lines expressing the H-*ras* oncogene were obtained and maintained on 200 μg/ml G418 (Bischoff *et al*., 1991). Four of five H-*ras* expressing 041 (tel+) clones formed tumors in nude mice with a latency period of 2–3 weeks. Similarly, 5/7 H-*ras* expressing 087 (tel−) clones formed tumors in nude mice with a latency period of 1–3 weeks without detection of telomerase activity (data not shown) (Bischoff *et al*., 1991). The nontumorigenic *ras*-expressing fibroblast 087 clones, have the mutant form of p53 and grow as cell lines without any indication of senescence. After an additional 50 PD in culture, the two 087 (tel−) *ras*-expressing nontumorigenic cell clones became tumorigenic in nude mice. No telomerase activity was detected in 087 (tel−) *ras*-expressing lines that became tumorigenic (data not shown). Figure 5 is a TRAP gel showing telomerase activity of representative 087-*ras* (tel−) clones and 041-*ras* (tel+) clones. The tumors derived from 041 cells all retained telomerase activity (Figure 5). None of the clones (041 or 087) expressing only pSV2-neo (control) formed tumors in nude mice.

*Somatic cell hybrids between 041 or 087 and HT1080*

Somatic cell hybrids were made between 041 (tel+, p53−) X HT1080 (tel+, p53+) as well as 087 (tel−, p53−) X HT1080 (tel+, p53+). We wanted to determine if the cell hybrids would continue dividing, undergo cellular senescence, or growth arrest. Somatic cell hybrids were formed between a telomerase positive, hygromycin resistant fibrosarcoma cell line HT1080, expressing wild type p53, and tumorigenic *ras*-transformed 041 (tel+) and 087 (tel−) fibroblasts

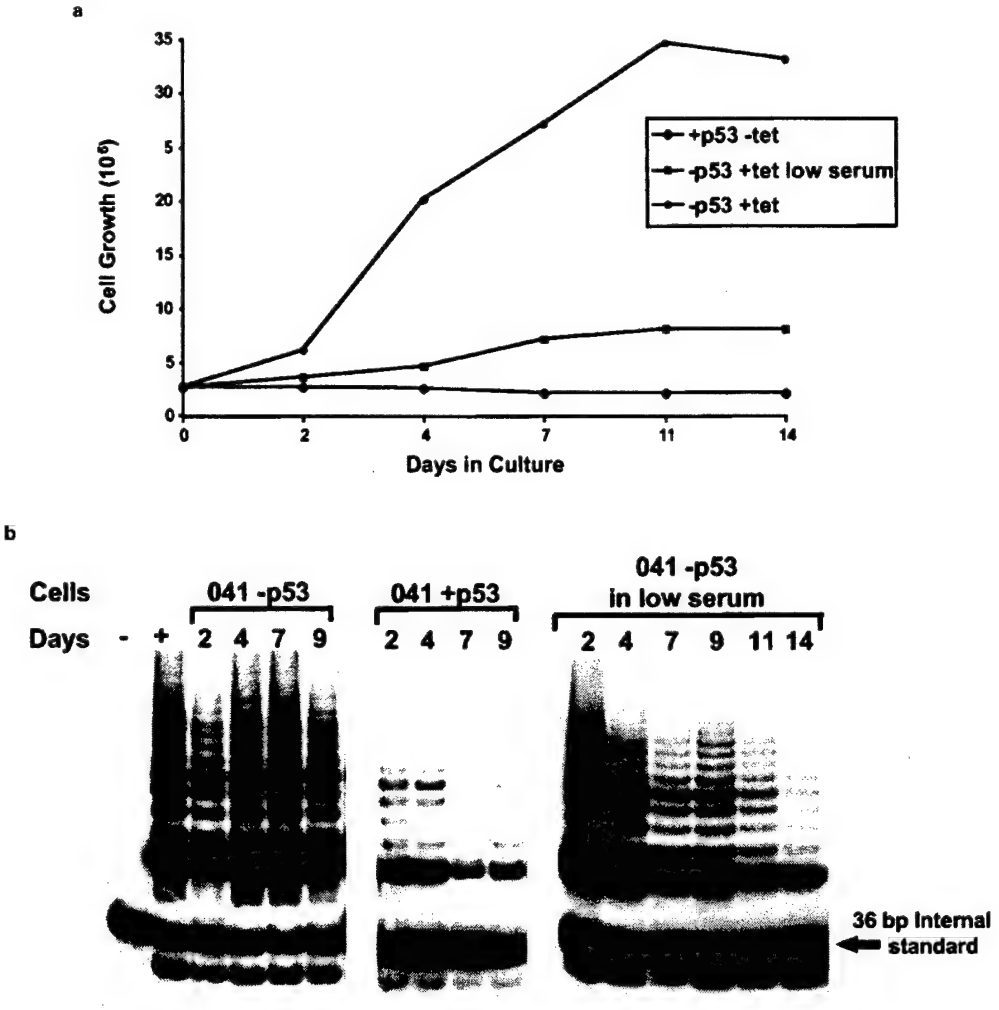


**Figure 4** Growth analysis and telomerase activity of 041 cells transfected with wild type p53 and a tetracycline-inducible promoter system. In the presence of tetracycline, wild type p53 is expressed. (**a**) growth curve in terms of numbers ($10^6$) of cells over 14 days in culture. Test groups include: [−p53, +tet]; [−p53, +tet, 0.75% serum]; [+p53, −tet]. (**b**) TRAP gel results of the same test sets as in (**a**) showing that in the presence of wild type p53 there is a 5–10-fold increase in the internal telomerase assay standard (ITAS) signal compared to telomerase activity signal versus 041 cells lacking wild type p53. Also note that the telomerase inhibition in the cells containing induced wild type p53 occurred after only 48 h whereas the cells in low serum conditions show comparable telomerase inhibition after approximately 2 weeks

containing the gene for neomycin (G418) resistance. Hybrid clones resistant to both hygromycin and G418 readily formed from crosses between HT1080 (tel+, p53+) cells and tumorigenic *ras*-transformed 087 (tel−, p53−) cells. However, there were very few clones obtained between HT1080 (tel+, p53+) and tumorigenic *ras*-transformed 041 (tel+, p53−) cells (Table 2). The three HT1080/041 *ras* cell hybrid clones that formed were telomerase positive but senesced rapidly. All of the hybrid clones tested (10/10) between 087 *ras* (tel−) and HT1080 (tel+) were telomerase positive and grew indefinitely. Southern blot analysis with a telomere-specific probe was performed using genomic DNA prepared from the HT1080-LFS fibroblast somatic cell hybrids. The hybridization revealed a pattern of DNA fragments that corresponded to the expected telomere lengths from each parent cell line (data not shown).

## Discussion

We found that clones from LFS fibroblast cell strains can spontaneously immortalize utilizing either a telomerase dependent or independent mechanism. While telomerase positive immortal LFS cells have stable telomere lengths and high levels of the telomerase RNA (hTR) component, immortal telomerase negative LFS cells lines have long and heterogenous telomere lengths and no observed increase in hTR levels greater than their corresponding preimmortal cell strains (Figure 3c and d). This suggests, at least in LFS, that some cell strains are committed at an early point to a telomerase positive or telomerase negative immortalization pathway.

The TRF analysis in 087 cells revealed two major populations of telomeres. Because the lower band remains unvarying in length throughout culturing,

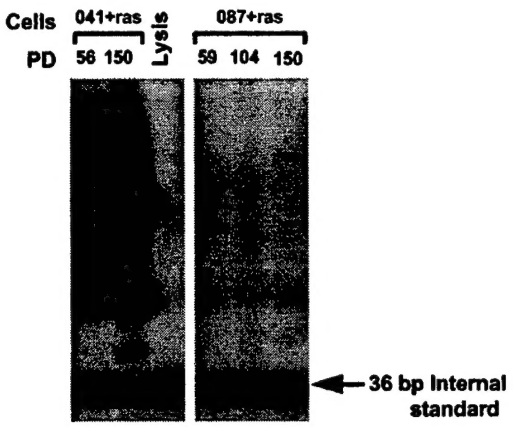


**Figure 5** Comparative telomerase activity of representative *ras*-transformed, tumorigenic 087 and 041 clones from nude mice. After resection of the tumors, cultures were re-established and cells harvested for telomerase activity at increasing PD. Lysis buffer lane is the negative control. 041 cells retain telomerase positivity while 087 cells remain telomerase negative regardless of tumorigenicity or PD

**Table 2** Summary of somatic cell hybrid colony formation and telomerase activity between HT1080 cells and 087 or 041 cells

| *Cell line* | *Efficiency*[a] | *#Colonies tested by TRAP* | *Telomerase activity* |
|---|---|---|---|
| HT1080 | ND | ND | +[b] |
| 087ras | ND | ND | +[b] |
| 041ras | ND | ND | −[b] |
| HT1080 × 087*ras* | 250 | 10 | 10 |
| HT1080 × 041*ras* | 3 | 3 | 3 |

[a]Number of hybrid colonies formed. [b]Telomerase activity assayed from parent cell lines. ND−not done

one possibility is that the longer telomere population is undergoing recombinant events and breakage-fusions-bridge cycles. Alternatively, the shorter telomere population in these cells may serve as the minimum number of TTAGGG repeats required for telomeric function. As the telomere size decreases below this threshold, the cells reenter crisis and a signal may be sent to begin lengthening the telomeres by an as yet unknown mechanism (Lansdorp *et al.*, 1996). Another possibility for the observed heterogenous telomere length and lack of telomerase activity could involve telomeric binding proteins as previously described (Chong *et al.*, 1995). For example, telomeric binding proteins may prevent the longer telomeric population from undergoing recombinational events that would maintain that length. As the telomeres shorten, the lack of bound proteins could either allow access of the ends to recombinational events or signal a negative feedback loop that initiates recombination to increase the telomere length.

Induction of wildtype p53 expression in a tet-inducible promoter in 041 (tel+) cells resulted in growth arrest with a corresponding inhibition in telomerase activity (Agarwal *et al.*, 1995). This loss of telomerase activity occurred significantly faster than telomerase inhibition observed under low serum conditions. However, these results do not indicate that there is a direct interaction between wild type p53 and telomerase activity, merely which telomerase activity is downregulated in cells exiting the cell cycle (Holt *et al.*, 1997). This is consistent with previous observations which show that quiescent cells have reduced telomerase activity (Buchkovich and Greider, 1996; Holt *et al.*, 1996b). While this is the most likely explanation, our results do not rigorously exclude the possibility that p53 could directly regulate the telomerase holoenzyme.

Tumorigenicity studies in nude mice of *ras* transformed 041 and 087 cells showed that even with tumor formation, the status of telomerase activity did not change. Our results using LFS fibroblast cells suggests that activation of telomerase activity is not a requirement for immortalization or tumorigenicity since *ras*-transformed 087 cells formed tumors in nude mice without reactivation of telomerase activity. These results are in agreement with those recently described in a study by (Blasco *et al.*, 1997) in which a telomerase knockout mouse was generated by deleting the gene encoding the telomerase RNA component from the mouse germline. Mice homozygous null for telomerase activity were observed to form tumors at frequencies comparable to normal mice (Blasco *et al.*, 1997). However, cells transformed with oncogenes could form tumors when reintroduced into mice. The 087 LFS skin fibroblasts do not appear to require a functional telomerase since they maintain their telomeres by an alternative lengthening mechanism. Whether there is a difference in metastatic capability and telomere status requires further investigation. Another consideration is the p53 status in these cells. One study (Tainsky *et al.*, 1995) showed that genomic instability due to p53 germline mutations progresses preneoplastic lesions to cancer in human cells. In this present study of LFS fibroblasts, previously characterized for their genomic instability (Bischoff *et al.*, 1990), positive telomerase activity did not appear to be required for tumor formation. The 087 (tel−) cells formed tumors in nude mice as readily as the 041 (tel+) cells.

Immortal 041 cells that have a p53 frameshift mutation at amino acid 184 resulting in a truncated product and null for the wild type protein, may have the remaining components of the p53 pathway intact, thus leading to complementation and growth suppression in the wild type expressing HT1080 × 041 hybrids. One study (Bryan *et al.*, 1995) reported that some somatic cell hybrids between telomerase positive and telomerase negative cell lines recommenced proliferation after exhibiting cellular senescence. Unlike Bryan *et al.* (1995) we did not observe reversible cellular senescence in the somatic cell hybrids generated in this study. In contrast, the continued proliferation capability of the HT1080/087 hybrid clones may be due to the presence of the p53 mutant 248 acting as a dominant negative, abrogating the wild type p53 function of the HT1080 cells. However, the poor efficiency of generating HT1080/041 hybrids may indicate differing mechanisms of complementation for inactivation of the p53 pathway. Because 041 cells are essentially null for p53, the introduction of the wild type p53 from HT1080 cells may cause a cell cycle arrest that remains separate from telomerase activity.

The results from the somatic cell hybrid experiments taken together with the TRF results are consistent with the hypothesis that the wild-type p53 expressed in the HT1080/087 hybrid clones may recognize the long and heterogenous population of telomeres as damaged DNA resulting in a checkpoint growth arrest. The resulting effect would be available telomerase enzyme unable to bind to and replace telomeric TTAGGG repeats and thus telomeres continue to shorten. As the telomeres reach a critical length, p53 may have limited telomere accessibility due to conformational changes, or there may be an unknown mechanism that would allow telomerase to outcompete p53 for the telomeric ends by somehow superseding the p53 binding strategy.

The ALT pathway does not appear to be frequent in primary tumors. It can be observed when viral oncoproteins (e.g. SV40 large T antigen) may predispose certain cells in culture (primarily fibroblasts) to the ALT pathway. Thus, in rare instances, the viral oncogene would integrate into a region(s) that would disrupt the activation of telomerase, such as the RNA component of telomerase or the functional telomerase gene. Our data suggests that such a hypothesis is unlikely since the immortalized cell lines obtained in the present study were spontaneous events. Possibly, it is cell strain specific genetic mutations since we have shown in this study and previous studies (Shay *et al.*, 1995) from patients with p53 germline mutations, the immortalization pathways are consistently and reproducibly different in their activation of telomerase activity, telomere structure, and telomerase RNA expression.

In summary, the results from this study suggest that whether cells immortalize via telomerase reactivation or the ALT pathway may be cell strain specific. Our results also suggest that the immortalization pathway may be genetically predetermined. Evidence for this includes that 087 (tel−) cells clonally and spontaneously immortalized from eight different experiments, never had detectable telomerase activity while the 041 cell immortalization events reactivated telomerase. Telomerase reactivation appears to involve the stabilization of the telomerase lengths whereas the ALT pathway appears to characteristically support long and heterogenous telomeres. Thus, the spontaneous immortalization of LFS cells requires both loss of p53 function and a mechanism to maintain telomeres.

## Materials and methods

### *Cell culture*

The cell lines studied (041 and 087) were derived from primary tissues obtained by skin biopsy from patients with Li-Fraumeni Syndrome. Characterization and immortalization of these cells *in vitro* was previously described (Bischoff *et al.*, 1990). 041 cells contain a frameshift point deletion at codon 184 (GAT−GAA) which generates the translation of 60 aa from the resulting frameshift that is not normally in the p53 protein, followed by a premature stop codon rendering the cell line null for p53 activity. 087 cells contain a missense point mutation at codon 248 (Arg−Trp). The growth and maintenance of these LFS fibroblasts was performed as previously described (Bischoff *et al.*, 1990). All cells were grown in modified Eagle's medium with 10% fetal calf serum and antibiotics.

### *Cell preparation for telomerase analysis*

Detection of telomerase activity in cultured cells requires the extension of an oligonucleotide that serves as the substrate for the telomerase enzyme (TS), followed by PCR amplification of the resultant products with the forward (TS) and reverse (CX) primers. Details of the telomeric repeat amplification protocol (TRAP assay) are reported elsewhere (Holt *et al.*, 1996a; Kim *et al.*, 1994; Piatyszek *et al.*, 1995). TRAP assays were performed using the Oncor TRAPeze™ kit (Gaithersburg, MD). PCR products were electrophoresed on 10% polyacrylamide gels, and the gels were analysed either using PhosphorImaging System from Molecular Dynamics (Sunnyvale, CA) or dried and placed on Kodak Bio Max™ Film (Rochester, NY) overnight. Telomerase activity produces a processive 6 bp RNase sensitive ladder of amplification products. The 36 bp internal standard permits quantitation of relative telomerase activity levels by calculating the ratio of the internal standard to the telomerase ladder.

### *Telomerase RNA and* in situ *hybridization*

For telomerase RNA analysis, cells were prepared as follows: 50 000 cells were plated per chamber in a 2-chamber slide (Nalge-Nunc, Milwaukee, WI) and allowed to attach overnight. The slides were rinsed in PBS and placed in cold acetone for 20 min. Cells were then prepared for hybridization following established protocols (Jordan, 1990). Briefly, cells were cross-linked in 4% paraformaldehyde (Sigma, St. Louis, MO), permeabilized in 0.05% Triton X-100 (Sigma), and deproteinized in 0.2 N HCl (Sigma), deproteinized a second time with Proteinase K (1 μg/ml) (Gibco), at 37°C. The cells were cross-linked again in 4% paraformaldehyde, followed by acetylation with 0.25% acetic anhydride (Sigma) in 0.1 M triethanolamine (Sigma).

### *Probe preparation*

The template used to generate antisense and sense control probes consisted of the human telomerase RNA (hTR) (Geron Corp., Menlo Park, CA) cDNA sequence (560 nucleotides) in a pGEM-5Z plasmid (Feng *et al.*, 1995). Single-stranded RNA probes labeled with [$\alpha^{35}$S] UTP were synthesized according to manufacturer's instruction (Ambion, Austin, TX). As previously described (Yashima *et al.*, 1997) transcripts were alkaline hydrolyzed to generate an average length of 200 nt for efficient hybridization and purified with G-50 columns (Boerhinger Mannheim, Indianapolis, IN). After ethanol precipitation, the probes were resuspended in 30 μl of 100 mM DTT. Specific activity was approximately $3 \times 10^7$ c.p.m./μg of template DNA.

### *Hybridization and washing*

Hybridization solution consisted of 50% deionized formamide, 0.3 M NaCl, 20 mM Tris-HCl (pH 7.5), 5 mM EDTA, 10 mM $NaH_2PO_4$ (pH 8.0), 10% dextran sulfate, 1 × Denhardt's, 500 μg/ml total yeast RNA, 10 mM DTT and 50 000 c.p.m./μl of the $^{35}$S-labeled RNA probe. Slides were hybridized overnight at 50°C. Washes were performed at 50°C in 5 × SSC, 10 mM DTT, then 65°C in 50% formamide, 2 × SSC, 10 mM DTT. The cells were then washed twice in 0.4 M NaCl, 10 mM Tris-HCl (pH 7.5), 5 mM EDTA before treatment with RNase A followed by washes in 2 × SSC and 0.1 × SSC. The slides were dehydrated in a graded ethanol series and dipped in Kodak NTB-2 nuclear track emulsion. After drying, the slides were stored in a light-tight box with desiccant at −80°C for 3−4 weeks. Slides were developed in Kodak

Dektol developer, rinsed with water, fixed, rinsed again, counterstained with Gill's Hematoxylin (Fisher, Pittsburgh, PA) and coverslipped with Permount (Sigma). Photomicrography was performed on an Olympus BH-2 microscope using Kodak-400 *Elite*™ film.

*Telomere length measurement*

DNA from cultured cells was isolated by dialysis and digested with a six enzyme mix consisting of 10 U each *Hinf*I, *Alu*I, *Cfo*I, *Hae*III, *Msp*I and *Rsa*I. 10 μg of digested DNA was electrophoresed on 1.0% agarose gels using field inversion gel electrophoresis (FIGE) (Bio-Rad, Hercules, CA) with forward voltage 180 V, reverse voltage 120 V, for 20 h. Gels were denatured in high salt buffer (0.5 M NaOH, 1.5 M NaCl) for 15 min, dried under vacuum at 50°C for 45 min and equilibrated in neutralization buffer (0.5 M Tris-HCl, pH 8, 1.5 M NaCl) 2 times for 15 min. The gels were preincubated in hybridization buffer (5 × SSC, 5 × Denhardt's solution, 0.5 M sodium pyrophosphate, 10 mM disodium hydrogen phosphate) at 37°C for 4 h. Hybridization was done using fresh buffer and the radiolabeled telomeric probe $(TTAGGG)_4$ for 12 h. Hybridized gels were washed 3 times for 7 min each with 0.1 × SSC at room temperature and analysed using the PhosphorImaging System from Molecular Dynamics. Terminal Restriction Fragment (TRF) lengths were estimated based on electrophoresis of 1 kb and high molecular weight ladders (Gibco).

*Western analysis*

Cells were harvested at approximately 80% confluence and analysed as previously described (Gillespie and Hudspeth, 1991). Briefly, 20 μg of protein extract was run under 10% SDS–PAGE conditions. Resolved protein was transferred to ECL™ Nitrocellulose membrane (Amersham, Arlington Heights, IL). For p53, monoclonal antibody DO-1 (Oncogene Science, Cambridge, MA) was applied as per manufacturers instructions and detection was performed using Tropix™ chemiluminescent reagents (Bedford, MA). Blots were exposed to Kodak X-ray film (Rochester, NY).

*Somatic cell hybrids*

Cells for preparation of somatic cell hybrids were harvested by trypsinization from rapidly growing cell cultures. Somatic cell hybrids were formed by mixing $3 \times 10^6$ cells of each pair HT1080($hygro^R$) with 087ras($neo^R$) or HT1080($hygro^R$) with 041ras($neo^R$), centrifuging at 800 r.p.m. for 6 min, and washing once in 10 ml of serum free media, RPMI 1640. The cells were recentrifuged at 800 r.p.m. for 6 min and resuspended in 1 ml of 50% polyethyleneglycol 1500 (Boehringer Mannheim) in RPMI 1640 prewarmed to 37°C. The cells were kept for 1 min at 37°C in a water bath. After 1 min, 1 ml of medium was added, and after 2 min, 2 ml of medium was added. This mixture was kept for 4 min at 37°C, and then 4 ml of medium was added for a final volume of 8 ml. The mixture was then centrifuged at 800 r.p.m. for 6 min and resuspended gently in RPMI 1640. The washed cells were then centrifuged at 800 r.p.m. for 6 min and resuspended in MEM with 10% FBS and plated at $1 \times 10^6$ cells per 100 mm tissue culture plate. Drug selection was initiated 24 h later in MEM with 10% FBS using both 100 mg/ml of hygromycin and 200 mg/ml G418. Double drug resistant colonies were picked 3–4 weeks later and used for further studies.

*Tetracycline inducible response promoter*

The TR-9 cells are immortal 041 cells that contain a repressible wt-p53 expression cassette. Cells were generously supplied by Stark and Agarwal. Stock cultures were maintained in 1 mg/ml tetracyline, 600 mg/ml G418 and 50 mg/ml of hygromycin. For experiments, TR-9 cells were seeded at $2 \times 10^6$ per 100 $mm^2$ tissue culture plate in the presence of 600 mg/ml G418 and 50 mg/ml hygromycin. In cultures in which the wild type p53 was to be repressed, tetracycline was added to 1 mg/ml. Cells were harvested at day 2, 4, 7, 9, 11 and 14 for cell counting, p53 expression and telomerase assays. The growth of the cells is almost immediately halted after removal of tetracycline from the medium. For the early times and for culture in which the wild type p53 was expressed, 2–3 plates of cells were harvested, pooled and counted.

**Acknowledgements**

We would like to thank Drs A Agarwal and G Stark for supplying the TR-9 cells. Special thanks to Dr SE Holt for critical reading of the manuscripts as well as JF Train and B Squires for technical assistance. This work was supported in part by the US Army Postdoctoral Grant DAMD17-94-J-4023 (LSG), National Institutes of Health Training Grant CA-09299 (EK), National Institutes of Health core grant CA-16672 to the MDACC and a grant from National Institutes of Health CA-P01 34936 (MAT and LCS).

**References**

Agarwal ML, Agarwal A, Taylor WR and Stark GR. (1995). *Proc. Natl. Acad. Sci. USA*, **92**, 8493–8497.

Avery OT, MacLeod CM and McCarty M. (1944). *J. Exp. Med.*, **79**, 137–158.

Avilion AA, Piatyszek MA, Gupta J, Shay JW, Bacchetti S and Greider CW. (1996). *Cancer Res.*, **56**, 645–650.

Bacchetti S and Counter C. (1995). *Int. J. Oncol.*, **7**, 423–432.

Band V, Dalal S, Delmolino L and Androph YEJ. (1993). *EMBO J.*, **12**, 1847–1852.

Barrett JC. (1993). *Molecular Genetics of Nervous System Tumors*, Levine AJ and Schmidek HH (eds). Wiley-Liss: New York, pp 61–72.

Bischoff F, Strong L, Yim S, Pathak S, Pratt D, Grant G, Sicillano M, Giovanella B and Tainsky M. (1991). *Oncogene*, **6**, 183–186.

Bischoff FZ, Yim SO, Pathak S, Grant GMJ, S, Giovanella BC, Strong LC and Tainsky MA. (1990). *Cancer Res.*, **50**, 7979–7984.

Blackburn EH. (1991). *Nature*, **350**, 569–573.

Blackburn EH. (1994). *Cell*, **77**, 621–623.

Blasco M, Lee H-W, Hande M, Samper E, Lansdorp P, DePinho R and Grieder C. (1997). *Cell*, **91**, 25–34.

Bryan TM, Engelzou A, Gupta J, Bachetti S and Reddel RR. (1995). *EMBO J.*, **14**, 4240–4248.

Buchkovich K and Greider CW. (1996). *Mol. Biol. Cell*, **7**, 1443–1454.

Chong L, van Steensel B, Broccoli D, Erdjument-Bromage H, Hanish J, Tempst P and de Lange T. (1995). *Science*, **270**, 1663–1667.

Counter CM, Avilion AA, LeFeuvre CE, Stewart NG, Greider CW, Harley CB and Bacchetti S. (1992). *EMBO J.*, **11**, 1921–1929.
Duncan EJ, Whitaker NJ, Moy EL and Reddel RR. (1993). *Exp. Cell Res.*, **205**, 337–344.
Eliyahu D, Raz A, Gruss P, Givol D and Oren M. (1984a). *Nature*, **312**, 646–649.
Feng J, Funk WD, Wang SS, Weinrich SL, Avilion AA, Chiu CP, Adams RR, Chang E, Allsopp RC, Yu J, Le S, West MD, Harley CB, Andrews WH, Greider CW and Villeponteau B. (1995). *Science*, **269**, 1236–1239.
Gao Q, Hauser SH, Liu XL, Wazer DE, Madoc-Jones H and Band V. (1996). *Cancer Res.*, **56**, 3129–3133.
Gillespie PG and Hudspeth AJ. (1991). *Proc. Natl. Acad. Sci. USA*, **88**, 2563–2567.
Gollahon LS and Shay JW. (1996). *Oncogene*, **12**, 715–725.
Gossen M and Bujard H. (1992). *Proc. Natl. Acad. Sci. USA*, **89**, 5547–5551.
Graham FL and Smiley J. (1977). *J. Gen. Virol.*, **36**, 59–74.
Greider CW. (1991). *Curr. Opin. Cell Biol.*, **3**, 444–451.
Gutman A and Wasylyk B. (1991). *Trends Genetics*, **7**, 49–54.
Harley CB. (1991). *Mutat. Res.*, **256**, 271–282.
Harley CB, Fletcher AB and Greider CW. (1990). *Nature*, **345**, 458–460.
Harley CB, Kim NW, Prowse KR, Weinrich SL, Hirsch KS, West MD, Bacchetti S, Hirte HW, Counter CM, Greider CW, Piatyszek MA, Wright WE and Shay JW. (1994). *Cold Spring Harbor Symposia on Quantitative Biology*, pp 307–315.
Harley CB and Villaponteau B. (1995). *Curr. Opin. Genetics Develop.*, **5**, 249–255.
Holt SE, Aisner DL, Shay JW and Wright WE. (1997). *Proc. Natl. Acad. Sci. USA*, **94**, 10687–10692.
Holt SE, Norton JC, Wright WE and Shay JW. (1996a). *Methods Cell Science*, **18**, 237–248.
Holt SE, Wright WE and Shay JW. (1996b). *Mol. Cell. Biol.*, **16**, 2932–2939.
Hsiao R, Sharma HW, Ramakrishnan S, Keith E and Narayanan R. (1997). *Anticancer Res.*, **17**, 827–832.
Huschtscha LL and Holliday R. (1983). *J. Cell Sci.*, **63**, 77–99.
Jordan C. (1990). *In Situ Hybridization Histochem.*, Chesselet M-F (ed) CRC Press: Boston, pp 61–63.
Karlsson C, Stenman G, Vojta PJ, Bongcam-Rudloff E, Barrett JC, Westermark B and Paulsson Y. (1996). *Cancer Res.*, **56**, 241–245.
Kim NW, Piatyszek MA, Prowse KR, Harley CB, West MD, Ho PL, Coviello GM, Wright WE, Weinrich SL and Shay JW. (1994). *Science*, **266**, 2011–2015.
Lansdorp PM, Verwood NP, Van de Rijke FM, Dragowska V, Little M-T, Dirks RW, Raap AK and Tanke HJ. (1996). *Hum. Mol. Genet.*, **5**, 685–691.
Lemoine NR, Staddon S, Bond J, Wyllie FS, Shaw JJ and Wynford-Thomas D. (1990). *Oncogene*, **5**, 1833–1837.
Mayne LV, Priestley A, James MR and Burkes JR. (1986). *Exp. Cell Res.*, **162**, 530–538.
Mayne LV, Priestley A, James MR and Burke JR. (1986). *Exp. Cell Res.*, **162**, 530–538.
McCormick JJ and Maher VM. (1988). *Mutat. Res.*, **199**, 273–291.
Murnane JP, Sabatier L, Marder BA and Morgan WF. (1994). *EMBO J.*, **13**, 4953–4962.
Ohmura H, Tahara H, Suzuki M, Ide T, Shimizu M, Yoshida MA, Tahara E, Shay JW, Barrett JC and Oshimura M. (1995). *Jap. J. Cancer Res.*, **86**, 899–904.
Olovnikov AM. (1973). *J. Theoretical Biol.*, **41**, 181–190.
Pereira-Smith OM. and Smith JR. (1988). *Proc. Natl. Acad. Sci. USA*, **85**, 6042–6046.
Piatyszek MA, Kim NW, Weinrich SL, Keiko H, Hiyama E, Wright WE and Shay JW. (1996). *Methods Cell Sci.*, **17**, 1–15.
Rainey WH, Sawetawan C, Shay JW, Michael MD, Mathis JM, Kutteh W, Byrd W and Carr BR. (1994). *J. Clin. Endocrinol. Metab.*, **78**, 705–710.
Rogan EM, Bryan TM, Hukku B, Maclean K, Chang AC, Moy EL, Englezou A, Warneford SG, Dalla-Pozza L and Reddel RR. (1995). *Mol. Cell. Biol.*, **15**, 4745–4753.
Ross SR, Linzer DI, Flint SJ and Levine AJ. (1978). *Persistent viruses, Vol. 11.* Stevens JG *et al.* (eds). Academic Press: New York, pp 469–484.
Sarnow P, Ho YS, Williams J and Levine AJ. (1982). *Cell*, **28**, 387–394.
Sasaki M, Honda T, Yamada H, Wake N, Barrett JC and Oshimurs M. (1994). *Cancer Res.*, **54**, 6090–6093.
Scheffner M, Werness BA, Huibregtse JM, Levine AJ and Howley PM. (1990). *Cell*, **63**, 1129–1136.
Shay JW and Bacchetti S. (1997). *Euro. J. Cancer*, **5**, 787–791.
Shay JW, Brasiskyte D, Ouellette M, Piatyszek MA, Werbin H, Ying Y and Wright WE. (1994). *Meth. Mol. Genet.*, **5**, 263–280.
Shay JW, Pereira-Smith OM and Wright WE. (1991a). *Exp. Cell Res.*, **196**, 33–39.
Shay JW, Tomlinson G, Piatyszek MA and Gollahon LS. (1995). *Mol. Cell. Biol.*, **15**, 425–432.
Shay JW, Van Der Haegen BA, Ying Y and Wright WE. (1993a). *Exp. Cell Res.*, **209**, 45–52.
Shay JW and Wright WE. (1996). *Curr. Opin. Oncol.*, **8**, 66–71.
Shay JW, Wright WE, Brasiskyte D and Van Der Haegen BA. (1993b). *Oncogene*, **8**, 1407–1413.
Shay JW, Wright WE and Werbin H. (1991b). *Biochim. Biophys. Acta*, **1072**, 1–7.
Slingerland JM, Jenkins JR and Benchimol S. (1993). *EMBO J.*, **12**, 1029–1037.
Tainsky M, Bischoff F and Strong L. (1995). *Can. Metast. Rev.*, **14**, 43–48.
Tsutsui T, Fujino T, Kodama S, Tainsky MA, Boyd J and Barrett JC. (1995). *Carcinogenesis*, **16**, 25–34.
Tsutsui T, Tanaka Y, Matsudo Y, Hasegawa K, Fujino T, Kodama S and Barrett J. (1997). *Mol. Carcin.*, **18**, 7–18.
Van Der Haegen BA and Shay JW. (1993). *In Vitro Cell. Devel. Biol.*, **29A**, 180–182.
Watanabe S, Kanda T and Yoshiike K. (1993). *Jpn. J. Cancer Res.*, **84**, 1043–1049.
Watson JD. (1972). *Nature*, **239**, 197–201.
Wazer DE, Liu XL, Chu Q, Gao Q and Band V. (1995). *Proc. Natl. Acad. Sci. USA*, **92**, 3687–3691.
Werness BA, Levine AJ and Howley PM. (1990). *Science*, **248**, 76–79.
Wright WE, Brasiskyte D, Piatyszek MA and Shay JW. (1996). *EMBO J.*, **15**, 1734–1741.
Wright WE, Pereira-Smith OM and Shay JW. (1989). *Mol. Cell. Biol.*, **9**, 3088–3092.
Wright WE and Shay JW. (1992). *Exp. Gerontol.*, **27**, 383–389.
Wyllie FS, Lemoine NR, Barton CM, Dawson T, Bond J and Wynford-Thomas D. (1993). *Mol. Carcinog.*, **7**, 83–88.
Yashima K, Milchrug S, Gollahon LS, Maitra A, Saboorian MH, Shay JW and Gazdar AF. (1991). *Clinical Cancer Res.*, **4**, 229–234.